Elemental localization of the von Economo neuron and the fork neuron in the insular cortex in humans and macaque monkeys

Dissertation

zur Erlangung des Grades eines

Doktors der Naturwissenschaften

der Mathematisch-Naturwissenschaftlichen Fakultät

und

Medizinischen Fakultät

der Eberhard Karls Universität Tübingen

vorgelegt von

Felicitas Marietta Horn

aus Albstadt-Ebingen, Baden-Württemberg, Deutschland

Juni 2019

Tag der mündlichen Prüfung:	12.09.2019
Dekan der Math.-Nat. Fakultät:	Prof. Dr. W. Rosenstiel
Dekan der Medizinischen Fakultät:	Prof. Dr. I. B. Autenrieth
1. Berichterstatter:	Dr. Henry Evrard
2. Berichterstatter:	Prof. Dr. Dr. Hans-Otto Karnath
Prüfungskommission:	PD Dr. Axel Lindner
	Prof. Dr. Uwe Ilg

Ich erkläre, dass ich die zur Promotion eingereichte Arbeit mit dem Titel:

„Elemental localization of the von Economo neuron and the fork neuron within the insular cortex in humans and macaque monkeys“

selbständig verfasst, nur die angegebenen Quellen und Hilfsmittel benutzt und wörtlich oder inhaltlich übernommene Stellen als solche gekennzeichnet habe. Ich versichere an Eides statt, dass diese Angaben wahr sind und dass ich nichts verschwiegen habe. Mir ist bekannt, dass die falsche Abgabe einer Versicherung an Eides statt mit Freiheitsstrafe bis zu drei Jahren oder mit Geldstrafe bestraft wird.

Tübingen, _____ _____

Datum Unterschrift

Elemental localization of the von Economo neuron and fork neuron in the insular cortex in humans and macaque monkeys

Felicitas M. Horn

Functional and Comparative Neuroanatomy Laboratory, Werner Reichardt Center for Integrative Neuroscience, Tuebingen, Germany

Max Planck Institute for Biological Cybernetics, Tuebingen, Germany

International Max Planck Research School, Tuebingen, Germany

Abstract

The cerebral cortex of mammalian species is parcellated into discrete areas, or modules. Some of these modules share common features amongst most mammals; however, between higher and lower mammalian species, deviations in size, subdivisions, cellular features and connectivity of these modules exist. The cortex of higher mammals like primates, has expanded and has subdivided many times resulting in a complex neural system built of smaller modules acting in concert and forming functional networks. In line with this, in primates, the insular cortex has been shown to consist of smaller, unique modules, each having a specific structure and function. Furthermore, the research presented here, identified that in the anterior agranular and the dysgranular insula of macaque monkeys one of each of these architectonic area harbors two specialized neuronal morphotypes, the von Economo neurons (VEN) and the fork neurons (FN), whilst in the human anterior insula there are five distinct architectonic areas hosting these neurons. More than a century ago, Brodmann defined this kind of containment of specialized neuronal morphotypes with a specific cytoarchitectonic area of the primate cerebral cortex as “elemental localization”, because it suggests shared evolutional, developmental, and functional features between the specialized neurons and their host area. The discovery of novel elemental localizations within the primate brain 1) supports the theory that the ventral anterior insular cortex as well as the adjacent orbital prefrontal cortex are heterogeneously organized into smaller areas rather than being lumped together into a larger, homogeneous periallocortical (agranular) sector, and 2) provides an exclusive experimental advantage for the examination of the VEN areas and its two specialized neuronal morphotypes, VEN and FN, which are linked to internal bodily state representation and neuropsychiatric disorders.

Introduction

The insular cortex

Topology and morphology

The primate insular cortex is a distinct cortical lobe, which is often referred to as the "fifth lobe", situated in the depth of the Sylvian fissure (Fig. 1A). It is hidden by the overlaying opercula of the frontal, parietal and temporal lobes and has a triangular shape with its apex pointing anteroventrally. Its demarcation is formed by the circular sulcus, which consists of a superior peri-insular sulcus (SPS) separating the insular cortex from the frontoparietal operculum, and the inferior peri-insular sulcus (IPS), forming the border to the superior surface of the temporal lobe. In humans, an anterior peri-insular (APS) sulcus separates the insular cortex from the orbital gyri (Fig. 1A'). The caudal end of the insular cortex is formed by the fusion of the SPS and IPS in the fundus of the Sylvian fissure. A central insular sulcus divides the insular cortex into a larger anterior and a smaller posterior lobule. The anterior lobule is generally formed by three short gyri: the anterior, the middle, and the posterior short gyri (s1-3 in Fig. 1A'). The posterior lobule consists of two long gyri, the anterior and posterior long gyri (l1-2 in Fig. 1A'). The gyri are radially oriented towards the most anteroventral point of the insula forming the pole of the insular cortex, which is demarcated by the junction of the APS and IPS. The pole is close to -but clearly separable from- the apex, which is formed by the junction of the inferior end of all or some of the short gyri and forms the most lateral part of the insular cortex (Naidich et al., 2004). In addition to the anterior and posterior lobules, some insular cortices have a more or less well developed accessory gyrus and a transverse gyrus (Afif and Mertens, 2010; Brockhaus, 1940; Kurth et al., 2010; Mesulam and Mufson, 1985; Naidich et al., 2004; Rosen et al., 2015; Wysiadecki et al., 2018). These two gyri approximately overlapping with the region termed frontoinsula (FI; (von Economo, 1925)) that harbors a high concentration of two specialized neuronal morphotypes: the spindle-shaped von Economo neurons (VEN), which is accompanied systematically by the triangular-shaped Fork neurons (FN) (Evrard et al., 2012; von Economo, 1925).

In macaque monkeys, the insular cortex is nearly completely smooth (lissencephalic) with only an incipient convexity in the ventral part of the insula (Fig.

1B"), and in many cases, there is a shallow but distinct groove anteriorly (Evrard, 2019; Mesulam and Mufson, 1985). The region, which is anterior to that groove harbors the VEN and FN and therefore is suggested to be the macaque homolog of the human FI (Evrard et al., 2012, Horn and Evrard, in preparation) (Fig. 1).

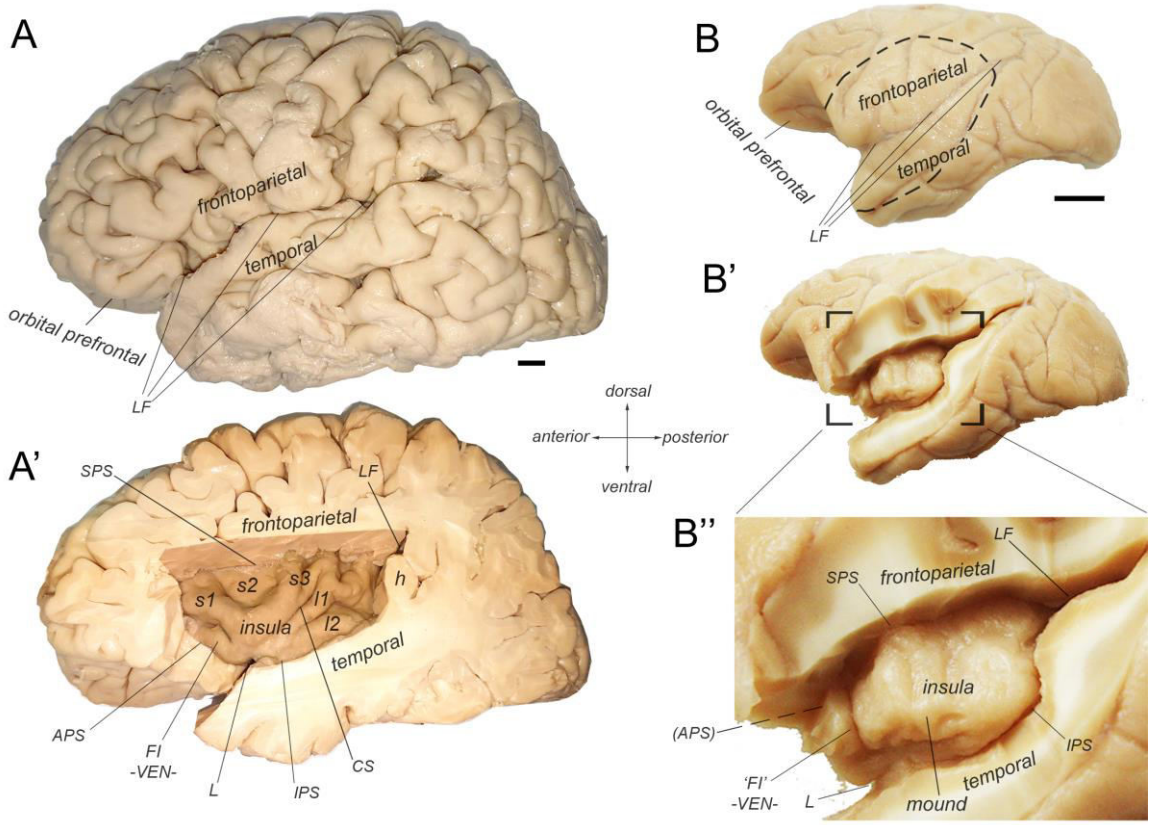

Figure 1: Morphology and location of the insular cortex in humans (A-A') and macaque monkeys (B-B'-B"). A. Lateral view of a human left hemisphere. The insular cortex is hidden by the opercula of the frontal, parietal, and temporal lobes. A'. Insular cortex and its demarcation after removal of the opercula. The three short gyri of the anterior insular lobule are labeled s1-3; the long gyri of the posterior lobule l1 and l2. The accessory gyrus is assumed to overlap with the FI, that harbors the VEN and FN. B. Lateral aspect of a cynomolgus macaque monkey brain. B' and B''. Lissencephalic insular cortex that has only an incipient bulge and a shallow anterior sulcus that marks the region containing the VEN and FN. Abbreviations: APS: anterior peri-insular sulcus; CS: central insular sulcus; FI: frontoinsula; h: Heschel's gyrus; L: limen insula; LF: lateral (Sylvian) fissure; IPS: inferior peri-insular sulcus; SPS: superior per-insular insular sulcus. Scale bar represents 1 cm. Human brain photographs by F.M. Horn. Monkey photographs by H.C. Evrard. Figure composite by H.C. Evrard.

Architectonic parcellation

Since the beginning of the 20th century, anatomists studied the organization of the primate cerebral cortex, including the insular cortex, based on cyto- and myeloarchitectonic criteria (Brockhaus, 1940; Brodmann, 1909; Retzius, 1896; 1902; Rose, 1928; Vogt, 1910; von Economo, 1925). Their maps, however, showed considerable variations in the gross organization of the insular cortex. Based on differences in lamination and the presence of the inner granular layer 4 (granularity), Brodmann simply divided the human insular cortex into an anterior agranular and a posterior granular sector. However, in his publication, he pointed out that this division cannot be taken as final and must await further investigation (Brodmann, 1909). Von Economo and Koskinas divided the insula into three sectors: an anterior agranular region called area frontoinsularis, a dysgranular area called praecentralis insulae and a posterior granular area called postcentralis insulae (von Economo, 1925). Brockhaus, who additionally used myeloarchitectonic criteria and Rose agreed with the tripartition described by von Economo and Koskinas, but they further parcellated each sector into no less than 26 and 31 subareas, respectively (Brockhaus, 1940; Rose, 1928). While Rose described sharp borders between the subareas, Brockhaus and von Economo & Koskinas reported rather gradual transitions (Brockhaus, 1940; von Economo, 1925).

Current architectonic studies of the insular cortex in humans and macaque monkeys also describe a similar trichotomous organization, and nowadays it is widely accepted that the primate insular cortex can be divided into three different main sectors: an anteroventral agranular sector, an intermediate dysgranular sector, and an antero- and posterodorsal granular sector (Evrard et al., 2014; Gallay et al., 2012; Jones and Burton, 1976; Mesulam and Mufson, 1982b; 1985; Morel et al., 2013; Roberts and Akert, 1963). Similar to the description of Rose who only examined the cytoarchitecture of one human, one baboon, and one lemur, but did not examine the macaque insular cortex, a recent study using both cyto- and myeloarchitectonic comparison of the macaque insular cortex demonstrated that the three main sectors can be further parcellated into smaller, architectonically distinct areas that are sharply delimited (Carmichael and Price, 1994; Evrard et al., 2014). The authors consistently identified four granular (Idfa, Idfp, Igd, Igv), four dysgranular (Idd, Idm, Idv, Ivfp) (Evrard et al., 2014), and seven agranular areas (Iai, Ial, Iam, Iamp, Iap, Iapl, Ivfa) (Carmichael and Price, 1994; Evrard et al., 2014). Additionally, an observer-

independent measurement of laminar optical density of the posterior lobule of the human insular cortex stained to reveal cell bodies concluded that the human posterior lobule consists of six areas, including two posterior granular regions Ig1 and Ig2, three medial dysgranular regions Id1, Id2 and Id3, followed anteriorly by an agranular area Iag1 (Kurth et al., 2010). Although this map is still incomplete, it was found that the arrangement of the architectonic areas within the human posterior insular cortex is highly similar to that in macaques. In contrast to Carmichael and Price and Evrard and Kurth and colleagues, other groups describe that the transition between the three main sectors occurs rather gradually and they combine the different smaller cytoarchitectonic areas of the macaque AIC into larger, periallocortical (agranular), proisocortical (dysgranular), and eulaminate (granular) regions (Barbas and Pandya, 1989; Mesulam and Mufson, 1982b; Morel et al., 2013). Furthermore, Morel and colleagues, who used multiple immunohistological stains in addition to cyto- and myeloarchitectonic stains, claimed that multiarchitectonic comparison of borders and connectivity patterns could be neglected in the determination of architectonic borders (Morel et al., 2013), despite shown differently (Glasser et al., 2016; Luppino et al., 1991; Zilles et al., 2002). However, the parcellation of the three main insular sectors into smaller modules with sharp borders is in line with the theory that the entire cerebral cortex is a heterogeneous structure organized into smaller regions, which are built of unique anatomical and functional modules (Northcutt and Kaas, 1995). This theory has already been established in the late 19th century by anatomists such as Paul Flechsig, Alfred Campbell, Korbinian Brodmann and Oscar and Cécile Vogt (Brodmann, 1909; Campbell, 1904; Flechsig, 1898; Vogt, 1910) and has been supported by studies that used a wide variety of approaches (Geyer et al., 1996; Geyer et al., 1997; Luppino et al., 1991; Northcutt and Kaas, 1995; Zeki et al., 1991; Zhao et al., 2001; Zilles et al., 2002). For example, Luppino and colleagues used electrophysiological stimulation in the mesial agranular frontal cortex in macaque monkeys and demonstrated that the rostral and caudal portions of this cortical area, which are distinct in terms of their cytoarchitecture and connectivity pattern to other areas of the brain or the spinal cord, also have different motor representations (Luppino et al., 1991). Within the human cerebral cortex, transmitter receptor densities reflected the cyto- and myeloarchitectonic boundaries of cortical areas (Zilles et al., 2002), and transcriptional profiling analysis of the hippocampus in mice revealed different expression profiles for the different architectonic regions CA1, CA3, and dentate gyrus (Zhao et al., 2001).

Furthermore, in a recent tract-tracing study in macaque monkeys, labeling patterns in the insular cortex produced by anterograde and retrograde tracers, which were injected in other brain areas, overlapped precisely with the previously defined architectonic borders of the unique areas of the insula (Krockenberger et al., *submitted*). This overlap shows that each architectonic area of the insular cortex has a specific hodological pattern confirming the theory of the cortical parcellation. The modular organization of the cortex into smaller distinct areas, which harbor different types of receptors, different cell types, and different numbers of layers, enables the emergence of new functional abilities. An evolutionary increase in the number of functionally distinct cortical areas, such as in the human brain, might reflect the increased complexity of cortical processing (Kaas, 2011). Furthermore, it is suggested that the volume of a brain area is related to the capacity for information processing which is necessary for the performance of a task. With the growth of the areal volume, the amount of neurons increases and local cortical circuitries and interconnectivity between brain areas are modified. Hence the fine-tuned cortical processing is improved (Bauernfeind et al., 2013; Hofman, 2014; Kaas, 2000).

Functional organization of the primate insular cortex

The insula cortex plays a role in a multitude of processes ranging from interoception, to somatosensory and motor functions and is involved in complex processes like emotions and cognition (Butti and Hof, 2010). Its exact functional organization, however, is not fully understood. Electro-cortical stimulation in epilepsy patients as well as lesion and clinicopathological studies and functional magnetic resonance imaging (fMRI)-studies enabled scientists to reveal several functions of the insula that are critical for behavior, emotion, and cognition. Furthermore, structural connectivity studies like in-vivo diffusion-weighted imaging, functional connectivity studies (resting state fMRI) in humans, as well as electrophysiological recordings, electrical microstimulations, and tract-tracing studies in macaque monkeys contributed to the understanding of the insula functions.

The primate insular cortex is suggested to integrate interoceptive afferents, encompassing all sensations of the physiological state of the whole body like warmth, cold, itch, pain, sensual touch, hunger or thirst, bowel distension, and others (Craig,

2002). Interoceptive afferents shape all ongoing emotional, cognitive, and behavioral events to autonomically regulate and motivate behavior for the maintenance of homeostasis (Craig, 2002; 2009b). Differing from exteroceptive signals, which are linked to sensorimotor processing (e.g. mechanoreception, vision, proprioception), interoceptive signals reflect the homeostatic status of the organs and tissues of the body and are linked to subjective qualities (Strigo and Craig, 2016). Craig and his team proposed that the homeostatic state of the body is represented by a primate-specific spino-thalamo-cortical pathway in which interoceptive afferents from the body are conveyed by modality selective, small-diameter afferent Aδ- and C-fibers to spinal lamina 1 neurons (Craig et al., 1994). These small-diameter afferent fibers carry information from the viscera, heart, pharynx, and tongue and travel along with the vagal and glossopharyngeal nerves, which project to neurons of the solitary tract nucleus (NTS). Both, the projections of the neurons in the spinal lamina 1 and of the NTS, terminate in a somatotopographic order in two thalamic subnuclei: the posterior part of the ventromedial nucleus of the thalamus (VMpo) and the basal part of the ventral medial nucleus of the thalamus (VMb), respectively. VMb and VMpo send thalamocortical representations of interoceptive signals to the anterior dorsal fundus of the insula (Idfa) and the posterior dorsal fundus of the insula (Idfp), respectively (Craig, 2014). Injections of anterograde tracers in VMpo, guided by microelectrode recordings, showed a somatotopic representation of interoception within Idfp from anterior (head and face) to posterior (foot) while vagal and gustatory afferent representations, relayed by the VMb are located in Idfa. Thus, Idfa and Idfp together form the so-called primary interoceptive cortex (PIC) (Craig, 2014; Evrard and Craig, 2015; Pritchard et al., 1986). Based on single-unit recordings, tract tracing, and imaging studies, a working model of the primate insular cortex proposes that the integration process occurs in a posterior-to-mid-to-anterior progression with the PIC constituting the first cortical relay (Craig, 2002).

Craig further suggested that all sensory interoceptive information mapped initially within the PIC is re-represented in the intermediate dysgranular insular cortex and that in this region the primary interoceptive afferent stimuli are integrated with multi-modal higher-order cortical salient emotional, hedonic, homeostatic, and environmental activity (Craig, 2009a). Furthermore, by employing microelectrode recordings, Schneider and colleagues have shown that due to innocuous tactile

stimulation of the monkey's limbs, head, trunk, or entire body, the activity in the mid-insula revealed a similar anteroposterior topography like in the PIC (Schneider et al., 1993). Additionally, labeling in the dysgranular insula that was produced by anterograde and retrograde tracer injections into somatosensory cortex S1 and S2 confirmed this somatotopic anteroposterior representation within the dysgranular insular cortex in macaque monkeys (Burton et al., 1995; Mesulam and Mufson, 1982a).

In this model, the integrated interoceptive information eventually unifies within the AIC and is further integrated with motivational, social, and cognitive conditions represented in other cortical areas via reciprocal connections with cortical and subcortical areas, limbic, reward circuit components, and executive control regions (for review see (Augustine, 1996)). It is suggested that within the AIC emotions and cognitive feelings are colored by the subjective, interoceptive feeling states from the body (Craig, 2002). A wealth of imaging studies in humans show a strong activation of the AIC in subjective bodily reactions, emotional and cognitive feelings, and motivation: the AIC was activated in interoceptive processes like the detection of one's own heartbeat (Critchley et al., 2004), subjective rating of temperature (Craig et al., 2000), and subjective awareness of gastric or oesophageal distension (Phillips et al., 2003; Stephan et al., 2003). Furthermore, emotive stimuli, such as images of the own child or the romantic partner, caused activation of the AIC, mainly on the left side (Bartels and Zeki, 2004; Leibenluft et al., 2004). The right AIC was activated in unpleasant and pleasant emotions such as fear (Critchley et al., 2002), disgust (Jabbi et al., 2008), anger and (recall induced) sadness (Damasio et al., 2000; Lane et al., 1997), sexual arousal and joy (Ortigue et al., 2007; Takahashi et al., 2008), and trust (Winston et al., 2002). The AIC also plays a crucial role in high-level social-emotional processes, such as empathy and empathy for other's pain (Singer et al., 2009; Singer et al., 2004), compassion for psychological, physical, and social pain, as well as admiration for skills, virtue and moral (Immordino-Yang et al., 2009). Additionally, the AIC is involved in cognitive feelings, such as time perception (Craig, 2009a), recognition of the self (Devue et al., 2007), the "feeling-of-knowing" whilst recalling words (Kikyo et al., 2002), or deception (Baumgartner et al., 2013). Furthermore, the AIC is strongly activated by salient or novel stimuli that are embedded in the stream of all modalities, suggesting an essential function of the AIC in the detection of salient stimuli across all

incoming input and in determining the priority of the stimulus based on present goals (Crottaz-Herbette and Menon, 2006; Downar et al., 2002; Michel, 2017).

The AIC is conjointly activated with the anterior cingulate cortex (ACC) in multiple contexts, suggesting a close functional relationship between these two brain regions (Medford and Critchley, 2010). Both the AIC and ACC are cortical structures of the salience network (SN), which is involved in detecting relevant internal and extrapersonal stimuli to initiate, maintain, and adjust cognitive control functions and eventually guide behavior (Dosenbach et al., 2006; Menon and Uddin, 2010; Seeley et al., 2007). Furthermore, Sridharan and colleagues described that the SN, and particularly the right AIC, is switching between two main brain networks, which are involved in cognitive processes (Sridharan et al., 2008). While the AIC activates the central-executive network (CEN), it deactivates the default-mode network (DMN) (Menon and Uddin, 2010). The CEN and SN are classically active during demanding cognitive tasks; the DMN is active during resting state, but also during intrinsic processing like self-referential processing, monitoring of oneself, or rumination, and it gets deactivated if subjects are engaged in tasks with external cues (Greicius et al., 2003; Schneider et al., 2008; Sridharan et al., 2008).

The AIC and the ACC also share a unique anatomical feature, which is the presence of two specialized types of neurons: the VEN and the FN (Allman et al., 2010). The AIC and the ACC together with the VEN and FN have been proposed to play a role in interoceptive predictive coding (Critchley and Seth, 2012). The predictive coding model postulates that the brain is an adaptive system that strives to optimize homeostasis, counteract disorder, and minimize free energy (Friston, 2010). In order to achieve this, the brain is suggested to use internal generative models of the sensations caused by past somatosensory input from the body or the environment to predict upcoming events. Continuously generated predictions about the world, which are based on the generative models, are compared with actual incoming sensory signals. The brain aims to minimize the difference between the predictions (top-down signals) and the actual sensation (bottom-up signals), which is the so-called ‘prediction error’ (Barrett and Simmons, 2015). Prediction errors are permanently used to update the generative models in an endless flow of prediction error minimization (Friston, 2002; 2010). Furthermore, the integration of predictions with incoming sensory input has been considered to be fundamental for subjective awareness (Tononi and Koch, 2008). Such

a predictive coding model is also suggested for the processing of interoception. In this model, predictions about interoceptive input are generated and resulting prediction errors are used for homeostatic regulations (Barrett and Simmons, 2015). The AIC is proposed to constitute a cortical interface between the meta-representation of all bottom-up interoceptive activities and top-down predications from higher order cortical regions (e.g. ACC, PFC). It has been suggested that the communication between the AIC and the ACC is mediated by their specific population of VEN and FN, since, due to their long and large axons, they support rapid signal propagation (Craig, 2009b), which is necessary for the fast updating of the generative models (Critchley and Seth, 2012). They further mediate information exchange between the AIC and the ACC with distant targets, such as subcortical nodes responsible for autonomic control, like the periaqueductal gray (PAG), and the relay of afferent interoceptive input, like the parabrachial nucleus (PBN). The integration of top-down and bottom-up activation within the AIC, supported by VEN and FN, is proposed to be crucial for the generation of predictions that further drive autonomic effector systems to achieve homeostasis (Craig, 2009b; Uddin, 2015) and for the conscious perception of oneself (the 'material me'), the environment, and other people and their feelings. Thus, the AIC is suggested to be the underlying neural substrate for human (self-) awareness (Craig, 2009b).

Ontogeny of the insular cortex

In human corticogenesis, the insular cortex is one of the first cortices that develops and differentiates. Its development starts already in the sixth gestational week (GW), in approximately the region that will eventually become the limen insula. In the 13-18th GWs, the demarcation of the insular cortex by the peri-insular limiting sulci and the central insular sulcus occurs. The growth of the insular cortex is slower than the surrounding structures, hence, starting at the 20th GW, the insular cortex is buried deep within the lateral fissure by progressively being covered by the frontal, the parietal, and the temporal opercula. In the early development of the telencephalon, the insular cortex is a lissencephalic structure located on the lateral surface of the left and right hemisphere. The insular sulci start to define only in the 20-22th GWs. Growth and development of the insular cortex are asymmetrical, with a right-sided dominance. At

birth, the insular gyral and sulcal pattern is almost the same as in adulthood (Afif et al., 2007; Cunningham, 1891; Haller, 1906).

Von Economo and Fork neurons

Morphology

As mentioned above, the human and macaque AIC and ACC harbor two specialized neuronal morphotypes the VEN and the FN (Allman et al., 2010; Evrard et al., 2012). Both neurons are cortical layer 5b projection neurons with atypical morphology, based on which they can be distinguished from the typical pyramidal neurons (PN). The von Economo neuron has an elongated spindle-shaped perikaryon oriented radially towards the cortical surface with a thick apical dendrite and an equally thick and unique basal dendrite and a central nucleus with several nucleoli. VEN and FN have a small number of dendritic spines and the basal dendrite has a narrow dendritic arborization spanning the cortical layers but missing the typical basal tuft of PN (Nimchinsky et al., 1999; von Economo, 1926; Watson et al., 2006). They have been named von Economo neurons after Constantin von Economo, who provided their first detailed description (Allman et al., 2005; von Economo, 1926). However, earlier documentation by many classical neuroanatomists exists that states the presence of these neurons. (Betz, 1881; Ramón y Cajal, 1901-1902; Vogt and Vogt, 1919). The fork neuron, which is systematically accompanying the VEN, has a triangular perikaryon, which is prolonged by a thick basal dendrite and a bifid or 'forked' apical dendrite that is responsible for its name (Ngowyang, 1932). In humans and macaque monkeys, VEN and FN are larger than their neighboring PN and larger than the fusiform cells in cortical layer 6. Furthermore, human VEN and FN are slightly bigger than macaque VEN and FN (Evrard et al., 2012; Nimchinsky et al., 1999; Nimchinsky et al., 1995).

Localization

Across all primate species described to possess VEN and FN, like humans, great apes, or macaque monkeys, the highest densities of these neurons have been found in humans and African great apes (chimpanzee, bonobo, gorilla) (Allman et al., 2010;

Evrard et al., 2012; Nimchinsky et al., 1999). In the human cortex, the highest concentration of these two special neuronal morphotypes has been discovered in the ventral agranular AIC, called frontoinsula (FI) and in a rostrocaudal gradient within the ACC. In macaque monkeys, the highest number of VEN and FN was found in the ventral agranular AIC and, to a lesser extent, in the ACC (Allman et al., 2010; Evrard et al., 2012; von Economo, 1925). However, smaller numbers have also been found in other limbic areas, such as the entorhinal cortex and the subiculum (Ngowyang, 1932), the superior frontal cortex (Brodmann area 9) (Fajardo et al., 2008; Nimchinsky et al., 1999), and the medial portion of the frontal pole (Brodmann area 10) (Gonzalez-Acosta et al., 2018). Within the macaque AIC and the human FI, VEN and FN are forming one or more clusters, respectively, that are regionally limited instead of being broadly dispersed over the entire AIC (Evrard et al., 2012; Nimchinsky et al., 1999; Ramón y Cajal, 1901-1902; Seeley et al., 2006). Within the framework of this thesis, the VEN and FN cluster were systematically observed in and around a distinct curvature directly anterior to the limen insula, which is similar to the primary localization of VEN and FN at the crown of the gyri in most other species containing VEN and FN (see below) (Allman et al., 2010; Raghanti et al., 2015). In macaque monkeys, a second cluster of VEN and FN was present in and around the mound area of the dysgranular insular cortex (DIC), posterior to the limen insula. In the human FI, the VEN and FN were distributed over five distinct architectonic areas; this shows not only an enlargement but also a multiplication of the VEN areas. My in-depth examinations of the cyto- and myeloarchitectonic organization of the AIC and the DIC in both macaque species and the FI in humans revealed that the VEN and FN cluster(s) were consistently overlapping with sharp architectonic borders. The exact distribution of VEN and FN within the macaque AIC and DIC and the human FI is described in more detail in the attached manuscripts. Likewise, preliminary examinations of other primates such as lesser apes (e.g. gibbon), old world monkeys (e.g. baboon) and new world monkeys (e.g. spider monkey), as well as chimpanzees and orangutans are suggesting the limitation of these neurons to one architectonic area within the AIC (Evrard et al., in preparation). The regional cortical limitation of VEN and FN within the primate AIC was also similar in great apes, dolphins, whales, and elephants. All these species have big and highly encephalized brains and complex social behavior (Butti et al., 2011; Butti et al., 2009; Hakeem et al., 2009; Hof and Van der Gucht, 2007). Therefore, these neurons were initially suggested to play a role in interoceptive processes involved in social

interactions (Butti et al., 2011; Butti et al., 2009; Hakeem et al., 2009; Hof and Van der Gucht, 2007). More recently, VEN and FN were also found in some other species, such as sheep, pig, cow, deer, horse, rock hyrax, and pygmy hippopotamus, indicating that these neurons are not limited to species with big brains and complex social behavior. In these species, the distribution of VEN and FN was either limited to specific cortical regions (e.g. cow) or ubiquitously dispersed over the entire cortex (pygmy hippopotamus, common zebra) (Butti and Hof, 2010; Raghanti et al., 2015). However, these two neurons are not permanently present throughout phylogeny. Therefore it seems that VEN and FN either evolved repeatedly and independently or form an ancestor mammalian neuron that has been lost in several species (Hakeem et al., 2009; Raghanti et al., 2010).

Evidence for implication in long-distance excitatory projections

The VEN and the FN have been proposed to be atypical excitatory projection neurons with distant targets since they are immunoreactive for the non-phosphorylated filament protein SMI-32, which is typically expressed in pyramidal neurons with long-range distance projections (Hof et al., 1995; Nimchinsky et al., 1995). Furthermore, connectivity studies in humans and macaque monkeys showed that within the human ACC, VEN were retrogradely labeled by injections of a lipophilic dye in the cingulum bundle (Nimchinsky et al., 1995). In macaque monkeys, VEN of the AIC have been shown to project to the ACC, the ipsilateral mid-insula, and the contralateral AIC (Evrard et al., 2012). However, even stronger labelling has been produced by retrograde tracers injected into the subcerebral nuclei PAG and PBN, pivotal homeostatic centers in the midbrain and brainstem, respectively, suggesting that the main projection targets of VEN and FN are rather subcerebral regions (Evrard H.C. et al., *in preparation*). This is supported by the fact that VEN and FN express the transcription factors FEZF2, which are key regulators for the fate and differentiation of cortical layer 5 neuronal subtypes that project to subcerebral and callosal targets (Cobos and Seeley, 2015; Harb et al., 2016). Only recently resting-state functional connectivity MRI studies in humans with coma-causing lesions in the brainstem indicated that the left insular VEN area is functionally connected to the PBN (Fischer et al., 2016).

The excitatory nature of VEN and FN is indicated by their use of glutamate as their major output neurotransmitter (Dijkstra et al., 2018; Evrard et al., 2012). In addition to the evidence for glutamate synthesis, VEN and FN are entirely devoid of typical cortical interneuron markers such as Calbindin, Calretinin, and Parvalbumin, which are characteristic markers for GABAergic interneurons in the cerebral cortex (Hendry et al., 1989; Hof and Nimchinsky, 1992). The voluminous size and large diameter axons of VEN and FN, enabling fast conduction speeds, as well as their bipolar morphology, suggest that they are specialized for a rapid integration and relay of simple rather than detailed information to distant target regions across large brains (Allman et al., 2010; Evrard et al., 2012). The connectivity pattern of these neurons in humans and macaque monkeys still needs further exploration, but the connectivity patterns in both species are suggested to be similar (Evrard et al., 2012; Fischer et al., 2016).

Evidence for implication in feeding, homeostatic, and neuro-modulatory functions

VEN and FN express several genes that are involved in the regulation of food processing and immune functions. These genes code for proteins including neuromedin B (NMB), gastrin-releasing peptide (GRP), activating-transcription factor 3 (ATF3), and interleukin 4 receptor (IL4Rα) (Allman et al., 2010; Stimpson et al., 2011). NMB and GRP are expressed, amongst other regions, in the gut and the brain and are involved in the regulation of the gastrointestinal tract (GI) activity: in the gut they play a role in processes like the release of digestive stomach enzymes, and in brain areas such as the insula they participate in gut control, digestive processes and appetite, and have powerful effects on immune cells and thus, the immune responses (Allman et al., 2010; Jensen et al., 2008). ATF3 is a protein known to be involved in cellular stress responses and, in spinal cord neurons, it controls sensitivity to pain (Chen et al., 1996; Latremoliere et al., 2008). Hence, AFT3-expression in VEN may indicate their involvement in pain sensitivity (Stimpson et al., 2011). IL4Rα is a receptor involved in immune responses to allergens and inflammatory reactions in the brain (Watanabe et al., 2008). Taken together, the VEN's and FN's gene expression profile suggests a role in the control of food intake, the modulation of autonomic responses, and in the monitoring of the gut and the homeostatic state of the individual's body (Allman et al., 2010; Stimpson et al., 2011). Furthermore, it is known that VEN and FN express genes

that are coding for neurotransmitter receptors implicated in social behavior and reward processing, such as the dopamine d3 receptor, the serotonin 2b receptor (5ht2br), and vasopressin 1a receptor (AVPR1A), as well as a protein associated with psychiatric diseases: the disrupted-in-schizophrenia-1 (DISC-1). DISC-1 is mostly expressed in the soma and dendrites of VEN and has been shown to reduce the branching of the secondary and tertiary dendrites, which could be causal for the lack of higher order branching in these neurons (Allman et al., 2010; Allman et al., 2005; Duan et al., 2007). These gene expression profiles underpin the hypothesis that VEN and FN are involved in the conscious perception of sensations that are arising from the body and eventually are generating cognitive feelings such as "gut feelings" or "intuition", which are crucial for conscious decision-making, especially in uncertain situations (Allman et al., 2005). VEN and FN also express the neurotransmitter-related genes vesicular monoamine transporter 2 (VMAT2), GABA receptor subunit θ (GABRQ), and adrenoreceptor α-1A (ADRA1A). These receptors are predominantly expressed by VEN and FN and only by a small subpopulation of the neighboring PN. The expression of these receptors suggests a specialized role for VEN and FN in cortical monoaminergic neurotransmission and autonomic functions (Dijkstra et al., 2018).

Ontogeny of the VEN and FN

Several studies on the ontogeny, morphology, and allocation of VEN and FN in humans and great apes by John Allman and colleagues (Allman et al., 2010, Allman et al., 2011, Allman et al., 2005) found that these two neurons appear in both the AIC and ACC in the late prenatal period, particularly in the 35th GW. At birth, the numbers of VEN and FN are low, only about 15% of the total number, but they increase postnatally. Eight months after birth, they reach a peak but the numbers than decrease again in some regions and at the age of four years, when the adult number of VEN and FN is attained, remain relatively constant. It is still unknown, whether these neurons migrate into the AIC and ACC during the postnatal development or if they emerge after birth by differentiation. In neonates, the number of VEN and FN in the FI is similar in both hemispheres; however, postnatally the distribution becomes asymmetric, with a higher number of these neurons on the right hemisphere. In the ACC, there is no such

asymmetry, and the adult number is similar to that at eight months (Allman et al., 2010; Allman et al., 2011; Allman et al., 2005).

Involvement of insular cortex and VEN in pathology

Insular cortex and neuropathological implications

The insular cortex and the ACC are the most common neuronal brain sites that are affected in a broad diversity of neuropsychiatric and neurodegenerative disorders (Goodkind et al., 2015; Nagai et al., 2007). As mentioned above, the insular cortex has been proposed to integrate interoceptive feelings with emotional, hedonic, homeostatic, and environmental activity represented in other brain regions. This integration eventually engenders subjective feeling states, mediates behavior, and shapes cognitive processes and emotions. The insula's engagement in manifold processes is further indicated by clinical studies.

Lesion studies, which provide means of evaluating the numerous insular functions, proposed different symptoms depending on the site of insular damage (Jones et al., 2010). Lesions within the posterior insula have been shown to affect the representation of interoceptive afferents such as changes in temperature (Baier et al., 2014; Jones et al., 2010). Another study examined stroke patients with anosognosia for hemiplegia/hemiparesis and showed that lesions in the right posterior insula were linked to deficits in the sense of agency and body ownership (Karnath and Baier, 2010; Karnath et al., 2005). These studies support the proposed role of the posterior insula in the representation of somatosensory, proprioceptive, and mechanoreceptive activity and the representation of the body scheme (Karnath and Baier, 2010; Mesulam and Mufson, 1985; Schneider et al., 1993). In contrast, a case report showed the loss of speech comprehension and emotions that are produced by music after damage in the anterior insula (Griffiths et al., 2004). A different study showed that patients with anterior insular cortex lesions revealed significantly impaired discrimination accuracy to others' pain (Gu et al., 2012). Hence, these and other studies suggest that lesions in the anterior insula are associated with social and emotional deficits and language disturbances (Jones et al., 2010).

In addition, multiple psychiatric and neurodegenerative disorders with atypical feeling states accompanied by impaired social-emotional behaviors, have been

attributed to insular dysfunctions and gray matter alterations. One frequently studied mental disorder involving the insular cortex is schizophrenia, a psychotic disorder characterized by distorted social-emotional behaviors. Schizophrenic patients suffer from several positive symptoms, such as hallucinations, hearing of voices, and mostly paranoid delusions, as well as negative symptoms like anergia, social withdrawal, emotional blunting, and loss of experiencing pleasure (Brune et al., 2011; Schultz et al., 2007). In first-episode and chronic schizophrenia patients or patients with schizophreniform disorders, several neuroimaging studies showed a reduction of gray matter volume in mostly the left or bilateral insular cortex, as well as alterations in the number, distribution, and morphology of VEN and FN (see below) (Crespo-Facorro et al., 2000; Goldstein et al., 1999; Wright et al., 1999); for review see also (Nagai et al., 2007). It is assumed that dysfunctions of the AIC contribute to the symptoms in schizophrenic patients since they show an increase of AIC activation during auditory hallucinations and psychotic symptoms (Shergill et al., 2000; Surguladze et al., 2001). Non-psychotic mood disorders, such as depression (major depressive disorder; MDD) and bipolar disorder, are also associated with altered insular functions and a reduction of volume and gray matter density in the AIC. Likewise, gray matter volume reduction was measurable in first episodes of depression in MDD and bipolar disorder (Lai and Wu, 2014; Stratmann et al., 2014; Takahashi et al., 2010; Wise et al., 2017); for review see also (Sliz and Hayley, 2012).

Addictive disorders like alcoholism, cigarette craving, and other types of addiction to drugs like cocaine or heroin were negatively correlated with gray matter volume in the AIC (Franklin et al., 2002; Gardini and Venneri, 2012; Makris et al., 2008; Morales et al., 2014; Moreno-Lopez et al., 2012; Naqvi et al., 2014; Sutherland et al., 2016). In Anorexia nervosa, no morphological change of the insular cortex has been reported; however, in anorexic patients, a disconnection or dysfunction of the insular cortex is proposed to alter the integration and regulation of interoceptive, sensory, autonomic, and emotional stimuli leading to abnormal visual and subjective perception of one's body (Nunn et al., 2008). Functional and structural deficiencies have also been implicated in anxiety. It is assumed that altered activity of the AIC and ACC lead to increased anxiety and panic levels due to heightened interoceptive awareness. It is furthermore suggested that increased sensitivity of bodily feelings or their misinterpretation might be crucial to anxiety and panic attacks (Clark et al., 1997; Paulus and Stein, 2010; Terasawa et al., 2013). Furthermore, in several types of

dementia e.g. Alzheimer's Disease (AD), behavioral variant of the frontotemporal dementia (bvFTD), insular cortex pathology has been associated with the missing sense of the self. In neurodegenerative diseases like multiple sclerosis (MS) or Huntington's disease (HD) insular cortex pathology has been linked to emotional dysfunctions (MS, HD) (Loffler et al., 2016; Seeley et al., 2006).

As mentioned before, the AIC has multiple reciprocal connections with corticolimbic structures (e.g. ACC, amygdala) and components of the reward circuit (e.g. ventral striatum, nucleus accumbens, orbitofrontal cortex) that are important for the processing of errors, interoceptive prediction signals, anticipation, salient stimuli, motivation to reward stimuli, action planning, and assessment of the environmental stimuli in relation to the context. The AIC is suggested to constitute a hub of meta-awareness, which is crucial for the integration of all transient salient stimuli, interoceptive and autonomic feeling states; it is also suggested to play a role in the evaluation of the possible impact of these stimuli on the self (Paton et al., 2006; Paulus and Stein, 2006; Simmons et al., 2004; Simmons et al., 2006; Terasawa et al., 2013). Alterations in the processes the insula is involved in and dysfunctions of the insula are probably based on gray matter volume reduction and decreased functional connectivity. The role of the AIC in the generation of emotion, motivation, and particularly addiction is further supported by the high concentration of several receptors in the AIC, such as dopamine receptors D1, μ-opioid receptors, and corticotropin releasing factor 1 receptor. These receptors may support the insula's involvement in pain modulation, reward effects by drug abuse, and stress related motivation to take drugs (Baumgartner et al., 2006; Hurd et al., 2001; Sanchez et al., 1999). All the pathological changes in the AIC and the VEN and the FN could result in abnormal feeling states, impaired social-emotional behavior, and disturbed affective processing in multiple mental disorders (Goodkind et al., 2015; Nagai et al., 2007; Namkung et al., 2017).

VEN and FN in pathology

VEN and FN play a role in several neuropsychiatric diseases that lead to distortion in social and emotional behavior. Studying the role of these neurons in clinicopathological conditions was driven by William Seeley's findings of specific VEN and FN alterations in brains of bvFTD patients, investigated post mortem (Seeley

et al., 2006; Seeley et al., 2008; Seeley et al., 2012). bvFTD is a neurodegenerative syndrome that engenders distorted social behavior (e.g. empathy and moral sensibility) and metacognitive judgment, as well as a loss of self-conscious emotions and experiences, and theory of mind, (Butti et al., 2013; Kim et al., 2012; Seeley, 2008). bvFTD is an early age-of-onset type of dementia that appears in the fifth or sixth decade of life and is characterized by progressive gray matter atrophy in the orbital prefrontal cortex and, in particular, the FI and the ACC. Both are regions harboring high concentrations of VEN and FN (Kim et al., 2012; Rosen et al., 2002; Seeley, 2008; Seeley et al., 2006). It is suggested that the beginning of the syndrome starts with the focal degeneration of the FI and the ACC before spreading to the rostral forebrain (Broe et al., 2003). The depletion of VEN and FN in the FI and the ACC occurs in a very early stage when deficits in social-emotional behavior start to appear. In bvFTD patients, the number of VEN and FN was reduced by 60%, whereas the local PN numbers were not affected. The few VEN and FN that did not perish revealed prominent morphological alterations. In AD, VEN and FN are not targeted in the early stages; however, in the late stages, there are discrepancies in the literature regarding the theory if they are affected or not (Gefen et al., 2018; Kim et al., 2012). In bvFTD it has been shown that the severity of the symptoms was correlated with the stage of VEN and FN degeneration as well as anatomical and functional changes of the VEN and FN (Kim et al., 2012; Seeley et al., 2008). The correlation between the bvFTD severity and VEN and FN degeneration along with their location in two key regions of a network that incorporates social-emotional, visceral-autonomic, and cognitive information, suggest a role of these neurons in the integration of this information and in generating awareness of subjective feelings (Craig, 2009b; Kim et al., 2012; Seeley, 2008).

VEN and FN are also selectively reduced in agenesis of the corpus callosum (AgCC), another neurological disorder that is characterized by deficits in empathy, social judgment, self- and social awareness, impaired humor, and problems in the comprehension of affective and figurative language (Kaufman et al., 2008). Post-mortem stereological analyses of brains with partial or complete AgCC showed a significant reduction of VEN and FN in relation to the total number of neurons in the FI and the ACC. The degree of callosal agenesis correlated with the degree of VEN and FN reduction, while ischemic or stroke-induced lesion in the corpus callosum did not affect the number of VEN and FN. Furthermore, the symptoms described in patients

with AgCC do not manifest themselves in patients with an injured corpus callosum caused by stroke (Allman et al., 2010; Kaufman et al., 2008).

Early-onset schizophrenia, a subgroup of schizophrenia, has also been linked to alterations in VEN and FN in the ACC; Brune and colleagues found a reduction of VEN within the ACC in the post-mortem brains of patients who had diagnoses of that type of schizophrenia (Brune et al., 2011).

Furthermore, VEN and FN express DISC-1, a protein which plays a crucial role in neuron migration during development and signaling processes and is proposed to be involved in enhanced cognitive abilities in humans (Allman et al., 2010; Soares et al., 2011). Studies on the interaction between DISC-1 and other proteins have shown that it is involved in many pathways that are relevant in neuropsychiatric disorders, such as depression, bipolar disorder, and schizophrenia; it, therefore constitutes a risk factor for neuropsychiatric disorders (Soares et al., 2011). It is suggested that VEN and FN, as well as DISC-1, have undergone evolutionary modifications and are therefore more vulnerable to dysfunctions appearing in various neuropsychiatric disorders (Allman et al., 2010).

Patients with autism spectrum disorders present a wide range of social, emotional, and introspective distortions. Therefore, VEN and FN were also examined in post-mortem brains of autistic patients. Several studies comparing the number of VEN and FN within the AIC and ACC suggested a dichotomy in VEN numbers in autistic patients: Kennedy and his team reported no difference in the total number or morphology of VEN and FN in the FI in autistic patients (Kennedy et al., 2007). Another neuropathological examination of VEN and FN in autistic children showed an increased ratio of both neurons compared to local PN and alterations in the distribution and morphology of VEN and FN in the FI (Santos et al., 2011). A further group, who analyzed VEN and FN in the ACC of post-mortem brains of autistic patients, found an increase of both neurons in one subgroup of patients and a decreased number of the same compared to PN in another subgroup. Furthermore, they also described alterations in the aforementioned gradual rostrocaudal distribution of VEN and FN within the cingulate cortex (Simms et al., 2009). Variations in the number of these neurons could be related to the distorted discrimination between oneself and others and between oneself and the external world (Allman et al., 2005).

Conversely, in suicide victims, the number of VENs in the ACC was increased (Brune et al., 2011). In ‘SuperAgers’ (80+) individuals, who maintained unusually good

cognitive performances, the number of VEN was significantly higher compared to average 80+year-old controls and individuals with mild cognitive impairment stage of AD. Their performance in episodic memory tests was better than or equal to healthy 50-60-year-olds. In SuperAgers, the cortical thickness of the ACC was also increased compared to their cognitively average 80+ year-old peers and compared to healthy 20-30 years younger individuals (Gefen et al., 2015; Rogalski et al., 2013).

The alterations in the VEN and FN number in several neuropsychiatric and neurodegenerative disorders, such as bvFTD, AgCC, schizophrenia, and autism - all sharing impaired social-emotional and self-related behavior - suggest a crucial contribution of these neurons in the processing of internal bodily states with social, emotional and cognitive information (Allman et al., 2005; Kaufman et al., 2008; Kim et al., 2012; Santos et al., 2011; Seeley et al., 2006).

Research Aims

Most of the research reviewed in the preceding section focused on the organization and function of the primate insular cortex and its specialized neurons, the VEN and FN. The parcellation of the insular cortex in macaque monkeys (Evrard et al., 2014) and in humans (Kurth et al., 2010) is in line with the theory of a parcellation of the entire cerebral cortex into small functional units with unique architecture and connections (Northcutt and Kaas, 1995). A high parcellation is proposed to reflect the capacity for enhanced cortical processing (Kaas, 2011). The differences between cortical areas presenting themselves in distinct connectivity patterns with other brain areas, distinct neuron densities, distinct laminar and fibrous structures, distinct densities of (transmitter) receptors, and distinct cellular structures (Kaas, 2011; Luppino et al., 1991; Zilles et al., 2002; Zilles et al., 2004). Several authors researching the insular cortex in humans described that the VEN and FN co-occur within small clusters, rather than being distributed broadly throughout the AIC (Evrard et al., 2012; Nimchinsky et al., 1999; Ramón y Cajal, 1901-1902; Seeley et al., 2006).

The VEN and FN are linked to social-emotional cognition, interoception, and autonomic regulations (Craig, 2009b; Seeley et al., 2006; von Economo, 1926) and they are involved in several neuropsychiatric illnesses characterized by a distortion of social and emotional behavior (Kaufman et al., 2008; Kim et al., 2012; Seeley et al., 2006). The exact function of these neurons is uncertain as of yet; however, understanding the relationship between them and their localization could be crucial in disclosing their overall role in the brain. Therefore, the first study in this body of work addresses the relationship between the distribution of the VEN and FN with the architectonic areas of the anterior insula in two species of macaque monkeys. The hypothesis of this study was that there is a robust relationship, a so-called elemental localization (EL) (Brodmann, 1909), between these neurons and one particular architectonic area in the macaque AIC. The EL suggests a common evolutionary and developmental fate, hodological pattern, and function; it offers an opportunity to examine the function of neurons by invasively studying the entire area for example with microelectrode recordings, functional imaging, and tracer injections into the VEN area.

The macaque ventral AIC, including the VEN area Ial, as well as the ventral and mound dysgranular - but not the dorsal dysgranular and granular insula insular cortex -

are heavily and mainly connected with cortical and subcortical limbic regions like the basal and lateral nuclei of the amygdala, ventral striatum, including the shell of the nucleus accumbens, and the limbic ACC (Chikama et al., 1997; Mufson et al., 1981; Stefanacci and Amaral, 2000). In addition to the similar connectivity profiles, both regions also have in common the presence of a prominent cortical convexity or mound. Our previous study revealed the localization of the VEN and FN mainly in and around this mound area in the AIC (Horn, F.M & Evrard, H.C, *in preparation*). Therefore, the second study examined the presence of VEN and FN, as well as the cyto- and myeloarchitecture, in the ventral and mound areas of the dysgranular insula in two species of macaque monkeys. It is hypothesized that the previously defined mound dysgranular area of the insula (Idm) also harbors clusters of VEN and FN. The finding of another EL within the macaque insula may help to identify the function of the VEN and FN and their host areas and by that increase the understanding of the functional organization of the insula.

Human subjective awareness of feelings and oneself seems to have no direct functional homolog in macaque monkeys. It has been suggested that the unique cognitive evolution in the human lineage might have emerged with neuroanatomical modifications such as a larger volume and higher parcellation of the cortex. Cytoarchitecture based volumetric histological analyses across primates revealed that in humans the insular cortex, and in particular the AIC, grew hyperallometrically in relation to the entire brain (Bauernfeind et al., 2013). Hence, the third study takes up the question whether the VEN and FN containing region within the FI in humans constitutes the enlarged but identical architectonic area as in macaque monkeys, or whether there are multiple distinct architectonic areas containing VEN and FN. Based on preliminary examinations, it was hypothesized that in the human FI there are at least three or more different architectonic areas. Comparison of the organization of the AIC, and in particular the VEN areas in primates, could contribute to the understanding of the neuroanatomical basis underlying the increased complexity and refinement of the unique cognitive capacities in healthy humans as well as to the understanding of malfunctions in the insular cortex in the diseased brain.

Abbreviations

ACC	Anterior cingulate cortex
AD	Alzheimer's Disease
AgCC	Agenesis of the corpus callosum
AIC	Anterior insular cortex
ALS	Anterior peri-insular sulcus
bvFTD	behavioral variant of the frontotemporal dementia
CBP	Calcium-binding proteins
CEN	Central-executive network
DIC	Dysgranular insular cortex
DISC-1	Disrupted-in-schizophrenia 1
DMN	Default mode network
EL	Elemental localization
FI	Frontoinsula
FN	Fork neuron
GABA	Gamma-Aminobutyric acid
Iai	Intermediate agranular area of the insula
Ial	Lateral agranular area of the insula
Iam	Medial agranular area of the insula
Iap	Posterior agranular area of the insula
Iapl	Posterior-lateral agranular area of the insula
Iapm	Posterior-medial agranular area of the insula
Idm	Mound dysgranular area of the insula
Idfa	Anterior area of the dorsal fundus of the insula
Idfp	Posterior area of the dorsal fundus of the insula
Igd	Dorsal granular insula
Igv	Ventral granular insula
IPS	Inferior peri-insular sulcus

Ivfa	Anterior area of the ventral fundus of the insula
NTS	Nucleus tractus solitarii, or solitary nucleus
PAG	Periaqueductal gray
PBN	Parabrachial nucleus
PIC	Primary interoceptive cortex
PN	Pyramidal neuron
SN	Salience network
SPS	Superior peri-insular sulcus
VEN	Von Economo neuron
VMpo	Ventromedial posterior nucleus of the thalamus
VMb	Ventral medial nucleus of the thalamus
VTA	Ventral tegmental area

References

Afif A, Bouvier R, Buenerd A, Trouillas J, Mertens P. 2007. Development of the human fetal insular cortex: study of the gyration from 13 to 28 gestational weeks. Brain Struct Funct 212(3-4):335-346.

Afif A, Mertens P. 2010. Description of sulcal organization of the insular cortex. Surg Radiol Anat 32(5):491-498.

Allman JM, Tetreault NA, Hakeem AY, Manaye KF, Semendeferi K, Erwin JM, Park S, Goubert V, Hof PR. 2010. The von Economo neurons in frontoinsular and anterior cingulate cortex in great apes and humans. Brain Struct Funct 214(5-6):495-517.

Allman JM, Tetreault NA, Hakeem AY, Park S. 2011. The von Economo Neurons in Apes and Humans. Am J Hum Biol 23(1):5-21.

Allman JM, Watson KK, Tetreault NA, Hakeem AY. 2005. Intuition and autism: a possible role for Von Economo neurons. Trends Cogn Sci 9(8):367-373.

Augustine JR. 1996. Circuitry and functional aspects of the insular lobe in primates including humans. Brain Res Brain Res Rev 22(3):229-244.

Baier B, zu Eulenburg P, Geber C, Rohde F, Rolke R, Maihofner C, Birklein F, Dieterich M. 2014. Insula and sensory insular cortex and somatosensory control in patients with insular stroke. Eur J Pain 18(10):1385-1393.

Barbas H, Pandya DN. 1989. Architecture and intrinsic connections of the prefrontal cortex in the rhesus monkey. J Comp Neurol 286(3):353-375.

Barrett LF, Simmons WK. 2015. Interoceptive predictions in the brain. Nat Rev Neurosci 16:419.

Bartels A, Zeki S. 2004. The neural correlates of maternal and romantic love. Neuroimage 21(3):1155-1166.

Bauernfeind AL, de Sousa AA, Avasthi T, Dobson SD, Raghanti MA, Lewandowski AH, Zilles K, Semendeferi K, Allman JM, Craig AD, Hof PR, Sherwood CC. 2013. A volumetric comparison of the insular cortex and its subregions in primates. J Hum Evol 64(4):263-279.

Baumgartner T, Gianotti LR, Knoch D. 2013. Who is honest and why: baseline activation in anterior insula predicts inter-individual differences in deceptive behavior. Biol Psychol 94(1):192-197.

Baumgartner U, Buchholz HG, Bellosevich A, Magerl W, Siessmeier T, Rolke R, Hohnemann S, Piel M, Rosch F, Wester HJ, Henriksen G, Stoeter P, Bartenstein P, Treede RD, Schreckenberger M. 2006. High opiate receptor binding potential in the human lateral pain system. Neuroimage 30(3):692-699.

Betz WA. 1881. Ueber die feinere Structur der Gehirnrinde des Menschen. Centralblatt fuer die Medicinischen Wissenschaften 19:193-195, 209-234.

Brockhaus H. 1940. Die Cyto-und Myeloarchitektonik des Cortex claustralis und des Claustrum beim Menschen. Journal für Psychologie und Neurologie 49:249-348.

Brodmann K. 1909. Vergleichende Lokalisationslehre der Grosshirnrinde in ihren Prinzipien dargestellt und Grund des Zellenbaues. Leipzig: Verlag von Johann Ambrosius Barth.

Broe M, Hodges JR, Schofield E, Shepherd CE, Kril JJ, Halliday GM. 2003. Staging disease severity in pathologically confirmed cases of frontotemporal dementia. Neurology 60(6):1005-1011.

Brune M, Schobel A, Karau R, Faustmann PM, Dermietzel R, Juckel G, Petrasch-Parwez E. 2011. Neuroanatomical correlates of suicide in psychosis: the possible role of von Economo neurons. PLoS One 6(6):e20936.
Burton H, Fabri M, Alloway K. 1995. Cortical Areas within the Lateral Sulcus Connected to Cutaneous Representations in Area-3b and Area-1 - a Revised Interpretation of the 2nd Somatosensory Area in Macaque Monkeys. Journal of Comparative Neurology 355(4):539-562.
Butti C, Hof PR. 2010. The insular cortex: a comparative perspective. Brain Structure & Function 214(5-6):477-493.
Butti C, Raghanti MA, Sherwood CC, Hof PR. 2011. The neocortex of cetaceans: cytoarchitecture and comparison with other aquatic and terrestrial species. Ann N Y Acad Sci 1225:47-58.
Butti C, Santos M, Uppal N, Hof PR. 2013. Von Economo neurons: clinical and evolutionary perspectives. Cortex 49(1):312-326.
Butti C, Sherwood CC, Hakeem AY, Allman JM, Hof PR. 2009. Total number and volume of Von Economo neurons in the cerebral cortex of cetaceans. J Comp Neurol 515(2):243-259.
Campbell AW. 1904. Histological Studies on the Localisation of Cerebral Function. Journal of Mental Science 50 (211):651-662.
Carmichael ST, Price JL. 1994. Architectonic subdivision of the orbital and medial prefrontal cortex in the macaque monkey. J Comp Neurol 346(3):366-402.
Chen BPC, Wolfgang CD, Hai TW. 1996. Analysis of ATF3, a transcription factor induced by physiological stresses and modulated by gadd153/Chop10. Mol Cell Biol 16(3):1157-1168.
Chikama M, McFarland NR, Amaral DG, Haber SN. 1997. Insular cortical projections to functional regions of the striatum correlate with cortical cytoarchitectonic organization in the primate. J Neurosci 17(24):9686-9705.
Clark DM, Salkovskis PM, Ost LG, Breitholtz E, Koehler KA, Westling BE, Jeavons A, Gelder M. 1997. Misinterpretation of body sensations in panic disorder. J Consult Clin Psychol 65(2):203-213.
Cobos I, Seeley WW. 2015. Human von Economo Neurons Express Transcription Factors Associated with Layer V Subcerebral Projection Neurons. Cerebral Cortex 25(1):213-220.
Craig AD. 2002. How do you feel? Interoception: the sense of the physiological condition of the body. Nat Rev Neurosci 3(8):655-666.
Craig AD. 2009a. Emotional moments across time: a possible neural basis for time perception in the anterior insula. Philos T R Soc B 364(1525):1933-1942.
Craig AD. 2009b. How do you feel - now? The anterior insula and human awareness. Nat Rev Neurosci 10(1):59-70.
Craig AD. 2014. Topographically Organized Projection to Posterior Insular Cortex From the Posterior Portion of the Ventral Medial Nucleus in the Long-Tailed Macaque Monkey. Journal of Comparative Neurology 522(1):36-63.
Craig AD, Bushnell MC, Zhang ET, Blomqvist A. 1994. A thalamic nucleus specific for pain and temperature sensation. Nature 372(6508):770-773.
Craig AD, Chen K, Bandy D, Reiman EM. 2000. Thermosensory activation of insular cortex. Nat Neurosci 3(2):184-190.
Crespo-Facorro B, Kim J, Andreasen NC, O'Leary DS, Bockholt HJ, Magnotta V. 2000. Insular cortex abnormalities in schizophrenia: a structural magnetic resonance imaging study of first-episode patients. Schizophr Res 46(1):35-43.

Critchley H, Seth A. 2012. Will studies of macaque insula reveal the neural mechanisms of self-awareness? Neuron 74(3):423-426.
Critchley HD, Mathias CJ, Dolan RJ. 2002. Fear conditioning in humans: the influence of awareness and autonomic arousal on functional neuroanatomy. Neuron 33(4):653-663.
Critchley HD, Wiens S, Rotshtein P, Ohman A, Dolan RJ. 2004. Neural systems supporting interoceptive awareness. Nat Neurosci 7(2):189-195.
Crottaz-Herbette S, Menon V. 2006. Where and when the anterior cingulate cortex modulates attentional response: combined fMRI and ERP evidence. J Cogn Neurosci 18(5):766-780.
Cunningham DJ. 1891. Development of the Gyri and Sulci on the Surface of the Island of Reil of the Human Brain. J Anat Physiol 25(Pt 3):338-348.
Damasio AR, Grabowski TJ, Bechara A, Damasio H, Ponto LL, Parvizi J, Hichwa RD. 2000. Subcortical and cortical brain activity during the feeling of self-generated emotions. Nat Neurosci 3(10):1049-1056.
Devue C, Collette F, Balteau E, Degueldre C, Luxen A, Maquet P, Bredart S. 2007. Here I am: the cortical correlates of visual self-recognition. Brain Res 1143:169-182.
Dijkstra AA, Lin LC, Nana AL, Gaus SE, Seeley WW. 2018. Von Economo Neurons and Fork Cells: A Neurochemical Signature Linked to Monoaminergic Function. Cerebral Cortex 28(1):131-144.
Dosenbach NU, Visscher KM, Palmer ED, Miezin FM, Wenger KK, Kang HC, Burgund ED, Grimes AL, Schlaggar BL, Petersen SE. 2006. A core system for the implementation of task sets. Neuron 50(5):799-812.
Downar J, Crawley AP, Mikulis DJ, Davis KD. 2002. A cortical network sensitive to stimulus salience in a neutral behavioral context across multiple sensory modalities. J Neurophysiol 87(1):615-620.
Duan X, Chang JH, Ge S, Faulkner RL, Kim JY, Kitabatake Y, Liu XB, Yang CH, Jordan JD, Ma DK, Liu CY, Ganesan S, Cheng HJ, Ming GL, Lu B, Song H. 2007. Disrupted-In-Schizophrenia 1 regulates integration of newly generated neurons in the adult brain. Cell 130(6):1146-1158.
Evrard HC. 2019. The Organization of the Primate Insular Cortex. Frontiers in Neuroanatomy 13(43).
Evrard HC, Craig AD. 2015. Insular cortex. Brain Mapping: An Encyclopedic Reference: Elsevier. p 387-393.
Evrard HC, Forro T, Logothetis NK. 2012. Von Economo neurons in the anterior insula of the macaque monkey. Neuron 74(3):482-489.
Evrard HC, Logothetis NK, Craig AD. 2014. Modular architectonic organization of the insula in the macaque monkey. J Comp Neurol 522(1):64-97.
Fajardo C, Escobar MI, Buritica E, Arteaga G, Umbarila J, Casanova MF, Pimienta H. 2008. Von Economo neurons are present in the dorsolateral (dysgranular) prefrontal cortex of humans. Neurosci Lett 435(3):215-218.
Fischer DB, Boes AD, Demertzi A, Evrard HC, Laureys S, Edlow BL, Liu H, Saper CB, Pascual-Leone A, Fox MD, Geerling JC. 2016. A human brain network derived from coma-causing brainstem lesions. Neurology 87(23):2427-2434.
Flechsig PE. 1898. Neue Untersuchungen über die Markbildung in den menschlichen Grosshirnlappen. Neurologisches Centralblatt 17:977-996.
Franklin TR, Acton PD, Maldjian JA, Gray JD, Croft JR, Dackis CA, O'Brien CP, Childress AR. 2002. Decreased gray matter concentration in the insular,

orbitofrontal, cingulate, and temporal cortices of cocaine patients. Biol Psychiatry 51(2):134-142.
Friston K. 2002. Beyond phrenology: what can neuroimaging tell us about distributed circuitry? Annu Rev Neurosci 25:221-250.
Friston K. 2010. The free-energy principle: a unified brain theory? Nat Rev Neurosci 11(2):127-138.
Gallay DS, Gallay MN, Jeanmonod D, Rouiller EM, Morel A. 2012. The insula of Reil revisited: multiarchitectonic organization in macaque monkeys. Cereb Cortex 22(1):175-190.
Gardini S, Venneri A. 2012. Reduced grey matter in the posterior insula as a structural vulnerability or diathesis to addiction. Brain Res Bull 87(2-3):205-211.
Gefen T, Papastefan ST, Rezvanian A, Bigio EH, Weintraub S, Rogalski E, Mesulam MM, Geula C. 2018. Von Economo neurons of the anterior cingulate across the lifespan and in Alzheimer's disease. Cortex 99:69-77.
Gefen T, Peterson M, Papastefan ST, Martersteck A, Whitney K, Rademaker A, Bigio EH, Weintraub S, Rogalski E, Mesulam MM, Geula C. 2015. Morphometric and histologic substrates of cingulate integrity in elders with exceptional memory capacity. J Neurosci 35(4):1781-1791.
Geyer S, Ledberg A, Schleicher A, Kinomura S, Schormann T, Burgel U, Klingberg T, Larsson J, Zilles K, Roland PE. 1996. Two different areas within the primary motor cortex of man. Nature 382(6594):805-807.
Geyer S, Schleicher A, Zilles K. 1997. The somatosensory cortex of human: Cytoarchitecture and regional distributions of receptor-binding sites. Neuroimage 6(1):27-45.
Glasser MF, Coalson TS, Robinson EC, Hacker CD, Harwell J, Yacoub E, Ugurbil K, Andersson J, Beckmann CF, Jenkinson M, Smith SM, Van Essen DC. 2016. A multi-modal parcellation of human cerebral cortex. Nature 536(7615):171-178.
Goldstein JM, Goodman JM, Seidman LJ, Kennedy DN, Makris N, Lee H, Tourville J, Caviness VS, Jr., Faraone SV, Tsuang MT. 1999. Cortical abnormalities in schizophrenia identified by structural magnetic resonance imaging. Arch Gen Psychiatry 56(6):537-547.
Gonzalez-Acosta CA, Escobar MI, Casanova MF, Pimienta HJ, Buritica E. 2018. Von Economo Neurons in the Human Medial Frontopolar Cortex. Frontiers in Neuroanatomy 12.
Goodkind M, Eickhoff SB, Oathes DJ, Jiang Y, Chang A, Jones-Hagata LB, Ortega BN, Zaiko YV, Roach EL, Korgaonkar MS, Grieve SM, Galatzer-Levy I, Fox PT, Etkin A. 2015. Identification of a common neurobiological substrate for mental illness. JAMA Psychiatry 72(4):305-315.
Greicius MD, Krasnow B, Reiss AL, Menon V. 2003. Functional connectivity in the resting brain: a network analysis of the default mode hypothesis. Proc Natl Acad Sci U S A 100(1):253-258.
Griffiths TD, Warren JD, Dean JL, Howard D. 2004. "When the feeling's gone": a selective loss of musical emotion. J Neurol Neurosurg Psychiatry 75(2):344-345.
Gu X, Gao Z, Wang X, Liu X, Knight RT, Hof PR, Fan J. 2012. Anterior insular cortex is necessary for empathetic pain perception. Brain 135(9):2726-2735.
Hakeem AY, Sherwood CC, Bonar CJ, Butti C, Hof PR, Allman JM. 2009. Von Economo neurons in the elephant brain. Anat Rec (Hoboken) 292(2):242-248.
Haller B. 1906. Beiträge zur Phylogenese des Grosshirns der Säugetiere. Archiv für mikroskopische Anatomie 69((1)):117-222.

Harb K, Magrinelli E, Nicolas CS, Lukianets N, Frangeul L, Pietri M, Sun T, Sandoz G, Grammont F, Jabaudon D, Studer M, Alfano C. 2016. Area-specific development of distinct projection neuron subclasses is regulated by postnatal epigenetic modifications. Elife 5.

Hendry SH, Jones EG, Emson PC, Lawson DE, Heizmann CW, Streit P. 1989. Two classes of cortical GABA neurons defined by differential calcium binding protein immunoreactivities. Exp Brain Res 76(2):467-472.

Hof PR, Nimchinsky EA. 1992. Regional Distribution of Neurofilament and Calcium-Binding Proteins in the Cingulate Cortex of the Macaque Monkey. Cerebral Cortex 2(6):456-467.

Hof PR, Nimchinsky EA, Morrison JH. 1995. Neurochemical Phenotype of Corticocortical Connections in the Macaque Monkey - Quantitative-Analysis of a Subset of Neurofilament Protein-Immunoreactive Projection Neurons in Frontal, Parietal, Temporal, and Cingulate Cortices. Journal of Comparative Neurology 362(1):109-133.

Hof PR, Van der Gucht E. 2007. Structure of the cerebral cortex of the humpback whale, Megaptera novaeangliae (Cetacea, Mysticeti, Balaenopteridae). Anat Rec (Hoboken) 290(1):1-31.

Hofman MA. 2014. Evolution of the human brain: when bigger is better. Front Neuroanat 8:15.

Hurd YL, Suzuki M, Sedvall GC. 2001. D1 and D2 dopamine receptor mRNA expression in whole hemisphere sections of the human brain. J Chem Neuroanat 22(1-2):127-137.

Immordino-Yang MH, McColl A, Damasio H, Damasio A. 2009. Neural correlates of admiration and compassion. Proc Natl Acad Sci U S A 106(19):8021-8026.

Jabbi M, Bastiaansen J, Keysers C. 2008. A common anterior insula representation of disgust observation, experience and imagination shows divergent functional connectivity pathways. PLoS One 3(8):e2939.

Jensen RT, Battey JF, Spindel ER, Benya RV. 2008. International union of pharmacology. LXVIII. Mammalian bombesin receptors: Nomenclature, distribution, pharmacology, signaling, and functions in normal and disease states. Pharmacol Rev 60(1):1-42.

Jones CL, Ward J, Critchley HD. 2010. The neuropsychological impact of insular cortex lesions. J Neurol Neurosurg Psychiatry 81(6):611-618.

Jones EG, Burton H. 1976. Areal differences in the laminar distribution of thalamic afferents in cortical fields of the insular, parietal and temporal regions of primates. J Comp Neurol 168(2):197-247.

Kaas JH. 2000. Why is Brain Size so Important: Design Problems and Solutions as Neocortex Gets Bigger or Smaller. Brain and Mind 1(1):7-23.

Kaas JH. 2011. Neocortex in early mammals and its subsequent variations. Ann N Y Acad Sci 1225:28-36.

Karnath HO, Baier B. 2010. Right insula for our sense of limb ownership and self-awareness of actions. Brain Struct Funct 214(5-6):411-417.

Karnath HO, Baier B, Nagele T. 2005. Awareness of the functioning of one's own limbs mediated by the insular cortex? J Neurosci 25(31):7134-7138.

Kaufman JA, Paul LK, Manaye KF, Granstedt AE, Hof PR, Hakeem AY, Allman JM. 2008. Selective reduction of Von Economo neuron number in agenesis of the corpus callosum. Acta Neuropathol 116(5):479-489.

Kennedy DP, Semendeferi K, Courchesne E. 2007. No reduction of spindle neuron number in frontoinsular cortex in autism. Brain Cogn 64(2):124-129.

Kikyo H, Ohki K, Miyashita Y. 2002. Neural correlates for feeling-of-knowing: an fMRI parametric analysis. Neuron 36(1):177-186.
Kim EJ, Sidhu M, Gaus SE, Huang EJ, Hof PR, Miller BL, DeArmond SJ, Seeley WW. 2012. Selective frontoinsular von Economo neuron and fork cell loss in early behavioral variant frontotemporal dementia. Cereb Cortex 22(2):251-259.
Kurth F, Eickhoff SB, Schleicher A, Hoemke L, Zilles K, Amunts K. 2010. Cytoarchitecture and probabilistic maps of the human posterior insular cortex. Cereb Cortex 20(6):1448-1461.
Lai CH, Wu YT. 2014. Frontal-insula gray matter deficits in first-episode medication-naive patients with major depressive disorder. J Affect Disord 160:74-79.
Lane RD, Reiman EM, Ahern GL, Schwartz GE, Davidson RJ. 1997. Neuroanatomical correlates of happiness, sadness, and disgust. Am J Psychiatry 154(7):926-933.
Latremoliere A, Mauborgne A, Masson J, Bourgoin S, Kayser V, Hamon M, Pohl M. 2008. Differential implication of proinflammatory cytokine interleukin-6 in the development of cephalic versus extracephalic neuropathic pain in rats. J Neurosci 28(34):8489-8501.
Leibenluft E, Gobbini MI, Harrison T, Haxby JV. 2004. Mothers' neural activation in response to pictures of their children and other children. Biol Psychiatry 56(4):225-232.
Loffler LA, Radke S, Morawetz C, Derntl B. 2016. Emotional dysfunctions in neurodegenerative diseases. J Comp Neurol 524(8):1727-1743.
Luppino G, Matelli M, Camarda RM, Gallese V, Rizzolatti G. 1991. Multiple Representations of Body Movements in Mesial Area-6 and the Adjacent Cingulate Cortex - an Intracortical Microstimulation Study in the Macaque Monkey. Journal of Comparative Neurology 311(4):463-482.
Makris N, Oscar-Berman M, Jaffin SK, Hodge SM, Kennedy DN, Caviness VS, Marinkovic K, Breiter HC, Gasic GP, Harris GJ. 2008. Decreased volume of the brain reward system in alcoholism. Biol Psychiatry 64(3):192-202.
Medford N, Critchley HD. 2010. Conjoint activity of anterior insular and anterior cingulate cortex: awareness and response. Brain Struct Funct 214(5-6):535-549.
Menon V, Uddin LQ. 2010. Saliency, switching, attention and control: a network model of insula function. Brain Struct Funct 214(5-6):655-667.
Mesulam MM, Mufson EJ. 1982a. Insula of the Old-World Monkey .3. Efferent Cortical Output and Comments on Function. Journal of Comparative Neurology 212(1):38-52.
Mesulam MM, Mufson EJ. 1982b. Insula of the old world monkey. I. Architectonics in the insulo-orbito-temporal component of the paralimbic brain. J Comp Neurol 212(1):1-22.
Mesulam MM, Mufson EJ. 1985. The Insula of Reil in Man and Monkey. Peters A, Jones EG (eds) Association and Auditory Cortices Cerebral Cortex. Boston, MA: Springer, Boston, MA. p 179-226.
Michel M. 2017. A role for the anterior insular cortex in the global neuronal workspace model of consciousness. Conscious Cogn 49:333-346.
Morales AM, Ghahremani D, Kohno M, Hellemann GS, London ED. 2014. Cigarette exposure, dependence, and craving are related to insula thickness in young adult smokers. Neuropsychopharmacology 39(8):1816-1822.
Morel A, Gallay MN, Baechler A, Nyss M, Gallay DS. 2013. The Human Insula: Architectonic Organization and Postmortem Mri Registration. Neuroscience 236:117-135.

Moreno-Lopez L, Catena A, Fernandez-Serrano MJ, Delgado-Rico E, Stamatakis EA, Perez-Garcia M, Verdejo-Garcia A. 2012. Trait impulsivity and prefrontal gray matter reductions in cocaine dependent individuals. Drug Alcohol Depend 125(3):208-214.

Mufson EJ, Mesulam MM, Pandya DN. 1981. Insular interconnections with the amygdala in the rhesus monkey. Neuroscience 6(7):1231-1248.

Nagai M, Kishi K, Kato S. 2007. Insular cortex and neuropsychiatric disorders: a review of recent literature. Eur Psychiatry 22(6):387-394.

Naidich TP, Kang E, Fatterpekar GM, Delman BN, Gultekin SH, Wolfe D, Ortiz O, Yousry I, Weismann M, Yousry TA. 2004. The insula: anatomic study and MR imaging display at 1.5 T. AJNR Am J Neuroradiol 25(2):222-232.

Namkung H, Kim SH, Sawa A. 2017. The Insula: An Underestimated Brain Area in Clinical Neuroscience, Psychiatry, and Neurology. Trends Neurosci 40(4):200-207.

Naqvi NH, Gaznick N, Tranel D, Bechara A. 2014. The insula: a critical neural substrate for craving and drug seeking under conflict and risk. Ann N Y Acad Sci 1316:53-70.

Ngowyang G. 1932. Beschreibung einer Art von Spezialzellen in der Inselrinde-zugleich Bemerkungen über die v. Economoschen Spezialzellen. J Psychol Neurol 44:671-674.

Nimchinsky EA, Gilissen E, Allman JM, Perl DP, Erwin JM, Hof PR. 1999. A neuronal morphologic type unique to humans and great apes. Proc Natl Acad Sci U S A 96(9):5268-5273.

Nimchinsky EA, Vogt BA, Morrison JH, Hof PR. 1995. Spindle neurons of the human anterior cingulate cortex. J Comp Neurol 355(1):27-37.

Northcutt RG, Kaas JH. 1995. The emergence and evolution of mammalian neocortex. Trends Neurosci 18(9):373-379.

Nunn K, Frampton I, Gordon I, Lask B. 2008. The fault is not in her parents but in her insula--a neurobiological hypothesis of anorexia nervosa. Eur Eat Disord Rev 16(5):355-360.

Ortigue S, Grafton ST, Bianchi-Demicheli F. 2007. Correlation between insula activation and self-reported quality of orgasm in women. Neuroimage 37(2):551-560.

Paton JJ, Belova MA, Morrison SE, Salzman CD. 2006. The primate amygdala represents the positive and negative value of visual stimuli during learning. Nature 439(7078):865-870.

Paulus MP, Stein MB. 2006. An insular view of anxiety. Biol Psychiatry 60(4):383-387.

Paulus MP, Stein MB. 2010. Interoception in anxiety and depression. Brain Struct Funct 214(5-6):451-463.

Phillips ML, Gregory LJ, Cullen S, Coen S, Ng V, Andrew C, Giampietro V, Bullmore E, Zelaya F, Amaro E, Thompson DG, Hobson AR, Williams SC, Brammer M, Aziz Q. 2003. The effect of negative emotional context on neural and behavioural responses to oesophageal stimulation. Brain 126(Pt 3):669-684.

Pritchard TC, Hamilton RB, Morse JR, Norgren R. 1986. Projections of thalamic gustatory and lingual areas in the monkey, Macaca fascicularis. J Comp Neurol 244(2):213-228.

Raghanti MA, Spocter MA, Butti C, Hof PR, Sherwood CC. 2010. A comparative perspective on minicolumns and inhibitory GABAergic interneurons in the neocortex. Frontiers in Neuroanatomy 4.

Raghanti MA, Spurlock LB, Treichler FR, Weigel SE, Stimmelmayr R, Butti C, Thewissen JGMH, Hof PR. 2015. An analysis of von Economo neurons in the cerebral cortex of cetaceans, artiodactyls, and perissodactyls. Brain Structure & Function 220(4):2303-2314.

Ramón y Cajal S. 1901-1902. Studies on the human cerebral cortex IV: Structure of the olfactory cerebral cortex in men and mammals. Trabajos del Laboratorio de Investigaciones Biológicas de la Universidad de Madrid 1:1-140.

Retzius G. 1896. Das Menschenhirn. Stockholm: Koenigliche Buchdruckerei P.A. Norstedt und Soener.

Retzius G. 1902. Zur Morphologie der Insula Reili. Biologische Untersuchungen X.14-20.

Roberts TS, Akert K. 1963. Insular and opercular cortex and its thalamic projection in Macaca mulatta. Schweiz Arch Neurol Neurochir Psychiatr 92:1-43.

Rogalski EJ, Gefen T, Shi J, Samimi M, Bigio E, Weintraub S, Geula C, Mesulam MM. 2013. Youthful memory capacity in old brains: anatomic and genetic clues from the Northwestern SuperAging Project. J Cogn Neurosci 25(1):29-36.

Rose M. 1928. Die Inselrinde des Menschen und der Tiere. Journal of Physchology and Neurology 37:467-624.

Rosen A, Chen DQ, Hayes DJ, Davis KD, Hodaie M. 2015. A Neuroimaging Strategy for the Three-Dimensional in vivo Anatomical Visualization and Characterization of Insular Gyri. Stereotact Funct Neurosurg 93(4):255-264.

Rosen HJ, Gorno-Tempini ML, Goldman WP, Perry RJ, Schuff N, Weiner M, Feiwell R, Kramer JH, Miller BL. 2002. Patterns of brain atrophy in frontotemporal dementia and semantic dementia. Neurology 58(2):198-208.

Sanchez MM, Young LJ, Plotsky PM, Insel TR. 1999. Autoradiographic and in situ hybridization localization of corticotropin-releasing factor 1 and 2 receptors in nonhuman primate brain. J Comp Neurol 408(3):365-377.

Santos M, Uppal N, Butti C, Wicinski B, Schmeidler J, Giannakopoulos P, Heinsen H, Schmitz C, Hof PR. 2011. Von Economo neurons in autism: a stereologic study of the frontoinsular cortex in children. Brain Res 1380:206-217.

Schneider F, Bermpohl F, Heinzel A, Rotte M, Walter M, Tempelmann C, Wiebking C, Dobrowolny H, Heinze HJ, Northoff G. 2008. The resting brain and our self: self-relatedness modulates resting state neural activity in cortical midline structures. Neuroscience 157(1):120-131.

Schneider RJ, Friedman DP, Mishkin M. 1993. A Modality-Specific Somatosensory Area within the Insula of the Rhesus-Monkey. Brain Res 621(1):116-120.

Schultz SH, North SW, Shields CG. 2007. Schizophrenia: a review. Am Fam Physician 75(12):1821-1829.

Seeley WW. 2008. Selective functional, regional, and neuronal vulnerability in frontotemporal dementia. Curr Opin Neurol 21(6):701-707.

Seeley WW, Carlin DA, Allman JM, Macedo MN, Bush C, Miller BL, Dearmond SJ. 2006. Early frontotemporal dementia targets neurons unique to apes and humans. Ann Neurol 60(6):660-667.

Seeley WW, Crawford R, Rascovsky K, Kramer JH, Weiner M, Miller BL, Gorno-Tempini ML. 2008. Frontal paralimbic network atrophy in very mild behavioral variant frontotemporal dementia. Arch Neurol 65(2):249-255.

Seeley WW, Menon V, Schatzberg AF, Keller J, Glover GH, Kenna H, Reiss AL, Greicius MD. 2007. Dissociable intrinsic connectivity networks for salience processing and executive control. J Neurosci 27(9):2349-2356.

Seeley WW, Merkle FT, Gaus SE, Craig AD, Allman JM, Hof PR. 2012. Distinctive neurons of the anterior cingulate and frontoinsular cortex: a historical perspective. Cereb Cortex 22(2):245-250.
Shergill SS, Brammer MJ, Williams SC, Murray RM, McGuire PK. 2000. Mapping auditory hallucinations in schizophrenia using functional magnetic resonance imaging. Arch Gen Psychiatry 57(11):1033-1038.
Simmons A, Matthews SC, Stein MB, Paulus MP. 2004. Anticipation of emotionally aversive visual stimuli activates right insula. Neuroreport 15(14):2261-2265.
Simmons A, Strigo I, Matthews SC, Paulus MP, Stein MB. 2006. Anticipation of aversive visual stimuli is associated with increased insula activation in anxiety-prone subjects. Biol Psychiatry 60(4):402-409.
Simms ML, Kemper TL, Timbie CM, Bauman ML, Blatt GJ. 2009. The anterior cingulate cortex in autism: heterogeneity of qualitative and quantitative cytoarchitectonic features suggests possible subgroups. Acta Neuropathol 118(5):673-684.
Singer T, Critchley HD, Preuschoff K. 2009. A common role of insula in feelings, empathy and uncertainty. Trends Cogn Sci 13(8):334-340.
Singer T, Seymour B, O'Doherty J, Kaube H, Dolan RJ, Frith CD. 2004. Empathy for pain involves the affective but not sensory components of pain. Science 303(5661):1157-1162.
Sliz D, Hayley S. 2012. Major depressive disorder and alterations in insular cortical activity: a review of current functional magnetic imaging research. Front Hum Neurosci 6:323.
Soares DC, Carlyle BC, Bradshaw NJ, Porteous DJ. 2011. DISC1: Structure, Function, and Therapeutic Potential for Major Mental Illness. ACS Chem Neurosci 2(11):609-632.
Sridharan D, Levitin DJ, Menon V. 2008. A critical role for the right fronto-insular cortex in switching between central-executive and default-mode networks. Proc Natl Acad Sci U S A 105(34):12569-12574.
Stefanacci L, Amaral DG. 2000. Topographic organization of cortical inputs to the lateral nucleus of the macaque monkey amygdala: a retrograde tracing study. J Comp Neurol 421(1):52-79.
Stephan E, Pardo JV, Faris PL, Hartman BK, Kim SW, Ivanov EH, Daughters RS, Costello PA, Goodale RL. 2003. Functional neuroimaging of gastric distention. J Gastrointest Surg 7(6):740-749.
Stimpson CD, Tetreault NA, Allman JM, Jacobs B, Butti C, Hof PR, Sherwood CC. 2011. Biochemical Specificity of von Economo Neurons in Hominoids. Am J Hum Biol 23(1):22-28.
Stratmann M, Konrad C, Kugel H, Krug A, Schoning S, Ohrmann P, Uhlmann C, Postert C, Suslow T, Heindel W, Arolt V, Kircher T, Dannlowski U. 2014. Insular and hippocampal gray matter volume reductions in patients with major depressive disorder. PLoS One 9(7):e102692.
Strigo IA, Craig AD. 2016. Interoception, homeostatic emotions and sympathovagal balance. Philos Trans R Soc Lond B Biol Sci 371(1708).
Surguladze SA, Calvert GA, Brammer MJ, Campbell R, Bullmore ET, Giampietro V, David AS. 2001. Audio-visual speech perception in schizophrenia: an fMRI study. Psychiatry Res 106(1):1-14.
Sutherland MT, Riedel MC, Flannery JS, Yanes JA, Fox PT, Stein EA, Laird AR. 2016. Chronic cigarette smoking is linked with structural alterations in brain regions

showing acute nicotinic drug-induced functional modulations. Behav Brain Funct 12(1):16.
Takahashi H, Matsuura M, Koeda M, Yahata N, Suhara T, Kato M, Okubo Y. 2008. Brain activations during judgments of positive self-conscious emotion and positive basic emotion: pride and joy. Cereb Cortex 18(4):898-903.
Takahashi T, Yucel M, Lorenzetti V, Tanino R, Whittle S, Suzuki M, Walterfang M, Pantelis C, Allen NB. 2010. Volumetric MRI study of the insular cortex in individuals with current and past major depression. J Affect Disord 121(3):231-238.
Terasawa Y, Shibata M, Moriguchi Y, Umeda S. 2013. Anterior insular cortex mediates bodily sensibility and social anxiety. Soc Cogn Affect Neurosci 8(3):259-266.
Tononi G, Koch C. 2008. The neural correlates of consciousness: an update. Ann N Y Acad Sci 1124:239-261.
Uddin LQ. 2015. Salience processing and insular cortical function and dysfunction. Nat Rev Neurosci 16(1):55-61.
Vogt C, Vogt O. 1919. Allgemeinere Ergebnisse unserer Hirnforschung: Von Cécile und Oskar Vogt. 1. bis 4. Mitteilung. Mit 141 Textabbildungen und 5 Tafeln. 1. Mitteilung: Ziele und Wege unserer Hirnforschung. 2. Mitteilung: Das Wesen der topischen architektonischen Differenzen des Cortex cerebri. 3. Mitteilung: Die architektonische Rindenfelderung im Lichte unserer neuesten Forschungen. 4. Mitteilung: Die physiologische Bedeutung der architektonischen Rindenfelderung auf Grund neuer Rindenreizungen: Joh. Ambr. Barth.
Vogt O. 1910. Die myeloarchitektonische Felderung des menschlichen Stirnhirns. Journal für Psychologie und Neurologie 15:221.
von Economo C. 1926. Eine neue art spezialzellen des lobus cinguli und lobus insulae. Zeitschrift für die gesamte Neurologie und Psychiatrie 100:706-712.
von Economo CaK, Georg N. 1925. Die Cytoarchitektonik der Hirnrinde des Erwachsenen Menschen—Textband und Atlas mit 112 Mikrophotographischen Tafeln. Wien und Berlin: J. Springer.
Watanabe Y, Nunokawa A, Shibuya M, Kaneko N, Nawa H, Someya T. 2008. Association study of interleukin 2 (IL2) and IL4 with schizophrenia in a Japanese population. Eur Arch Psy Clin N 258(7):422-427.
Watson KK, Jones TK, Allman JM. 2006. Dendritic architecture of the von Economo neurons. Neuroscience 141(3):1107-1112.
Winston JS, Strange BA, O'Doherty J, Dolan RJ. 2002. Automatic and intentional brain responses during evaluation of trustworthiness of faces. Nat Neurosci 5(3):277-283.
Wise T, Radua J, Via E, Cardoner N, Abe O, Adams TM, Amico F, Cheng Y, Cole JH, de Azevedo Marques Perico C, Dickstein DP, Farrow TFD, Frodl T, Wagner G, Gotlib IH, Gruber O, Ham BJ, Job DE, Kempton MJ, Kim MJ, Koolschijn P, Malhi GS, Mataix-Cols D, McIntosh AM, Nugent AC, O'Brien JT, Pezzoli S, Phillips ML, Sachdev PS, Salvadore G, Selvaraj S, Stanfield AC, Thomas AJ, van Tol MJ, van der Wee NJA, Veltman DJ, Young AH, Fu CH, Cleare AJ, Arnone D. 2017. Common and distinct patterns of grey-matter volume alteration in major depression and bipolar disorder: evidence from voxel-based meta-analysis. Mol Psychiatry 22(10):1455-1463.
Wright IC, Ellison ZR, Sharma T, Friston KJ, Murray RM, McGuire PK. 1999. Mapping of grey matter changes in schizophrenia. Schizophr Res 35(1):1-14.

Wysiadecki G, Malkiewicz A, Rozniecki J, Polguj M, Haladaj R, Zytkowski A, Topol M. 2018. Anatomical variations of the insular gyri: A morphological study and proposal of unified classification. Clin Anat 31(3):347-356.

Zeki S, Watson JDG, Lueck CJ, Friston KJ, Kennard C, Frackowiak RSJ. 1991. A Direct Demonstration of Functional Specialization in Human Visual-Cortex. J Neurosci 11(3):641-649.

Zhao XY, Lein ES, He AQ, Smith SC, Aston C, Gage FH. 2001. Transcriptional profiling reveals strict boundaries between hippocampal subregions. Journal of Comparative Neurology 441(3):187-196.

Zilles K, Palomero-Gallagher N, Grefkes C, Scheperjans F, Boy C, Amunts K, Schleicher A. 2002. Architectonics of the human cerebral cortex and transmitter receptor fingerprints: reconciling functional neuroanatomy and neurochemistry. Eur Neuropsychopharm 12(6):587-599.

Zilles K, Palomero-Gallagher N, Schleicher A. 2004. Transmitter receptors and functional anatomy of the cerebral cortex. J Anat 205(6):417-432.

Statements of contributions

Manuscript I: Novel elemental localization in the primate brain

Felicitas M. Horn (FMH) and Dr. Henry C. Evrard (HCE) designed the research

HCE made the histological processing of the monkey brain tissue

FMH digitalized the brain sections and analyzed the data

FMH and HCE interpreted the results and wrote the manuscript

Prof. Dr. Nikos K. Logothetis (NKL) provided all the resources for the experiments

Manuscript II: Elemental localization of von Economo neurons in the dysgranular insula in macaque monkeys

FMH and HCE designed the research

HCE made the histological processing of the monkey brain tissue

FMH digitalized the brain sections and analyzed the data

FMH and HCE interpreted the results and wrote the manuscript

NKL provided all the resources for the experiments

Manuscript III: Evolutionary expansion of the von Economo neuron areas in the human anterior insular cortex

Prof. Dr. Bernhard Hirt and Dr. Thomas Shiozawa-Bayer provided the brain tissue

FMH and HCE designed the research

FMH made the histological processing of the human brain tissue

FMH digitalized the brain sections and analyzed the data

FMH and HCE interpreted the results and wrote the manuscript

NKL provided all the resources for the experiments

Appended Manuscripts

Manuscript I

Novel elemental localization in the primate cerebral cortex

Felicitas M. Horn[1,2,3], Nikos K. Logothetis[2,4], Henry C. Evrard[1,2,*]

[1]Functional and Comparative Neuroanatomy Laboratory, Werner Reichardt Center for Integrative Neuroscience, Tuebingen, Germany; [2]Max Planck Institute for Biological Cybernetics, Tuebingen, Germany; [3]International Max Planck Research School, Tuebingen, Germany; [4]Imaging Science and Biomedical Engineering, University of Manchester, Manchester, UK

*Corresponding author: Henry.Evrard@tuebingen.mpg.de

Keywords: architectonics, non-human primate, insular cortex, von Economo neuron, Fork neuron, interoception, autonomic nervous system, awareness, emotion, cognition, subjective feelings

Abstract

More than a century ago, Brodmann defined as “elemental localization” the containment of specialized neuronal morphotypes within specific cytoarchitectonic areas of the primate cerebral cortex. Such areal specificity suggested a shared evolution, development and functional implications between a specialized neuron and its host area. At the time, Brodmann emphasized two such localizations: the giant Betz cell in the primary motor cortex (BA4) and the large Meynert cell in the primary visual cortex (BA17). Here, we identified a novel elemental localization by showing that the large spindle-shaped von Economo neuron and its large bifid Fork neuron companion are strictly confined together inside one single small architectonic area, i.e. the lateral agranular area of the insula (IAL or ‘VEN area’), within the ventral anterior insular cortex in the rhesus and cynomolgus macaque monkeys. Precisely, the identification of the architectonic boundaries of IAL at low magnification predicted the distribution of the VEN and FN at high magnification, and vice versa. This distinctive relationship illustrates the remarkably strict overall nature of the parcellation of the primate cerebral cortex, despite a backdrop of inter-individual variability. The elemental localization offers a unique experimental advantage in the sense that it suggests functional commonalities between the cells and their host areas; studying the VEN area could give us clues on the functions of cells that are otherwise too rare to easily study in vivo. Finally, the present finding supports the view of a heterogeneous anterior insular cortex, justifying to a finer parcellation of the rather broad periallocortices.

Along with transcriptional patterning studies this EL has fundamental implications in the investigation and understanding of the development origin, connectivity and function of the VEN and FN which are likely bound to the origin and fate of their host area.

Introduction

The concept of a heterogeneous and highly compartmented primate cerebral cortex dates back to the late 19th century, when anatomists such as Flechsig, Campbell, Smith, Brodmann and the Vogt published the first architectonic maps of the human cerebral cortex (Brodmann, 1909; Campbell, 1904; Flechsig, 1898; Meynert, 1872; Smith, 1907; Vogt, 1910). Nowadays, it is widely accepted that the primate cortex can be parcellated into a substantial number of specialized areas that are each structurally, hodologically and functionally distinct. This areal multi-modal overlap has been validated in a wealth of studies using not only cyto- and myeloarchitectonics but also molecular, genetic, connectional and electrophysiological mapping (Eickhoff et al., 2007; Luppino et al., 1991; Zhao et al., 2001; Zirlinger et al., 2001). For example, electrophysiological stimulations in the mesial agranular frontal cortex in macaque monkeys showed that its architectonically distinct rostral and caudal cytoarchitectonic subdivisions have sharply distinct motor representations and connectivity patterns (Luppino et al., 1991). Zhao and colleagues showed different gene-expression profiles for the different architectonic regions of the hippocampus (CA1, CA3, and dentate gyrus) in mice (Zhao et al., 2001) and similarly, Zilles and colleagues found that different densities of transmitter receptors matched with the cyto- and myeloarchitectonic boundaries in adjacent cortical areas (Zilles et al., 2002).

In fact, already in 1909, such areal specificity was emphasized at the cellular level by Brodmann (Brodmann, 1909). He noted the exclusive existence of two well-known neuronal morphotypes, each located within one particular architectonic area: the giant Betz cell and large Meynert cell, both atypical projection neurons located within layer 5 of the primary motor area (BA4 or M1) and the primary visual area (BA17 or V1), respectively. He defined this specific allocation as “elemental localization” (EL). The concept of EL suggests that the specialized neuronal morphotypes share the evolutionary and developmental origins as well as function and neuronal connections of the architectonic area in which they are located.

In addition to the Betz and Meynert cells, the spindle-shaped von Economo neuron (VEN) and its bifid companion Fork neuron (FN) are two atypical morphotypes localized in the anterior insular cortex (AIC) and anterior cingulate cortex (ACC) in primates and a few other non-primate species (Evrard et al., 2012; Nimchinsky et al., 1999; Raghanti et al., 2015; von Economo, 1926) The VEN and FN are atypical cortical layer 5 projection neurons, linked to social-emotional

cognition, interoception and autonomic regulations (Craig, 2009; Seeley et al., 2006; von Economo, 1926). They are selectively depleted in various neuropsychiatric disorders including particularly frontotemporal dementia (FTD) (Kim et al., 2012; Nana et al., 2019) and they recently drew attention as a potentially crucial cellular contributor to the emergence of self-conscious feelings in humans (Allman et al., 2005; Butti et al., 2013).

Preliminary investigations of the VEN and FN distribution within the macaque insula suggest that these neurons were intermingled and formed consistently a small isolated cluster inside the broader ventral aspect of the AIC instead of straddling the entire AIC (Evrard et al., 2012). Prior examinations of the anatomical organization of the macaque insular cortex (or insula) revealed that the insula is parcellated into smaller, sharply-delimited subareas with seven agranular areas composing the AIC (Evrard et al., 2014), and it has been suggested that the VEN and FN cluster is exactly overlapping with one of these areas (Evrard et al., 2012). In the present study, we examined the exact areal distribution of these two neurons by analyzing the correspondence between the cyto- and myeloarchitecture of the ventral AIC on consecutive coronal sections of the left and right AIC from two species of macaque monkeys. We show a novel EL within the macaque insular cortex (IC) since Brodmann's discovery of such a specific spatial allocation 100 years ago: the large spindle-shaped VEN and its companion the FN, are exclusively located in one sharply-delimited architectonic area of the agranular anterior insula, the lateral agranular area of the insula (IAL), or 'VEN area'.

Material and Methods

The present data were obtained from the brains of three rhesus (*Macaca mulatta*) and three cynomolgus (*Macaca fascicularis*) macaque monkeys (3-8 years old; average weight 7.3 kg; 2 females). All housing and experimental protocols were implemented with great care to ensure animal welfare. They were approved by the local German authorities and they followed the European directive 2010/63/EU on the protection of animals used for experimental and other scientific purposes.

All the animals were used previously in the context of a separate study (i.e. fMRI and tract-tracing) that required euthanasia, transcardial perfusion and fixation of the brain. The procedures for the fixation, sectioning of the brain, and histological processing were described in detail

elsewhere (Evrard et al., 2014). Briefly, immediately after euthanasia with a lethal overdose of sodium pentobarbital (60–80 mg/kg i.v.), the brain was rinsed, fixed and cryoprotected using a sequence of transcardial perfusion including 0.9% heparinized saline at room temperature (RT), followed by 4% paraformaldehyde in phosphate buffer (0.1 M, pH 7.4, RT), and then by 4% paraformaldehyde and 5% sucrose in PB (0.1 M, pH 7.4, RT). The brain was then removed and further cryoprotected in 0.01 M PBS (pH 7.4) containing 30% sucrose and 0.1% sodium azide for at least 7 days at 4ºC. For histological processing, the brains were frozen and cut in 50 µm-thick coronal sections using a horizontal sliding microtome. The serial sections were then separated into six or eight sets of 1-in-6 or 1-in-8 series, respectively. In all cases, the first set was used for a standard Nissl stain using cresyl violet (0.16% in 3.75% ethanol); the second set was used for a standard Gallyas stain of myelin using silver nitrate (Gallyas, 1979). Among the remaining sets, some were used in immunohistochemistries for various proteins and the others were used for the separate examination of tract-tracing results.

All Nissl- and Gallyas-stained sections containing the insular cortex were digitally photomicrographed at one focal plane in the middle of the section and at a 0.4 µm in-plane resolution using a digitizing microscope (AxioScan.Z1; Carl Zeiss GmbH, Göttingen, Germany) equipped with a 10x/0.45 plan-apochromatic objective and a Hitachi HV-F202SCL digital camera (Hitachi Europe, Düsseldorf, Germany). The resulting pyramid files were converted into 'low magnification' jpg images that were used for the localization of the insular architectonic boundaries. In addition, the region of the Nissl-stained sections that contains the insula was digitally photomicrographed at 20 distinct consecutive focal planes (z-stack with a 1 µm inter-slice interval across a 21 µm range) and at a 0.2 µm in-plan resolution with, this time, a 20x/0.8 plan-apochromatic objective. The resulting 3-dimensional 'high magnification' images were used for the localization of the VEN and FN. Scrolling back and forth through the z-stack image allowed a clear visualization and verification of the cellular morphology, with an apparent visual sharpness of the objects that was similar to that experienced using conventional microscopy.

The two sets of images ('low' and 'high' magnifications) were analyzed in two separate phases by two independent observers (FMH and HCE). First, the localization of each VEN and FN occurring in the insula was charted using the high resolution images with a custom-designed software allowing to 'scroll' through the different slices of the z-stack of the pyramid image files (or 'virtual sections') in order to accurately recognize the different neuronal morphotypes. The

criteria for a neuron to considered as a VEN were a laminar localization in layer 5b, a unique basal dendrite and an equally thick apical dendrite, an elongated spindle-shaped perikaryon with a centered nucleus and nucleolus that is as large as or larger than the local pyramidal neurons, a rather symmetrical morphology along both the vertical and longitudinal axes (Nimchinsky et al., 1999). The criteria for a FN were a unique basal dendrite and a bifid or "forked" apical dendrite, a rather triangular perikaryon as large as or larger than the local pyramidal neurons (Ngowyang, 1932). Second, the Nissl- and Gallyas-stained sections were examined using the low magnification images to localize the cyto- and myeloarchitectonic boundaries of the insular areas, using criteria defined in a prior study (Evrard et al., 2014). This architectonic mapping was made with a relatively long time delay after the VEN and FN charting and without having any access to the charts in order to avoid a biased parcellation. Finally, the plots of the VEN and FN and the architectonic outline of the insular areas from both hemispheres were aligned in Adobe Illustrator (Adobe System Inc., San José, California, USA) for comparison of cell and border locations, and for the preparation of figures.

Results

General observation

Figure 1 shows four photomicrographs of representative VEN (Fig. 1A, C) and FNs (Fig. 1B, D) in the AIC in the rhesus (Fig. 1A, B) and cynomolgus (Fig. 1C, D) macaque monkeys. The examination of the high magnification z-stack images of the Nissl-stained insula confirmed the occurrence of the VEN and FN in the left and right AIC in both species (Evrard et al., 2012). The VEN were all large spindle-shaped neurons with a single large basal dendrite and an equally thick apical dendrite (Fig. 1A, C). Most VEN perikarya displayed the typical elongated and symmetrical morphology; other presented slight variations in size and shape, as described in prior reports in humans, great apes, and monkeys (Evrard et al., 2012; Nimchinsky et al., 1995). The soma of the FN had a characteristic triangular shape with a large basal dendrite and bifid apical dendrites (Fig. 1B, D) (Allman et al., 2011; Evrard et al., 2012; Ngowyang, 1932). Both the VEN and FN appeared consistently larger than their pyramidal neighbors, in agreement with the difference in perikaryal volume reported previously in humans and monkeys (Allman et al., 2011; Evrard et al., 2012).

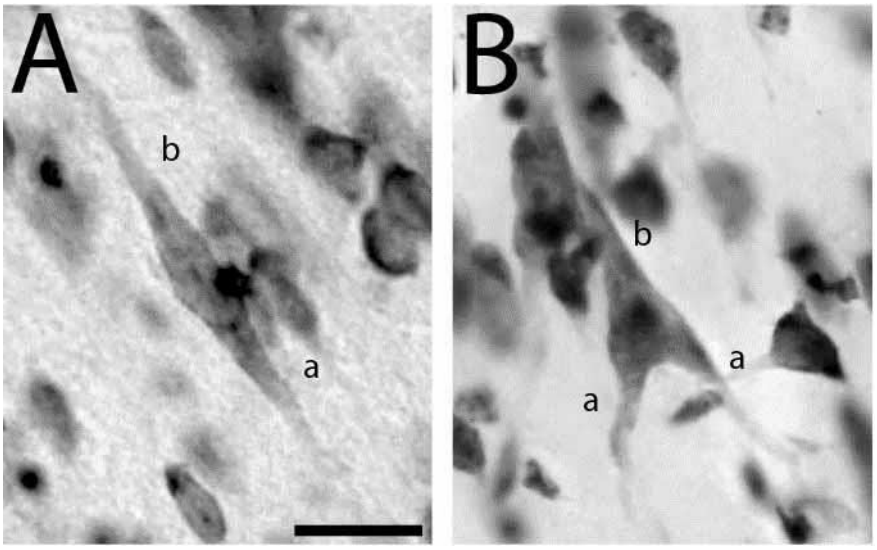

Figure 1: Example of VEN and FN morphology of a macaque monkeys
Photomicrographs of a VEN (**A**) and a FN (**B**) in the AIC of the macaque monkey, stained by using a standard Nissl technique; a and b indicate the apical and basal dendrites, respectively. Scale bar represents 20 μm.

Cluster distribution of the VEN and FN

Figure 2 shows representative plots of the localization of individual VEN and FNs in a series of consecutive coronal diagrams encompassing the entire posterior-to-anterior extent of the distribution of the cells in the left and right hemispheres in one cynomolgus (cm006; Fig. 2A) and one rhesus (rm013; Fig. 2B) macaque monkey. (For the other four subjects, see supplementary Fig. S1.) The plots, made based on high-magnification photomicrographs of Nissl-stained sections, revealed that the VEN consistently formed a compact cluster, which defined a small distinct sub-region within the broader agranular AIC. This cluster occurred in all six animals and in both hemispheres, despite an individual and hemispheric variability in the size and overall morphology of the AIC. The spatial delimitation of the VEN cluster was remarkably sharp rather than gradual, with a sudden and complete drop in the number of the VEN on all sides (anterior, posterior, lateral and medial).

Starting from the posterior levels, the VEN cluster occurred first just anterior to the limen insula, in a distinct convexity of the cortex, which anteriorly prolonged the point of junction between the orbital prefrontal and temporal cortices. Progressing anteriorly, the cluster remained co-existent with the convexity and then continued until its anterior end in a planer region, medial to the ending of the lateral sulcus and lateral to the lateral orbital sulcus.

The FNs were typically less numerous than the VEN (Evrard et al., 2012). They were not detected on every section. However, in the sections where they occurred, they were either mingled

with the VEN (e.g. Fig. 2A, third level, left) or slightly but distinctly shifted medially even sometimes to the point of reaching another area such as IAPM (e.g. Fig. 2B, third level, right). This 'floating' localization of the FN around the VEN cluster will be further described below.

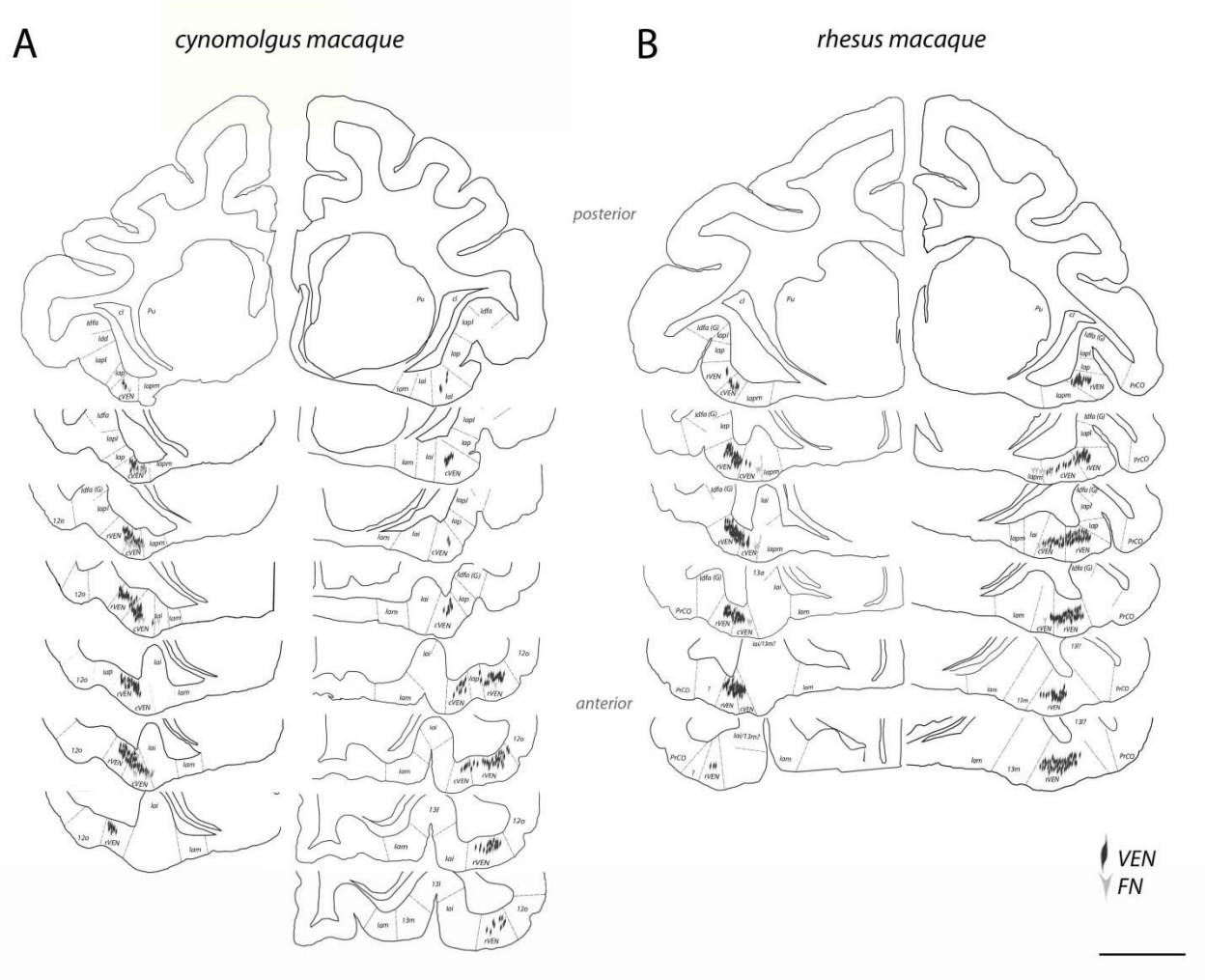

Figure 2: Localization of VEN and FN cluster within the macaque AIC
Computer generated drawings of coronal N Nissl stained sections showing the distribution of VEN and FNs across the left and right anterior insular cortices in a cynomolgus (**A**), and rhesus macaque monkey (**B**) in consecutive sections from anterior to posterior The borders of the areas are marked by the dashed lines; the white and grey matter are separated by a black line. *Abbreviations*: Cl, Claustrum; Iai, intermediate agranular insula; Ial, lateral agranular insula, Iam, medial anterior insula; Iap, posterior agranular insula; Iapl, posterior- lateral agranular insula; Iapm, posterior-medial anterior insula; Idfa, anterior area of the dorsal fundus of the insula; PrCO, precentral opercular area; Pu, Putamen; 12o, area 12o. Scale bars represent 5 mm.

Architectonic affiliation of the VEN cluster

The independent and temporally spaced examination of the low-magnification images of Nissl- and Gallyas-stained sections at and beyond the anteroposterior levels where the VEN and FNs had been detected revealed the distinct architectonic areas of the AIC and orbital prefrontal cortex (Carmichael and Price, 1994; Evrard et al., 2014). As illustrated in Figure 2 (and Fig. S1) and described in details below, the subsequent overlay of the architectonic maps drawn from the Nissl- and Gallyas-stained sections with the computer-generated charts of the VEN distribution revealed that the VEN were consistently clustered in one particular architectonic area of the AIC, the *lateral agranular area of the insula* (IAL), hereafter also interchangeably named 'VEN area'. Thus, the detection of the limits of the cluster of VEN at high magnification (e.g. as in Fig. 1, which does not allow architectonic parcellation) allowed to predict the localization of the architectonic boundaries of IAL, which were detectable only a lower magnification, and vice versa.

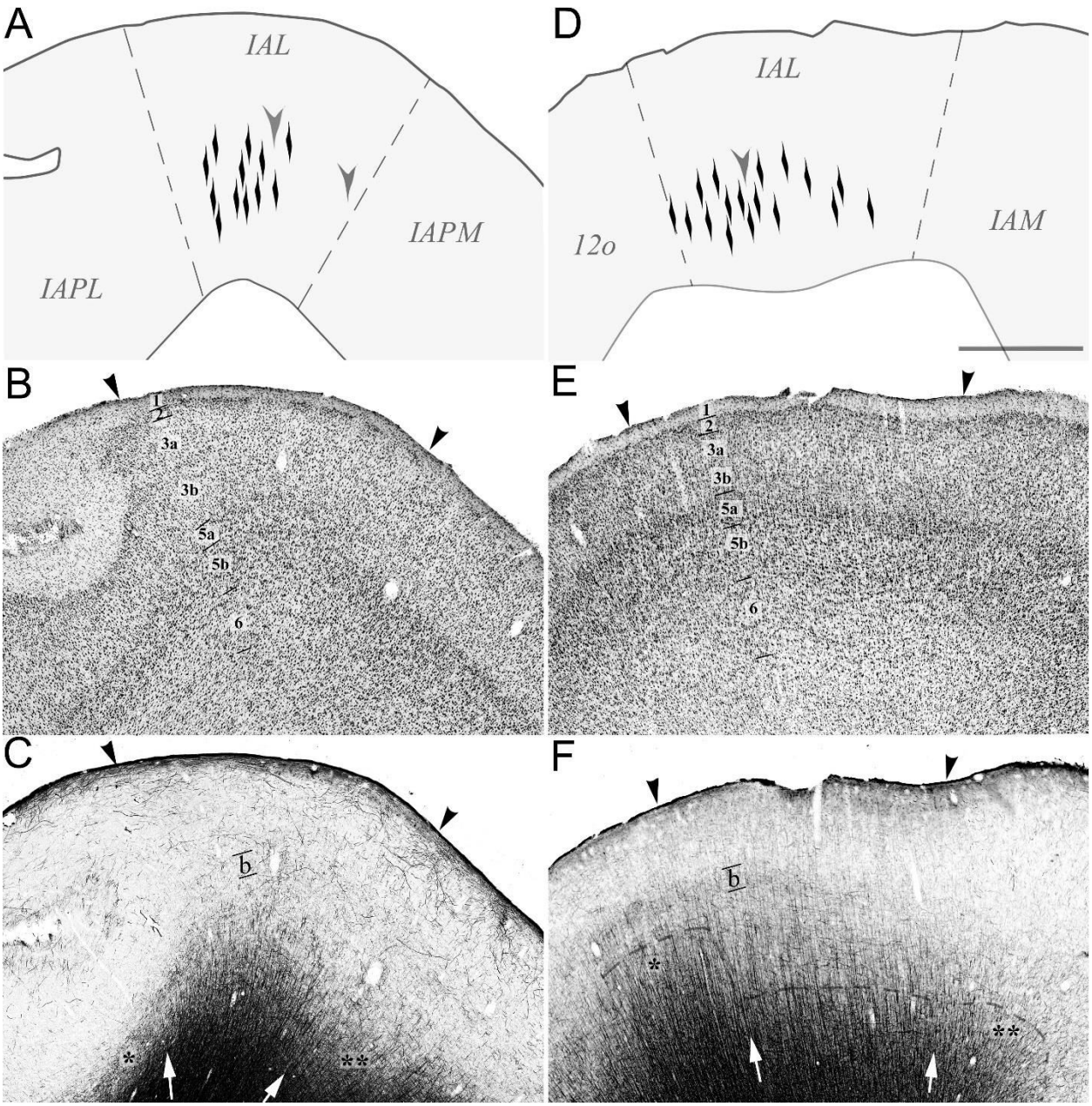

Figure 3 Cyto- and myeloarchitectonic features of IAL in a cynomolgus monkey

A-C show the localization of the VEN and FN and the cyto- and myeloarchitectonic features of IAL in a posterior level and **D-F** in an anterior level (**D-F**) in one cynomolgus monkey (cm006). The plots in **A and D** show the localization of the VEN and FNs within the caudal (**A**) and rostral (**D**) components of area IAL. Arrowheads mark the borders of these areas with their medial and lateral neighboring architectonic areas. The pairs of photomicrographs illustrate the cytoarchitectonic (**B, E)** and myeloarchitectonic characteristics (**C, F)** of the caudal and rostral components of area IAL in the agranular insula. The delimitation of the cortical layers 2-6 is indicated left in the mound of the insula in panel A and D; VEN and FNs are illustrated by the black spindles and the grey triangular shapes, respectively; the asterisks mark the characteristic shifts in the myelination patterns indicating the borders to the adjacent areas IAPL and IAPM or 12o and IAM (see text); b marks the outer band of Baillarger; left is dorsal, top is lateral; scale bar = 1000 μm.

Figures 3 and 4 show the cyto- and myeloarchitectonic features of IAL at a posterior (Fig. 3A-C and 4A-C) and an anterior (Fig. 3D-F and 4D-F) level in one hemisphere from one cynomolgus monkey (cm006; Fig. 3) and one hemisphere from one rhesus monkey (rm014; Fig. 4). (The other hemispheres of these two cases and both hemispheres of the other four cases are shown in supplementary Figures S3-8.)

At the posterior levels, IAL was bordered laterally by the *lateral posterior agranular area of the insula* (IAPL) and medially by the *median posterior agranular area of the insula* (IAPM). In the Nissl stain (Fig. 3B and 4B), IAL was characterized by a thin but very distinct layer 2, a broad layer 3 with a subtle subdivision into sub-layers 3a and 3b, a distinct but slightly vague separation between layers 3 and 5 with in some sections a feeble development of layer 4, a broad layer 5 made of conspicuously larger cells than in IAPL and IAPM and a distinct subdivision into sub-layers 5a and 5b, and a rather broad layer 6 with a diffuse separation from the white mater. The border with IAPL was sharp and marked by a suddenly less distinct layer 2 and by a thinner layer 5 made of two distinct rows (or "train tracks"; Carmichael and Price, 1994). The border with IAPM was equally sharp. It was characterized by the disappearance of layer 2 and by the very neat separation between a broad layer 3 and the thinner but very dense layer 5, which is the hallmark of IAPM (Carmichael and Price, 1994; Evrard et al., 2014). In the Gallyas stain (Fig. 3C and 4C), IAL was characterized by the presence of fan of straight radial fibers ending approximately at the border between sub-layers 5b and 5a, by a sparse but systematic outer band of Baillarger (b) that was slightly separated from the radial fibers (Fig. 3C) or directly in contact with them (Fig. 4C), and by sparse but distinct fibers that were randomly orientated in layer 3. The border with IAPL was marked by the sudden replacement of the rather long radial fibers with a thin plexus of rather horizontal fibers running along the highly myelinated white matter (*). The border with IAPM was marked by a sudden drop in the length of penetration of the grey matter by the radial fibers (**).

At the anterior levels, in particular in the planer cortex, IAL was typically but not exclusively bordered laterally by *orbital prefrontal area 12o* (12o) and by the *median agranular area of the insula* (IAM). In the Nissl stain (Fig. 3E and 4E), like in the anterior levels, IAL had a broad layer 3 with a subtle subdivision in sub-layers 3a and 3b, a slightly vague separation between layers 3 and 5, a broad layer 5 with large cells and a distinct subdivision into sub-layers 5a and 5b, and a rather broad layer 6 mingled with the white mater. However, unlike in the anterior levels, there was a distinct but not as sharply demarcated layer 2. The border with 12o was marked by a thinner

layer 3 and a denser layer 5 (and in particular sublayer 5a) in which the cells were however markedly smaller than in IAL. The border with IAM was marked by broader layers 3 and 5 that were however poorly separable and populated with also markedly smaller cells than in the layer 5 of IAL. In the Gallyas stain (Fig. 3F and 4F), IAL was characterized, like in the anterior levels, by straight radial fibers ending approximately at the limit between sub-layers 5b and 5a and a subtle outer band of Baillarger that was either slightly separated from (Fig. 3F) or directly abutting (Fig. 4F) the radial fibers. The border with 12o was marked by a sudden elongation and higher density of the radial fibers. The border with IAM was marked by a sudden drop of the length of the fibers and a more diffuse fan-like pattern (**).

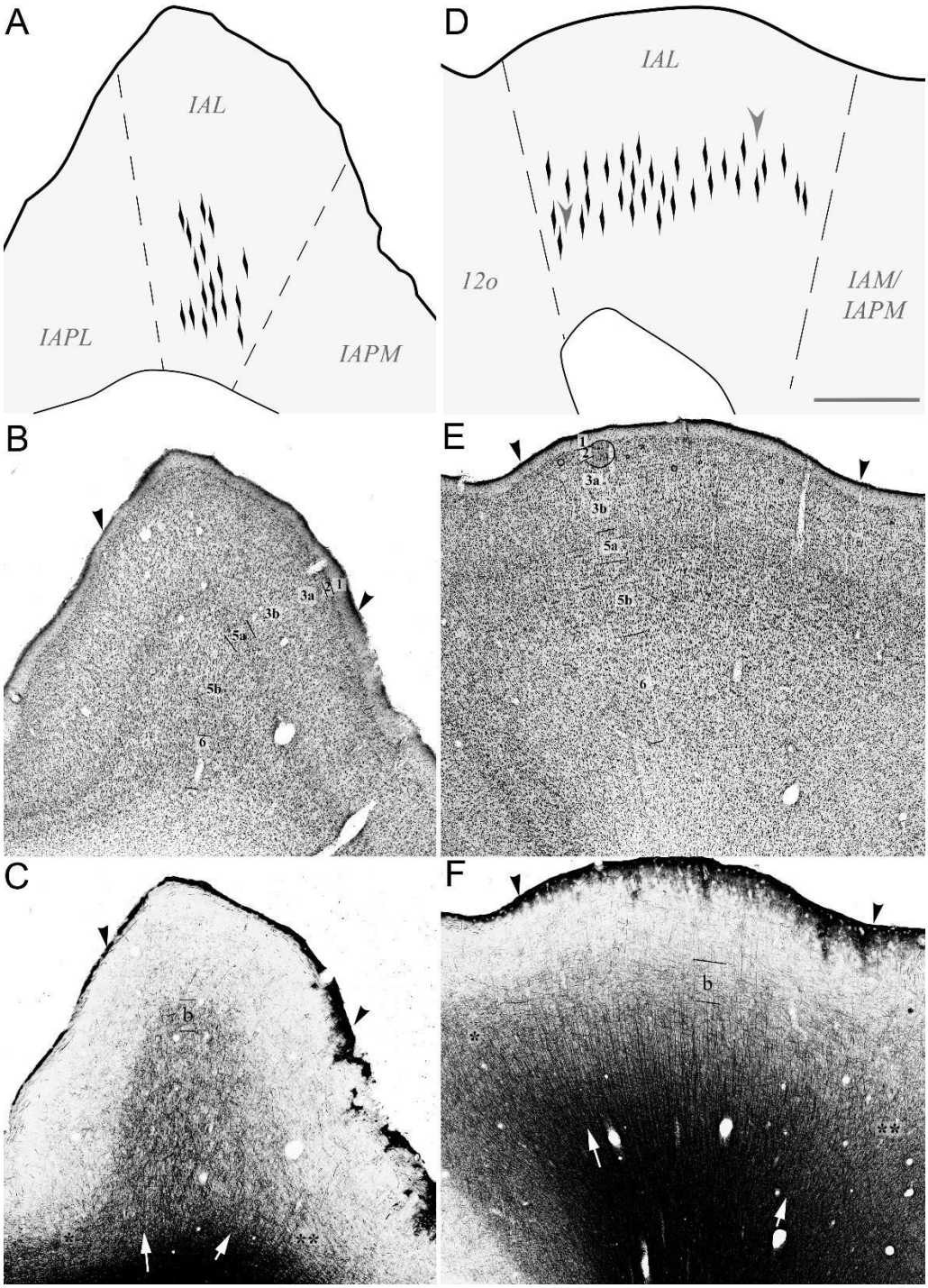

Figure 4 A-C Localization of the VEN and FN and the cyto- and myeloarchitectonic features of EVN

Manuscript II

Elemental localization of von Economo neurons in the dysgranular insula in macaque monkeys

Felicitas M. Horn[1,2,3], Nikos K. Logothetis[2,4], Henry C. Evrard[1,2,*]

[1]Functional and Comparative Neuroanatomy Laboratory, Werner Reichardt Center for Integrative Neuroscience, Tuebingen, Germany; [2]Max Planck Institute for Biological Cybernetics, Tuebingen, Germany; [3]International Max Planck Research School, Tuebingen, Germany; [4]Imaging Science and Biomedical Engineering, University of Manchester, Manchester, UK

*Corresponding author: Henry.Evrard@tuebingen.mpg.de

Keywords: architectonics, non-human primate, insular cortex, von Economo neuron, Fork neuron, interoception, autonomic nervous system, awareness, emotion, cognition, subjective feelings

Abstract

The insular cortex in macaque monkeys has been recently parcellated into 15 distinct architectonic areas, including 4 granular, 4 dysgranular, and 7 agranular areas. Some of these areas, in particular in the dysgranular sector, contained even smaller sub-areas that have each a distinct connectivity pattern with the rest of the brain, which is in line with the idea of a heterogeneous cerebral cortex comprising rather small structurally and functionally distinct modules. In addition of the modular architecto-hodological overlap, we recently showed that one ventral agranular area specifically contains two special neuronal morphotypes, the von Economo neuron (VEN) and the fork neuron (FN). In the present study, we demonstrated the existence of a second, spatially separate and sparser cluster of VEN and FN in the ventral dysgranular 'mound' area of the insula (Idm). In most cases where only one 'mound' occurred, the cluster coincided with the boundaries of a specific architectonic sub-area (Idm3). Notably, in cases where the ventral portion of the insula contained two mounds, the VEN occurred in two specific modules, one atop of each mound. The finding of a second cluster of VEN and FN in the macaque insula supports the idea of granular-to-dysgranular-to-agranular hierarchy in which dysgranular processing could already influence autonomic processes via direct efferent projections to the brainstem, leaving however the bulk of such regulation to the AIC. The existence of two distinct topologies (single versus double mound) is reminiscent of the single and double parallel cingulate sulci in humans. New functional and tracing studies are now clearly needed to compare the agranular and dysgranular VEN areas, and to determine if there exist any behavioral distinctions between single and double mounded monkeys.

Introduction

It is a widely accepted concept that the mammalian brain is not a homogeneous entity but has a topographic organization into unique modules with specific anatomical and functional properties and intra and inter-areal connections. However, the modules are not by themselves sufficient to accomplish sensory and motor functions or cognitive processes. The unique modules are grouped into larger, regionally distinct cortical areas (or subcortical nuclei), which are integrated into large-scale functional networks with a dynamic interaction and exchange of information underlying all cortical processes and behavior (Genon et al., 2018).

One cortical area that has been shown to be most frequently activated in functional neuroimaging studies is the insular cortex (Craig, 2009b; Duncan and Owen, 2000; Kurth et al., 2010). This cortical region plays a crucial role in the integration and representation of homeostatic feelings, which is the physiological status of all tissues of the body. Classical anatomical studies showed that the primate insular cortex is organized into three major sectors, a granular sector, a dysgranular sector , and an agranular sector (Evrard et al., 2014; Gallay et al., 2012; Mesulam and Mufson, 1982b; Morel et al., 2013; Rose, 1928) and it is suggested that each of these three sectors contributes individually to the overall role of the insular cortex (Evrard, 2019). The posterior granular insula is suggested to represent the actual, 'objective' physiological changes of the body (e.g. increase in temperature) that are subsequently integrated with homeostatic motor functions and salient multi-modal sensory input of the environment in the dysgranular sector. In the agranular insula, integration of motivational, social, emotional, and cognitive activity occurs and furthermore, in contrast to the objective representation within the granular sector, the agranular sector is active during the subjective perception of the physiological changes (Craig, 2009a). Another specialty of the anterior agranular insula is the presence of a high concentration of two specialized neuronal morphotypes, the von Economo neurons (VEN) and the fork neurons (FN). Within the entire brain, only the anterior cingulate cortex (ACC) has a similarly high numerical concentration of these two neurons.

The anterior insula and ACC, with the VEN and FN, are of clinical significance since they are the most commonly affected cortical regions in neuropsychiatric disorders (Goodkind et al., 2015; Nagai et al., 2007). Clinical and anatomical evidence suggests that the human anterior agranular insula, also referred to as frontoinsula (FI) (Allman et al., 2005), and the VEN and FN are fundamental for the generation of subjective feelings based on bodily states. The FI and in particular the VEN and FN are selectively depleted in the behavioral variant of the frontotemporal lobe dementia (bvFTD), which is characterized by deficits in social-emotional behavior and a loss of self-conscious experiences (Kaufman et al., 2008; Nana et al., 2019; Seeley et al., 2006). Recently these neurons drew attention as a potential crucial cellular contributor to the emergence of human self-conscious feelings (Allman et al., 2005; Craig, 2009; Butti et al., 2013).

Along with the concept of brain parcellation, Evrard and colleagues demonstrated that each of the three aforementioned insular sectors consists of distinct architectonic modules; they identified four granular, four dysgranular, and seven agranular modules (Evrard et al., 2014). So far, the exact functional organization of the primate insular cortex is uncertain as of yet, but it is already known that not just the insula as a whole but each individual module has a distinct

connectivity pattern with the rest of the brain (Krockenberger et al., *submitted*). Another recent anatomical study of the areal distribution of the VEN and FN within the agranular insula in macaque monkeys revealed an elemental localization of these neurons within one particular architectonic agranular area or module, called the lateral agranular area of the insula (Ial) (Horn, F.M & Evrard, H.C, *in preparation*). The ventral agranular insula, including Ial, as well as the ventral and mound dysgranular areas - but not the dorsal dysgranular and granular areas - have been shown to be densely interconnected with mostly limbic regions, such as the basal and lateral nuclei of the amygdala, ventral striatum, including the shell of the nucleus accumbens, and the limbic ACC (Chikama et al., 1997; Mufson et al., 1981; Stefanacci and Amaral, 2000). Additionally, the agranular and ventral dysgranular insula do not just share a similar connectivity profile but both regions also reveal a prominent cortical convexity or mound. Within the macaque agranular insula, the area containing VEN and FN is always particularly located in and around a similar but distinct cortical convexity, just anterior and in continuation with the limen insula (Horn et al., *in preparation*). Therefore, it was suggested that there could be another VEN area within the mound dysgranular insula. By analyzing the cyto-and myeloarchitecture of the dysgranular insula on consecutive coronal sections of the left and right hemisphere in two species of macaque monkeys, another VEN and FN cluster within the mound dysgranular insula has been identified. This finding increases the opportunity to invasively study the function of these neurons, and hence the area, which may eventually contribute to the understanding of the functional organization of the insula.

Material and Methods

The present data were obtained from the brains of three rhesus (*Macaca mulatta*) and three cynomolgus (*Macaca fascicularis*) macaque monkeys (3-8 years old; average weight 7.3 kg; 2 females). All housing and experimental protocols were implemented with great care to ensure animal welfare. They were approved by the local German authorities and they followed the European directive 2010/63/EU on the protection of animals used for experimental and other scientific purposes.

All the animals were used previously in the context of a separate study (i.e. fMRI and tract-tracing) that required euthanasia, transcardial perfusion and fixation of the brain. The procedures for the fixation, sectioning of the brain, and histological processing were described in detail elsewhere (Evrard et al., 2014). Briefly, immediately after euthanasia with a lethal

overdose of sodium pentobarbital (60–80 mg/kg i.v.), the brain was rinsed, fixed and cryoprotected using a sequence of transcardial perfusion including 0.9% heparinized saline at room temperature (RT), followed by 4% paraformaldehyde in phosphate buffer (0.1 M, pH 7.4, RT), and then by 4% paraformaldehyde and 5% sucrose in PB (0.1 M, pH 7.4, RT). The brain was then removed and further cryoprotected in 0.01 M PBS (pH 7.4) containing 30% sucrose and 0.1% sodium azide for at least 7 days at 4ºC. For histological processing, the brains were frozen and cut in 50 µm-thick coronal sections using a horizontal sliding microtome. The serial sections were then separated into six or eight sets of 1-in-6 or 1-in-8 series, respectively. In all cases, the first set was used for a standard Nissl stain using cresyl violet (0.16% in 3.75% ethanol); the second set was used for a standard Gallyas stain of myelin using silver nitrate (Gallyas, 1979). Among the remaining sets, some were used in immunohistochemistries for various proteins and the others were used for the separate examination of tract-tracing results.

All Nissl- and Gallyas-stained sections containing the insular cortex were digitally photomicrographed at one focal plane in the middle of the section and at a 0.4 µm in-plane resolution using a digitizing microscope (AxioScan.Z1; Carl Zeiss GmbH, Göttingen, Germany) equipped with a 10x/0.45 plan-apochromatic objective and a Hitachi HV-F202SCL digital camera (Hitachi Europe, Düsseldorf, Germany). The resulting pyramid files were converted into 'low magnification' jpg images that were used for the localization of the insular architectonic boundaries. In addition, the region of the Nissl-stained sections that contains the insula was digitally photomicrographed at 20 distinct consecutive focal planes (z-stack with a 1 µm inter-slice interval across a 21 µm range) and at a 0.2 µm in-plan resolution with, this time, a 20x/0.8 plan-apochromatic objective. The resulting 3-dimensional 'high magnification' images were used for the localization of the VEN and FN. Scrolling back and forth through the z-stack image allowed a clear visualization and verification of the cellular morphology, with an apparent visual sharpness of the objects that was similar to that experienced using conventional microscopy.

The two sets of images ('low' and 'high' magnifications) were analyzed in two separate phases by two independent observers (FMH and HCE). First, the localization of each VEN and FN occurring in the insula was charted using the high resolution images with a custom-designed software allowing to 'scroll' through the different slices of the z-stack of the pyramid image files (or 'virtual sections') in order to accurately recognize the different neuronal morphotypes. The criteria for a neuron to considered as a VEN were a laminar localization in layer 5b, a unique basal dendrite and an equally thick apical dendrite, an elongated spindle-shaped perikaryon with a centered nucleus and nucleolus that is as large as or larger than the local

pyramidal neurons, a rather symmetrical morphology along both the vertical and longitudinal axes (Nimchinsky et al., 1999). The criteria for a FN were a unique basal dendrite and a bifid or "forked" apical dendrite, a rather triangular perikaryon as large as or larger than the local pyramidal neurons (Ngowyang, 1932). Second, the Nissl- and Gallyas-stained sections were examined using the low magnification images to localize the cyto- and myeloarchitectonic boundaries of the insular areas, using criteria defined in a prior study (Evrard et al., 2014). This architectonic mapping was made with a relatively long time delay after the VEN and FN charting and without having any access to the charts in order to avoid a biased parcellation. Finally, the plots of the VEN and FN and the architectonic outline of the insular areas from both hemispheres were aligned in Adobe Illustrator (Adobe System Inc., San José, California, USA) for comparison of cell and border locations, and for the preparation of figures.

Results

A careful examination of the entire insular cortex using the high magnification pyramid image files revealed the presence of unequivocal VEN and FN in a in the dysgranular sector of the insula, precisely within the characteristic ventral convexity or 'mound', which has previously been defined as the 'mound dysgranular area of the insula, or Idm (Evrard et al., 2014). The VEN had the typical large spindle-shaped perikaryon with a unique thick basal dendrite and an equally thick apical dendrite (von Economo, 1926). The FN has the typical triangular perikaryon with a single thick basal dendrite and bifid apical dendrite (Ngowyang, 1932). Neither the VEN nor the FN were found in other parts of the insular cortex.

The VEN and FN in the mound region of the insula were generally sparser than in AIC (Evrard et al., 2012) but still co-mingled within one or two clusters - depending on the morphology of the mound - rather than being randomly dispersed. In our prior architectonic study, we illustrated that the mound can actually contain one convexity (single mound) or two adjacent convexities (double mound) separated by a shallow but distinct ridge (Evrard et al., 2014). In this study, the number of VEN areas was equivalent to the number of mounds. Figures 1 to 4 show sets of VEN and FN plots with their matching pair of Nissl and Gallyas photomicrographs. Figures 1, 2 and 3 illustrate cases with a single mound and a single VEN and FN cluster. Figure 4 illustrates cases with a double mound and a corresponding pair of VEN and FN clusters.

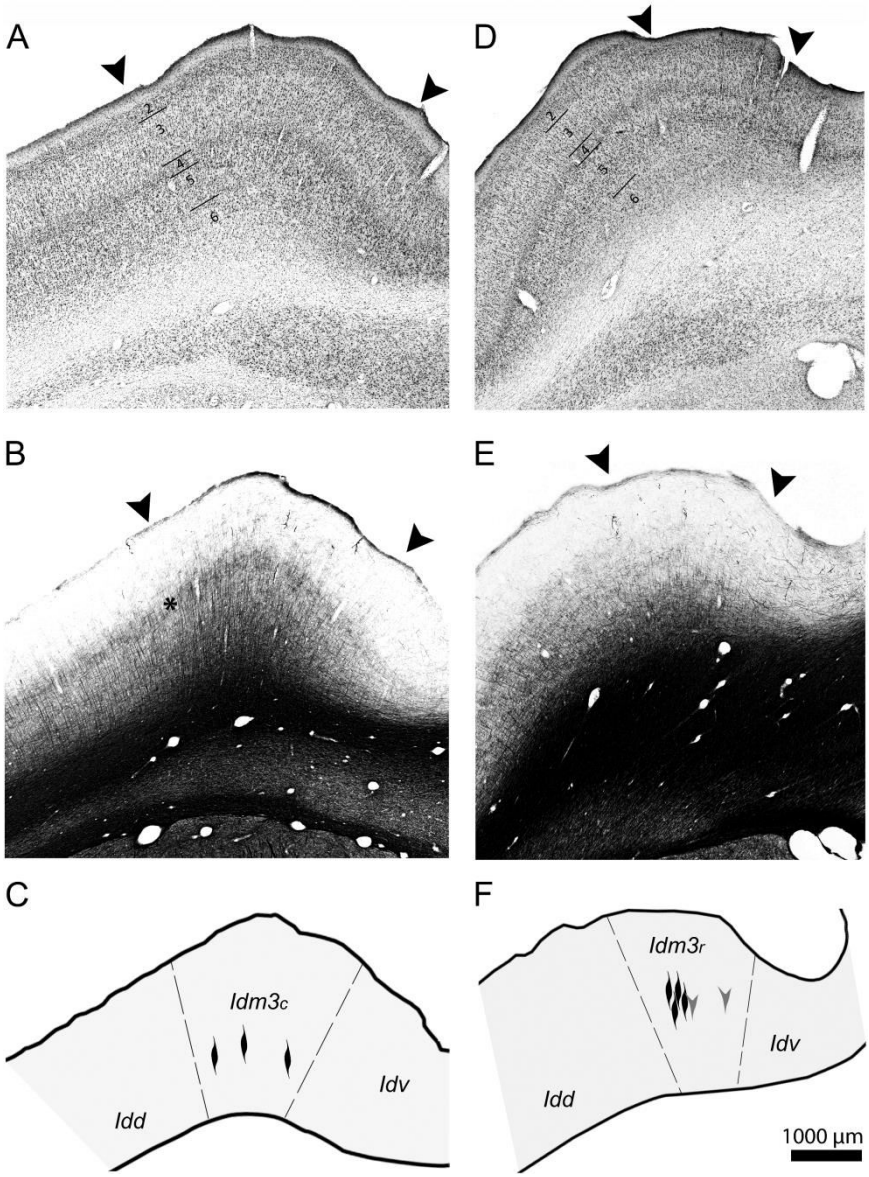

Figure 1: Medium-resolution photomicrographs of two adjacent coronal sections of the dysgranular insula of one rhesus monkey. A and **D** Nissl and **B** and **E** Gallyas (myelin) staining techniques. These pairs of photomicrographs illustrate the cyto- and myeloarchitectonic characteristics of the caudal (Idm3c) and rostral (Idm3r) components of area Idm3 in the dysgranular insula. A-C are sections taken from a more posterior plane, while **D-F** are sections taken from a more anterior plane. The plots in **C** and **F** show the localization of the VEN and FN within both components of area Idm3. Arrowheads mark the borders of these areas with their medial and lateral neighboring dysgranular regions Idd and Idm. The delimitation of the cortical layers 2-6 is indicated left in the mound of the insula in panel **A** and **D**; VEN and FN are illustrated by the black spindles and the grey triangular shapes, respectively; the asterisk marks the outer band of Baillarger; Idd: dorsal dysgranular area of the insula; Idm3: subarea 3 of the mound dysgranular area of the insula; Idm3c: caudal component of area Idm3; Idm3r: rostral component of area Idm3; Idv: ventral dysgranular area of the insula, left is dorsal, top is lateral; scale bar = 1000 µm.

In the single mound cases with a single VEN/FN cluster (4 out of 6; Fig. 1-3), the examination of the cyto- and myeloarchitectonic organization of the dysgranular insula revealed that the delimitation of the single VEN/FN cluster coincided ideally with the architectonic boundaries of the most ventral sub-area of Idm termed Idm3 (Evrard et al., 2014). Within that area, we, however, could systematically recognize a rostral and a caudal component: $Idm3_r$ and $Idm3_c$. In the Nissl stain, area $Idm3_r$ has a broad layer 2 and a less densely populated layer 3; the granule layer 4 is present, but the most prominent feature is the sublaminated layer 5; a lighter and less densely populated layer 5a as well as large and darkly stained neurons in layer 5b are forming a dark band giving it a striped appearance (Fig. 1D, Fig. 2 A, D, G). In the Gallyas stain, $Idm3_r$ shows an array of long vertical fibers ranging from layer 6 to 4 that are crossed by short and thin horizontal fibers (Fig. 1E, Fig. 2B, E, H).

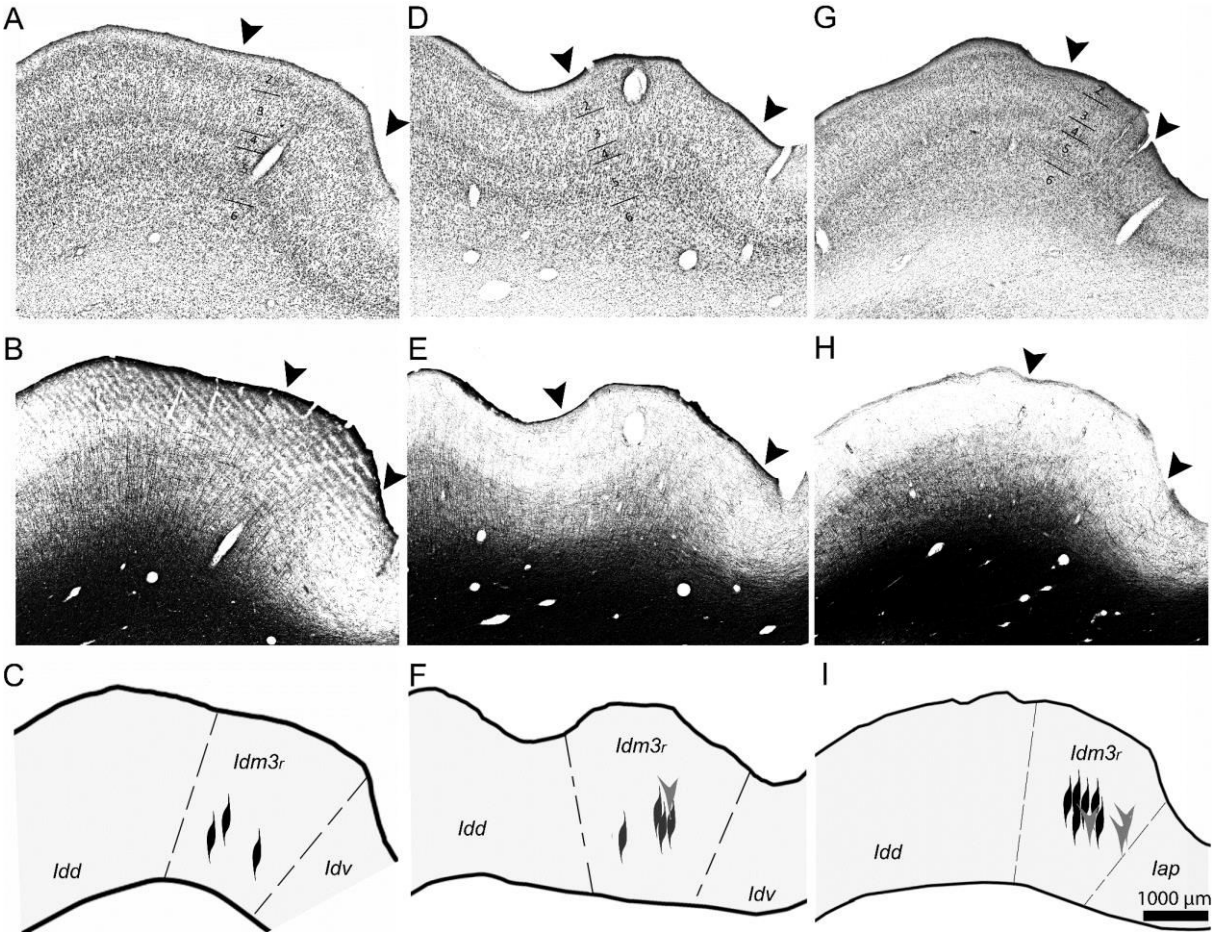

Figure 2: Medium-resolution photomicrographs of two adjacent coronal sections of the dysgranular insula of one cynomolgus (A-C) and two rhesus monkeys (D-I). The photomicrographs are taken at comparable levels. **A, D, G** Nissl and **B, E, H** Gallyas (myelin) staining techniques. These pairs of photomicrographs illustrate the cyto- and myeloarchitectonic characteristics of the rostral component of area Idm3 ($Idm3_r$) in the dysgranular insula in a more anterior plane. The plots in **C, F, I** show the localization of the VEN and FN within cortical area $Idm3_r$. Arrowheads mark the borders of these areas with their medial and lateral neighboring dysgranular regions Idd and Idv or Iap2. The delimitation of the cortical layers 2-6 is indicated left in the mound of the insula in panel **A, D** and **G**; VEN and FN are illustrated by the black spindles and the grey triangular shapes, respectively; Iap: posterior agranular area of the insula; Idd: dorsal dysgranular area of the insula; Idm3: subarea 3 of the mound dysgranular area of the insula; $Idm3_r$: rostral component of area Idm3; Idv: ventral dysgranular area of the insula, left is dorsal, top is lateral; scale bar = 1000 µm.

As for the difference between the two sub-areas, in the Nissl stain, $Idm3_r$ differs from $Idm3_c$ by its less prominent sublamination of layer 5. The striped appearance of $Idm3_r$ is not present. However, the columnar organization described is more prominent in $Idm3_c$ (Fig. 1A, Fig. 3 A, D, G). In the Gallyas stain, $Idm3_c$ also has an array of long and thick vertical fibers but with an increased density as compared to $Idm3_r$. This array is crossed by an outer band of Baillarger, which increases in thickness and density from ventral to caudal (Fig. 1B and Fig. 3 B, E, H). The rostrocaudal shift of cyto-and myeloarchitecture in Idm3 was robust in all the cases. Fig. 2 and 3 illustrate the cyto- and myeloarchitectonic characteristics of the rostral and caudal portion of Idm3. Photomicrographs of Nissl and Gallyas stained coronal sections are taken from one cynomolgus and two rhesus monkeys in an anterior (Fig. 2) and a more posterior plane (Fig. 3).

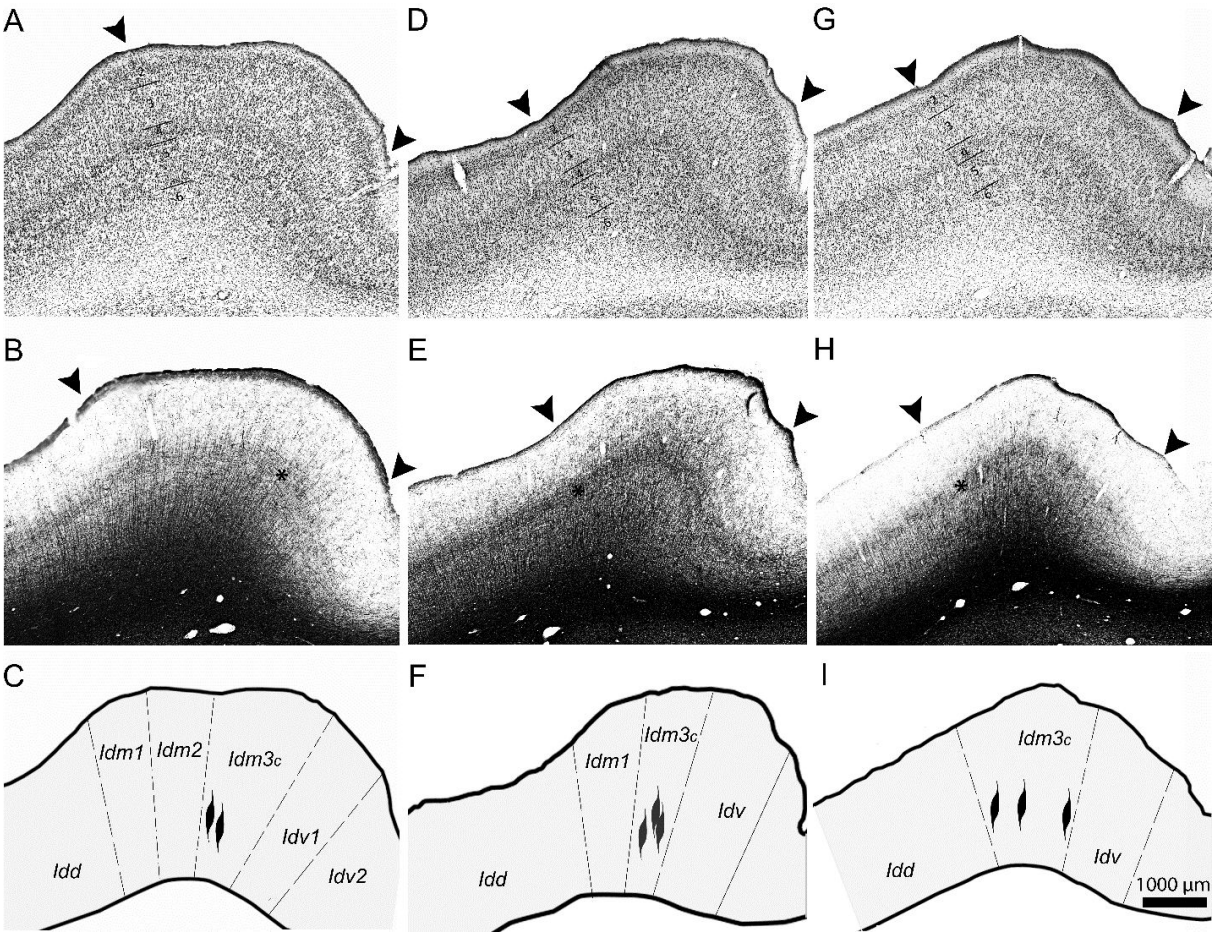

Figure 3: **Medium-resolution photomicrographs of two adjacent coronal sections of the dysgranular insula in one cynomolgus (A-C) and two rhesus monkeys (D-I).** The photomicrographs are taken at comparable levels. **A, D, G** Nissl and **B, E, H** Gallyas (myelin) staining techniques. These pairs of photomicrographs illustrate the cyto- and myeloarchitectonic characteristics of the caudal component of area Idm3 ($Idm3_c$) in the dysgranular insula in a more posterior plane as compared to Fig. 2. The plots in **C, F, I** show the localization of the VEN and FN within cortical area $Idm3_r$. Arrowheads mark the borders of these areas with their medial and lateral neighboring dysgranular regions Idd and Idv. The delimitation of the cortical layers 2-6 is indicated left in the mound of the insula in panel **A, D** and **G**; VEN and FN are illustrated by the black spindles and the grey triangular shapes, respectively; the asterisk marks the outer band of Baillarger; Idd: dorsal dysgranular area of the insula; Idm1-3: subareas 1-3 of the mound dysgranular area of the insula; $Idm3_c$: caudal component of area Idm3; Idv1-2: subareas 1-2 of the ventral dysgranular area of the insula, left is dorsal, top is lateral; scale bar = 1000 µm.

Two cases presented a double dysgranular mound. One monkey had two prominent mound areas on both, the left and right hemisphere, and the other monkey revealed two mound areas on only the left hemisphere. Interestingly, in both monkeys, the two mound areas contained VEN and FN. A comparison of the cytoarchitecture of these two mound regions revealed that the dorsal mound VEN cluster corresponded most closely to area Idm1 (Evrard et al., 2014) whereas the ventral VEN cluster corresponded to Idm3. The architectonic of Idm1 did not vary across its rostrocaudal extent (Fig. 4 A, B). The architectonic of Idm3 did vary and showed the same caudal and rostral sub-areas then in the single mound cases: $Idm3_c$ and $Idm3_r$ (Fig. 4 D, E). In the three cynomolgus monkeys examined, only one mound area was present.

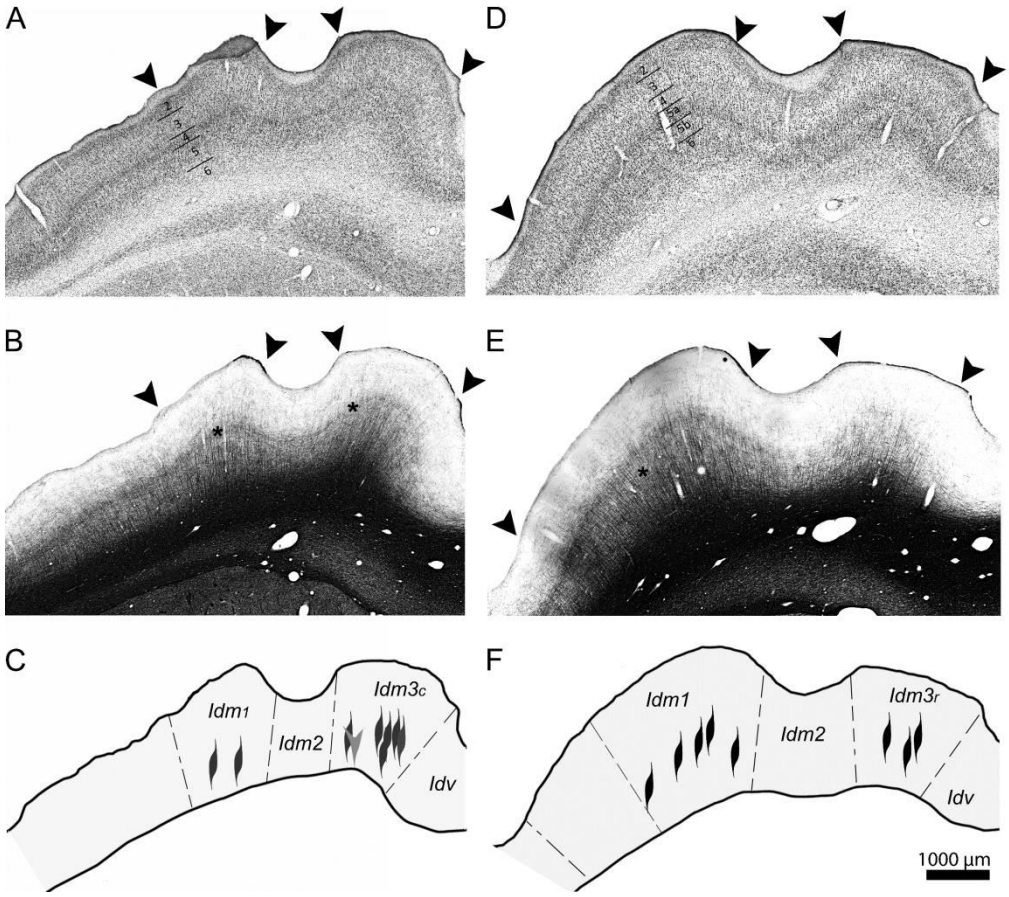

Figure 4: Medium-resolution photomicrographs of two adjacent coronal sections of the dysgranular insula of one rhesus monkey (**D-I**). **A** and **D**: Nissl and **B** and **E**: Gallyas (myelin) staining techniques. These pairs of photomicrographs illustrate the cyto- and myeloarchitectonic characteristics of Idm1 and the rostral and caudal components of Idm3 in the dysgranular insula. **A-C** displays sections from a more posterior plane, where the dorsal mound area is corresponding to Idm1 and the ventral mound area is formed by the caudal component of Idm3. **D-E** show a more anterior section where the dorsal mound area still corresponds to Idm1 but the ventral mound region is formed by the rostral component of Idm3. The plots in **C** and **F** show the localization of the VEN and FN within Idm1, Idm3r, and Idm3c. Arrowheads mark the borders of these areas with their medial and lateral neighboring dysgranular regions Idd and Idv. The delimitation of the cortical layers 2-6 is indicated left in the mound of the insula in panel **A** and **D**; VEN and FN are illustrated by the black spindles and the grey triangular shapes, respectively; the asterisk marks the outer band of Baillarger; Idd: dorsal dysgranular area of the insula; Idm1-3: subarea 1-3 of the mound dysgranular area of the insula; Idm3c: caudal component of area Idm3; Idm3r: rostral component of area Idm3; Idv: ventral dysgranular area of the insula, left is dorsal, top is lateral; scale bar = 1000 µm.

Discussion

Only recently our group demonstrated that in macaque monkeys the ventral agranular anterior insula has one distinct architectonic area harboring two specialized neuronal morphotypes, the VEN and FN. In macaque monkeys the VEN area, which was defined as the lateral agranular area of the insula (Ial) in a previous study (Evrard et al., 2014), is located in and around a distinct cortical convexity of the ventral agranular insula (Horn et al., *in preparation*). Likewise, in this study, we demonstrated the existence of a second sparser cluster of VEN and FN in the ventral dysgranular 'mound' area of the insula (Idm). In most cases only one 'mound' existed in the ventral dysgranular insula. In these cases, the VEN and FN cluster coincided with the architectonic boundaries of a specific sub-area (Idm3). In a few cases, the ventral portion of the insula contained two mounds both containing VEN and FN cluster. In these cases, the dorsal mound always coincided with the architectonic sub-area Idm1, while the ventral mound coincided with the sub-area Idm3. In this study, two cases had a double dysgranular mound; one case presented two mound areas on both, the left and right hemisphere, while the other monkey had two prominent mound areas on the left hemisphere, but only one mound on the right hemisphere. These interhemispheric differences show that the variation in the number of dysgranular mound areas is not case specific. The existence of two distinct topologies (single versus double mound) is reminiscent of the single and double parallel cingulate sulci in humans (Cachia et al., 2016). This group suggested further that the different topologies of cortical folding, which are already determined in early neurodevelopmental processes, reflect different cognitive abilities. Similar to the observation in macaque monkeys the different folding patterns of the ACC were not specific to the individual but differed between hemispheres. Furthermore, it has previously been shown that the primate brain reveals hemispheric asymmetries in many brain regions (Chiu and Damasio, 1980; Cunningham, 1891; Rosen et al., 2015), which could also explain the variety in the number of dysgranular mound areas containing VEN and FN between hemispheres and monkeys. However, more anatomical studies are needed to identify if the double mounded cases always contain two VEN areas. For a comparison of the agranular and dysgranular VEN areas and to determine if there exist any behavioral distinction between single and double mounded monkeys new functional and tracing studies are necessary to compare the agranular and dysgranular VEN areas,.

Besides, it was notably that in all the cases, the ventral mound was subdivided into a rostral and a caudal component, $Idm3_r$ and $Idm3_c$, respectively, that slightly varied in their architecture along the rostrocaudal axis. This rostrocaudal shift also existed in the agranular

VEN area as well as in one of the human VEN areas, VEN1, which is also situated at a distinct cortical convexity (Horn et al., *in preparation*). This rostrocaudal architectonic shift was not present in Idm1. The differences in cyto-and myeloarchitecture between the rostral and caudal portions in all VEN areas mentioned above were less compared to the adjacent areas. Therefore, it is suggested that the two components are rather sub-areas of one architectonic area instead of being two distinct architectonic areas.

Idm is part of the ventral dysgranular insula and together with the agranular insular cortex, including area Ial, it is heavily connected with cortical and subcortical regions of the limbic system. Retrograde tracers injected within the lateral dorsal, medial basal, cortical, and accessory basal nuclei of the amygdala labelled agranular and dysgranular regions and it has been shown that these connections are reciprocal (Mufson et al., 1981; Stefanacci and Amaral, 2000). Furthermore, injections of retrograde tracers in the agranular and ventral dysgranular insula showed the connectivity to the shell and ventral striatum including the shell of the nucleus accumbens (Chikama et al., 1997), and the cingulate cortex (Mesulam and Mufson, 1982c). The connectivity of the agranular and ventral dysgranular insula with the amygdala and the ventral striatum is suggested to convey somatosensory, visceral, auditory, and olfactory sensations and taste to the limbic system and to contribute to (reward-related) feeding behavior and autonomic regulations (Chikama et al., 1997; Mesulam and Mufson, 1982a; Mufson et al., 1981). It has been shown that these neurons express several proteins that play a role in processes for food regulation, the immune responses and pain sensitivity such as neuromedin B (NMB) and gastrin-releasing peptide (GRP), activating-transcription factor 3 (ATF3), and interleukin 4 receptor (IL4Rα) (Allman et al., 2010; Stimpson et al., 2011). The VEN's and FN's gene expression profile suggest a role in the control of food intake, the modulation of autonomic responses, and in the monitoring of the gut and the homeostatic state of one's body (Allman et al., 2010; Stimpson et al., 2011) and could support the role of the anterior agranular and ventral dysgranular insula in autonomic functions associated and feeding behavior.

Furthermore, retrograde tracer injection into the dorsolateral periaqueductal grey (PAG) produced labelling within the agranular and ventral dysgranular mound areas (An et al., 1998), in which the VEN areas are situated. More precisely, preliminary results of tract-tracing studies in our laboratory showed retrogradely labeled neurons in the agranular and both dysgranular VEN regions after injections of tracers into the lateral column of PAG (lPAG), while injections into the ventrolateral column of PAG only labelled the VEN area within the agranular insula. This suggests that the insular VEN and FN partly function together, but also have different roles. This idea is further supported by thalamo-insular projections within the primate cerebral

cortex. The primate insular cortex receives direct input from two thalamic nuclei, the ventral medial nucleus of the thalamus (VMb) and ventromedial posterior nucleus (VMpo) (Craig et al., 1994). Interoceptive afferents from the organs, which are conveyed by the spinal cord, and interoceptive afferents from the cranial nerves, which are transmitted by the NTS, are relayed in the VMb and VMpo, respectively, and terminate in the so called primary interoceptive cortex (PIC). In primates PIC occupies the anterior (Idfa) and posterior dorsal fundus of the insula (Idfp) (Craig, 2014; Evrard and Craig, 2015). Furthermore, it has been shown that the VMb projects primarily to Idfa and VMpo to Idfp (Craig, 2014). However, these two thalamic nuclei also have a second target site within the primate insular cortex; it has been shown that the VMb project directly to Ial (Carmichael and Price, 1995), while the VMpo projects to Idm (Craig, 2014) suggesting a different role of the VEN and the FN in the agranular and dysgranular insula. The different functions of these regions are uncertain as of yet. However, the presence of a second VEN and FN cluster in the dysgranular insula of macaque monkeys supports the idea of granular-to-dysgranular-to-agranular hierarchy in which dysgranular processing could already influence autonomic processes via direct efferent projections to the brainstem, however, leaving the majority of such regulation to the AIC.

The presence of a second VEN area is also in line with the elemental localization of the VEN in the agranular insula in macaque monkeys and humans (Horn, F.M. & Evrard, H.C. *in preparation*, Horn F.M. & Evrard, H.C. *in preparation*). In both species, all clusters of VEN and FN robustly overlap with the architectonic borders of specific architectonic areas, suggesting a common function, hodology, and fate for the neurons and their host area. The presence of two VEN areas within the insular cortex in macaque monkeys offers advantage for the examination of the VEN areas and its two specialized neuronal morphotypes. This may help to unravel the mystery of the functional organization of the primate insular cortex and could eventually be beneficial for the understanding of neuropsychiatric disorders involving the insular cortex and VEN and FN.

References

Allman JM, Tetreault NA, Hakeem AY, Manaye KF, Semendeferi K, Erwin JM, Park S, Goubert V, Hof PR. 2010. The von Economo neurons in frontoinsular and anterior cingulate cortex in great apes and humans. Brain Struct Funct 214(5-6):495-517.

Allman JM, Watson KK, Tetreault NA, Hakeem AY. 2005. Intuition and autism: a possible role for Von Economo neurons. Trends Cogn Sci 9(8):367-373.

An X, Bandler R, Ongur D, Price JL. 1998. Prefrontal cortical projections to longitudinal columns in the midbrain periaqueductal gray in macaque monkeys. J Comp Neurol 401(4):455-479.

Brodmann K. 1909. Vergleichende Lokalisationslehre der Grosshirnrinde in ihren Prinzipien dargestellt und Grund des Zellenbaues. Leipzig: Verlag von Johann Ambrosius Barth.

Cachia A, Borst G, Tissier C, Fisher C, Plaze M, Gay O, Riviere D, Gogtay N, Giedd J, Mangin JF, Houde O, Raznahan A. 2016. Longitudinal stability of the folding pattern of the anterior cingulate cortex during development. Developmental cognitive neuroscience 19:122-127.

Carmichael ST, Price JL. 1995. Limbic connections of the orbital and medial prefrontal cortex in macaque monkeys. J Comp Neurol 363(4):615-641.

Chikama M, McFarland NR, Amaral DG, Haber SN. 1997. Insular cortical projections to functional regions of the striatum correlate with cortical cytoarchitectonic organization in the primate. J Neurosci 17(24):9686-9705.

Chiu HC, Damasio AR. 1980. Human cerebral asymmetries evaluated by computed tomography. J Neurol Neurosurg Psychiatry 43(10):873-878.

Craig AD. 2009a. Emotional moments across time: a possible neural basis for time perception in the anterior insula. Philos Trans R Soc Lond B Biol Sci 364(1525):1933-1942.

Craig AD. 2009b. How do you feel - now? The anterior insula and human awareness. Nature Reviews Neuroscience 10(1):59-70.

Craig AD. 2014. Topographically Organized Projection to Posterior Insular Cortex From the Posterior Portion of the Ventral Medial Nucleus in the Long-Tailed Macaque Monkey. J Comp Neurol 522(1):36-63.

Craig AD, Bushnell MC, Zhang ET, Blomqvist A. 1994. A thalamic nucleus specific for pain and temperature sensation. Nature 372(6508):770-773.

Cunningham DJ. 1891. Development of the Gyri and Sulci on the Surface of the Island of Reil of the Human Brain. J Anat Physiol 25(Pt 3):338-348.

Duncan J, Owen AM. 2000. Common regions of the human frontal lobe recruited by diverse cognitive demands. Trends Neurosci 23(10):475-483.

Evrard HC. 2019. The Organization of the Primate Insular Cortex. Frontiers in Neuroanatomy 13(43).

Evrard HC, Craig AD. 2015. Insular cortex. Brain Mapping: An Encyclopedic Reference: Elsevier. p 387-393.

Evrard HC, Forro T, Logothetis NK. 2012. Von Economo neurons in the anterior insula of the macaque monkey. Neuron 74(3):482-489.

Evrard HC, Logothetis NK, Craig AD. 2014. Modular architectonic organization of the insula in the macaque monkey. J Comp Neurol 522(1):64-97.

Gallay DS, Gallay MN, Jeanmonod D, Rouiller EM, Morel A. 2012. The insula of Reil revisited: multiarchitectonic organization in macaque monkeys. Cereb Cortex 22(1):175-190.

Genon S, Reid A, Langner R, Amunts K, Eickhoff SB. 2018. How to Characterize the Function of a Brain Region. Trends in Cognitive Sciences Volume 22(Issue 4): 350-364,.

Goodkind M, Eickhoff SB, Oathes DJ, Jiang Y, Chang A, Jones-Hagata LB, Ortega BN, Zaiko YV, Roach EL, Korgaonkar MS, Grieve SM, Galatzer-Levy I, Fox PT, Etkin A. 2015. Identification of a common neurobiological substrate for mental illness. JAMA Psychiatry 72(4):305-315.

Kaufman JA, Paul LK, Manaye KF, Granstedt AE, Hof PR, Hakeem AY, Allman JM. 2008. Selective reduction of Von Economo neuron number in agenesis of the corpus callosum. Acta Neuropathol 116(5):479-489.

Kurth F, Eickhoff SB, Schleicher A, Hoemke L, Zilles K, Amunts K. 2010. Cytoarchitecture and probabilistic maps of the human posterior insular cortex. Cereb Cortex 20(6):1448-1461.

Mesulam MM, Mufson EJ. 1982a. Insula of the Old-World Monkey. III: Efferent Cortical Output and Comments on Function. Journal of Comparative Neurology 212(1):38-52.

Mesulam MM, Mufson EJ. 1982b. Insula of the old world monkey. I. Architectonics in the insulo-orbito-temporal component of the paralimbic brain. J Comp Neurol 212(1):1-22.

Mesulam MM, Mufson EJ. 1982c. Insula of the old world monkey. II: Afferent cortical input and comments on the claustrum. J Comp Neurol 212(1):23-37.

Morel A, Gallay MN, Baechler A, Nyss M, Gallay DS. 2013. The Human Insula: Architectonic Organization and Postmortem Mri Registration. Neuroscience 236:117-135.

Mufson EJ, Mesulam MM, Pandya DN. 1981. Insular interconnections with the amygdala in the rhesus monkey. Neuroscience 6(7):1231-1248.

Nagai M, Kishi K, Kato S. 2007. Insular cortex and neuropsychiatric disorders: a review of recent literature. Eur Psychiatry 22(6):387-394.

Nana AL, Sidhu M, Gaus SE, Hwang JL, Li L, Park Y, Kim EJ, Pasquini L, Allen IE, Rankin KP, Toller G, Kramer JH, Geschwind DH, Coppola G, Huang EJ, Grinberg LT, Miller BL, Seeley WW. 2019. Neurons selectively targeted in frontotemporal dementia reveal early stage TDP-43 pathobiology. Acta Neuropathol 137(1):27-46.

Ngowyang G. 1932. Beschreibung einer Art von Spezialzellen in der Inselrinde-zugleich Bemerkungen über die v. Economoschen Spezialzellen. J Psychol Neurol 44:671-674.

Nimchinsky EA, Gilissen E, Allman JM, Perl DP, Erwin JM, Hof PR. 1999. A neuronal morphologic type unique to humans and great apes. Proc Natl Acad Sci U S A 96(9):5268-5273.

Rose M. 1928. Die Inselrinde des Menschen und der Tiere. Journal of Physchology and Neurology 37:467-624.

Rosen A, Chen DQ, Hayes DJ, Davis KD, Hodaie M. 2015. A Neuroimaging Strategy for the Three-Dimensional in vivo Anatomical Visualization and Characterization of Insular Gyri. Stereotact Funct Neurosurg 93(4):255-264.

Seeley WW, Carlin DA, Allman JM, Macedo MN, Bush C, Miller BL, Dearmond SJ. 2006. Early frontotemporal dementia targets neurons unique to apes and humans. Ann Neurol 60(6):660-667.

Stefanacci L, Amaral DG. 2000. Topographic organization of cortical inputs to the lateral nucleus of the macaque monkey amygdala: a retrograde tracing study. J Comp Neurol 421(1):52-79.

Stimpson CD, Tetreault NA, Allman JM, Jacobs B, Butti C, Hof PR, Sherwood CC. 2011. Biochemical Specificity of von Economo Neurons in Hominoids. Am J Hum Biol 23(1):22-28.

von Economo C. 1926. Eine neue art spezialzellen des lobus cinguli und lobus insulae. Zeitschrift für die gesamte Neurologie und Psychiatrie 100:706-712.

Manuscript III

Evolutionary expansion of the von Economo neuron areas in the human anterior insular cortex

Felicitas M. Horn[1,2,3], Bernhard Hirt[4], Nikos K. Logothetis[2,5], Henry C. Evrard[1,2,*]

[1]Functional and Comparative Neuroanatomy Laboratory, Werner Reichardt Center for Integrative Neuroscience, Tuebingen, Germany; [2]Max Planck Institute for Biological Cybernetics, Tuebingen, Germany; [3]International Max Planck Research School, Tuebingen, Germany; [4]Institut für Klinische Anatomie und Zellanalytik, Eberhard Karls University of Tuebingen, Tuebingen, Germany; [5]Imaging Science and Biomedical Engineering, University of Manchester, Manchester, UK

*Corresponding author: Henry.Evrard@tuebingen.mpg.de

Abstract

The mammalian cerebral cortex is parcellated into many discrete areas, or modules. Some of these areas share common features amongst most mammals, however, between higher and lower mammalian species there are deviations in cortical size, subdivisions, and connectivity. In higher mammals, like primates, the cortex has expanded and was subdivided numerous times resulting in a complex neural system built of smaller modules, grouped within functional units, such as the insular cortex. In macaque monkeys, the insular cortex has been shown to be built of 15 smaller, unique structural and functional modules, with one particular anterior module containing two atypical layer 5b projection neurons, the von Economo neuron (VEN) and the fork neuron (FN). In humans, VEN and FN also occur in the ventral anterior insular cortex (AIC) (alsocalled in humans frontoinsula, FI). However, so far no model of the human anterior insular organization exists and whether the VEN and FN occur in one or more than one module remains unknown. A comparative study across primates has shown that in humans the anterior insula has grown hyperallometrically in relation to the rest of the insula. Here, we hypothesized that the anterior insular cortex in humans is not just larger, but also contains more than one VEN area. We used high- and low-magnification microscopy to analyze the areal distribution of the VEN and FN in the AIC in six human hemispheres. Freshly-fixed tissue from both hemispheres of three human brains were histologically processed and analyzed using pre-established multi-architectonic

comparison criteria. Upon independent examination of the VEN/FN distribution and AIC architecture, we showed that both neurons consistently occur in five distinct architectonic areas. The delimitation of the VEN/FN clusters sharply overlapped with the architectonic borders. The multiplication of the VEN areas in humans (five VEN areas) as compared to macaque monkeys (one VEN area) might be correlated with the disproportionate growth of the AIC in humans as compared to other primate species.

Introduction

Nowadays, it is a widely held view that the cerebral cortex of primates is highly parcellated into discrete units, or "modules", that are specific in terms of their architecture, function, and connectivity with other modules. They are grouped together forming differentiated functional systems (Glasser et al., 2016, Montgomery et al., 2016). It has been shown that mammals share neocortical equivalents, but there is also a high degree of interspecific variability amongst mammals as responses to selective pressures on behavioral changes during evolution (Ebbesson, 1980). It is known that an increase in the complexity of behavior is accompanied by quantitative anatomical changes of the cerebral cortex. Furthermore, it was suggested that these species-specific differences in brain anatomy, size, and functional complexities are due to parcellation processes during the evolution of complex behaviors and linked analytical capacities (Smaers et al., 2011). Therefore, higher parcellation indicates greater functional and structural modifications for more sophisticated cognitive processes (Ebbesson, 1980, Northcutt and Kaas, 1995). Comparison of the insular cortex across multiple mammalian species revealed great variability in its morphology, gyrification, and cytoarchitectonic organization: in lissencephalic, or animals, which have smooth-surfaced cortices, the insular cortex is located on the lateral surface of both hemispheres, and has a ventral agranular, and dorsal granular region, divided into an anterior and a posterior portion, respectively (Rose, 1928). In most gyrencephalic mammals, which have convolutions in the cortex, the insular cortex is buried behind the frontoparietal, and temporal opercula, or presents at least a partial infolding (Butti and Hof, 2010). Despite similar convolution patterns, the cytoarchitectonic organization differs between the species; whilst, for example, most cetaceans and artiodactyls, as well as bats, display and entirely agranular insular cortex; the hedgehog displays two agranular areas, a dorsal and a ventral agranular area (Butti and Hof, 2010,

Hof and Van der Gucht, 2007, Rose, 1928); whilst the dog's insular cortex is separated into one agranular and one dysgranular area (Salazar et al., 1988); (Butti and Hof, 2010, Rose, 1928). However, most mammals, e.g. primates reveal the classical tripartition into an agranular, a dysgranular, and a granular sector (Mesulam and Mufson, 1985, Rose, 1928). Furthermore, Evrard and his team showed the insular cortex in macaque monkeys can be further subdivided into no less than 15 different architectonic areas. Four of these areas are forming the dorsoposterior granular sector four are forming the intermediate dysgranular sector, and the remaining seven areas are forming the anterior insular cortex (AIC) (Evrard et al., 2014). The modular organization of the primate insular cortex is further underpinned by tract-tracing studies in macaque monkeys, demonstrating the exact overlap of architectonic borders with labelling patterns produced by antero- and retrograde tracers injected into other brain areas (Krockenberger et al., *submitted*). These findings suggest that each module of the primate insular cortex has a distinct hodological pattern and function. However, the architectonic organization of the entire human insular cortex has not been established yet, but examinations of the posterior insular cortex in humans, based on a probabilistic approach, revealed a similar overall organization to the posterior insular cortex in macaque monkeys (Kurth et al., 2010). Furthermore, a comparative study across several primate species suggests that the human insular cortex, and even more the ventral AIC, has grown hyperallometrically as compared to the rest of the cortex (Bauernfeind et al., 2013).

The AIC, together with the anterior cingulate cortex (ACC), is crucial for the integration of brain and bodily states. The AIC integrates interoceptive feelings with multimodal brain activity and is involved in the embodiment of emotional and cognitive processes, resulting in the representation of the homeostatic self. The AIC and ACC both are components of a large-scale network that is involved in detecting salient stimuli in the stream of all internal physiological (interoceptive) and external sensory signals for the adjustment of (social) behavior and autonomic functions to maintain or achieve homeostasis (Menon and Uddin, 2010). The AIC and ACC both host two specialized neurons, the von Economo neuron (VEN) and the fork neuron (FN). These neurons are specialized cortical layer 5b projection neurons. In humans and macaque monkeys, the highest concentration of these neurons has been found in the ACC, and the ventral AIC, which in humans is also referred to as frontoinsula (FI) (Allman et al., 2010, Evrard et al., 2012).

The FI and ACC, with their special neurons, are of clinical importance, since these cortical regions are most commonly affected in neuropsychiatric disorders (Goodkind et al., 2015, Nagai et al., 2007). VEN and FN are specifically vulnerable in many neuropsychiatric disorders with metacognitive deficits, such as impaired self-awareness and self-regulation and disturbed social conduct (Seeley et al., 2006, Kaufman et al., 2008). In particular, the behavioral variant of the frontotemporal dementia (bvFTD), characterized by social-emotional deficits and a loss of emotions related to the self, the selective depletion of VEN and FN in the ventral part of the AIC is one of the early onset makers. The severity of the clinical symptoms correlates with the degree of VEN and FN degeneration (Kim et al., 2012). However, the exact function of these neurons still remains unknown.

Recently, our laboratory has shown that the cluster of VEN and FN within the AIC in macaque monkeys was exactly overlapping with the architectonic borders of one specific insular area, previously defined as the lateral agranular area of the insula (Ial) (Evrard et al., 2014), or VEN area (Horn & Evrard, *in preparation*). Preliminary results now suggest that 1) within the human anterior insula the cluster of VEN and FN are exactly overlapping with architectonic areas and 2) there is not just one but several different architectonic VEN areas. Analysis of VEN and FN distribution based on cyto-and myeloarchitecture of the FI on consecutive coronal sections of the left and right hemisphere from three post-mortem human brains revealed that the human FI contains five specific architectonic VEN areas.

The exact localization of the VEN and FN within the human FI and comparison of the organization between humans and monkey revealing human specific insular areas could contribute to the understanding of neuropsychiatric disorders in which the insula and VEN are involved.

Material and Methods

Post-mortem specimens

The present data were obtained from the brains (left and right insulae) of three donating *H. s. sapiens* without any known neurodegenerative or neuropsychiatric disorders. The samples were obtained from the tissue bank of the Institut für Klinische Anatomie und Zellanalytik at the Eberhard Karls University of Tuebingen, after consent from the donors and approval of our experiments by the ethic commission of the faculty of medicine of the University of Tuebingen.

Tissue processing and histology

The brains were exhumed and fixed in 4% paraformaldehyde with a post-mortem interval of less than 24 hours. The insulae were dissected and cut into 1-2 cm thick coronal blocks. For cryoprotection the blocks were taken through ascending sucrose gradients (5-30% in 4% paraformaldehyde, pH 7.4) and stored at 4°C. For longtime storage the blocks were transferred to 0.01M phosphate-buffered saline (PBS, pH 7.4) with 30% Sucrose and 0.1% sodium azide and stored at 4°C.

For histological processing, the blocks of human insulae were frozen and cut into 50 µm-thick coronal sections with the use of a horizontal sliding microtome. Subsequently, the serial sections were separated into 10 sets of 1-in-10 series. In all three cases, the first set was used for a standard Nissl stain using a cresyl violet solution (0,25% cresyl violet, 2.35% glacial acetic acid, 1.35% sodium acetate, in $_{dd}H_2O$). The sections were mounted immediately on gelatinized glass slides. The second set was used for a standard Gallyas stain of myelin using silver nitrate (Gallyas, 1979). The sections were collected in a 1:1 solution of PBS and paraformaldehyde (0.01 M PBS: 10% paraformaldehyde) and stored for at least one week at 4°C. The remaining sets were stored in a glycerol solution for longtime storage at -20 °C.

Architectonic analysis and distribution of VEN and FN

All Nissl- and Gallyas-stained sections containing the insular cortex were digitally photomicrographed at one focal plane and at a 0.4 µm in-plane resolution using an Axio Scan.Z1

digitizing microscope equipped with a 10x/0.45 plan-apochromatic objective (Carl Zeiss GmbH, Göttingen, Germany). The resulting files were converted into 'low magnification' tif images (96 dpi resolution) that were used for the localization of the insular architectonic boundaries. Additionally, the region of the Nissl-stained sections containing the anterior insula was digitally photomicrographed at 20 distinct focal planes (z-stack with a 1 µm inter-slice interval across a 21 µm range) and at a 0.2 µm in-plan resolution using the Axio Scan.Z1 with, this time, a 20x/0.8 plan-apochromatic objective. The resulting 3-dimensional 'high magnification' images were used for the localization of the VEN and FN.

The two sets of images ('low' and 'high' magnifications) were analyzed in two separate phases by two independent observers (FMH and HCE). First, the localization of each VEN and FN occurring in the insula was charted using the high resolution images with a custom-designed software allowing to 'scroll' through the different slices of the z-stack in order to accurately recognize the different neuronal morphotypes. The criteria for a neuron to considered as a VEN were a laminar localization in layer 5b, a unique basal dendrite and an equally thick apical dendrite, an elongated spindle-shaped perikaryon with a centered nucleus and nucleolus that is as large as or larger than the local pyramidal neurons, a rather symmetrical morphology along both the vertical and longitudinal axes (Nimchinsky et al., 1999). The criteria for a FN were a unique basal dendrite and a bifid or "forked" apical dendrite, a rather triangular perikaryon as large as or larger than the local pyramidal neurons (Ngowyang, 1932). Second, the Nissl- and Gallyas-stained sections were examined using the low magnification images to localize the cyto- and myelo-architectonic boundaries of the insula, using criteria defined in our prior study on the architectonic areas in the macaque insular cortex (Evrard et al., 2014). This architectonic mapping was made using a relatively long delay after the VEN and FN charting and without having any access to the charts in order to avoid a biased parcellation. Finally, the plots of the VEN and FN and the architectonic outline of the insular areas from both hemispheres were finally aligned in Adobe Illustrator (Adobe System Inc., San José, California, USA) for comparison and for the preparation of figures.

Results

Cyto- and myeloarchitectonic features

Figures 1-6 illustrate medium-resolution photomicrographs of adjacent sections of the human agranular anterior insula processed with Nissl and Gallyas staining techniques from the left and right hemisphere of the three cases H003, H005, and H006. For differentiation of the VEN areas, cyto- and myeloarchitectonic features were examined. According to Brodmann's guidelines (Brodmann, 1909) cytoarchitectonic features (Nissl staining) included the thickness, the sublamination, the distinctiveness of the layers, as well as the neuronal size, the staining intensity, and the packing density. Myeloarchitectonic features (Gallyas staining) included their length or vertical expansion over cortical layers 2 -6, the density, the thickness, orientation of the fibers, and the presence of the outer Band of Baillarger, or line of Gennari (marked by an asterisk), which comprises a thick continuous horizontal plexus at the level of the cortical layer 4.

In both, the Nissl and Gallyas stained sections, the medial and lateral limits of most VEN areas were rather abrupt than gradual. These sharp borders between the insular areas were robustly reproducible in all cases. The cyto-and myeloarchitectonic borders were mostly matching each other. Arrow heads mark these borders between the VEN areas and their medial and lateral adjacent areas.

Architectonic features of the VEN areas

In all human insulae the VEN and FN were clustered within a rather vast region (or 'VEN domain') inside the ventral agranular region of anterior insula, or FI, with no apparent extension in the dorsal anterior insula or the dysgranular and granular insula. The VEN domain was delimited by an abrupt appearance of VEN and FN. Similar to what has been reported in macaque monkeys (Horn, F.M. & Evrard, H.C., *in preparation*), a comparison of the localization of the human VEN domain with the architectonic parcellation of the anterior insula revealed that its overall outer limit exactly overlapped with sharp architectonic boundaries. The domain consisted of five architectonic VEN areas that were labeled *VEN1, VEN2, VEN3, VEN4,* and *VEN5,* and each of them had distinct cyto-and myeloarchitectonic characteristics. In all cases, *VEN 1* was divided into a rostral and a caudal part (Fig. 1). In the Nissl stain (Fig. 1A) the rostral part of *VEN 1* (*VEN 1r*) is characterized

by a thin layer 2; a broader and sublaminated layer 3 containing larger neurons; a sublaminated layer 5, with a thinner but compact layer 5a, containing small neurons, and a broader layer 5b with large and darkly stained pyramidal neurons (PY), VEN and FN; and a broad layer 6. In the Gallyas stain *VEN 1r* reveals a vertical array of thick fibers extending over layer 6 to 5, in a fan like fashion (Fig 1B). It contains an outer band of Baillarger, few shorter fibers in layer 3 running horizontally, and a very light horizontal plexus near the pial surface. The caudal part of *VEN 1* is distinguished from the rostral part by its more distinct lamination.

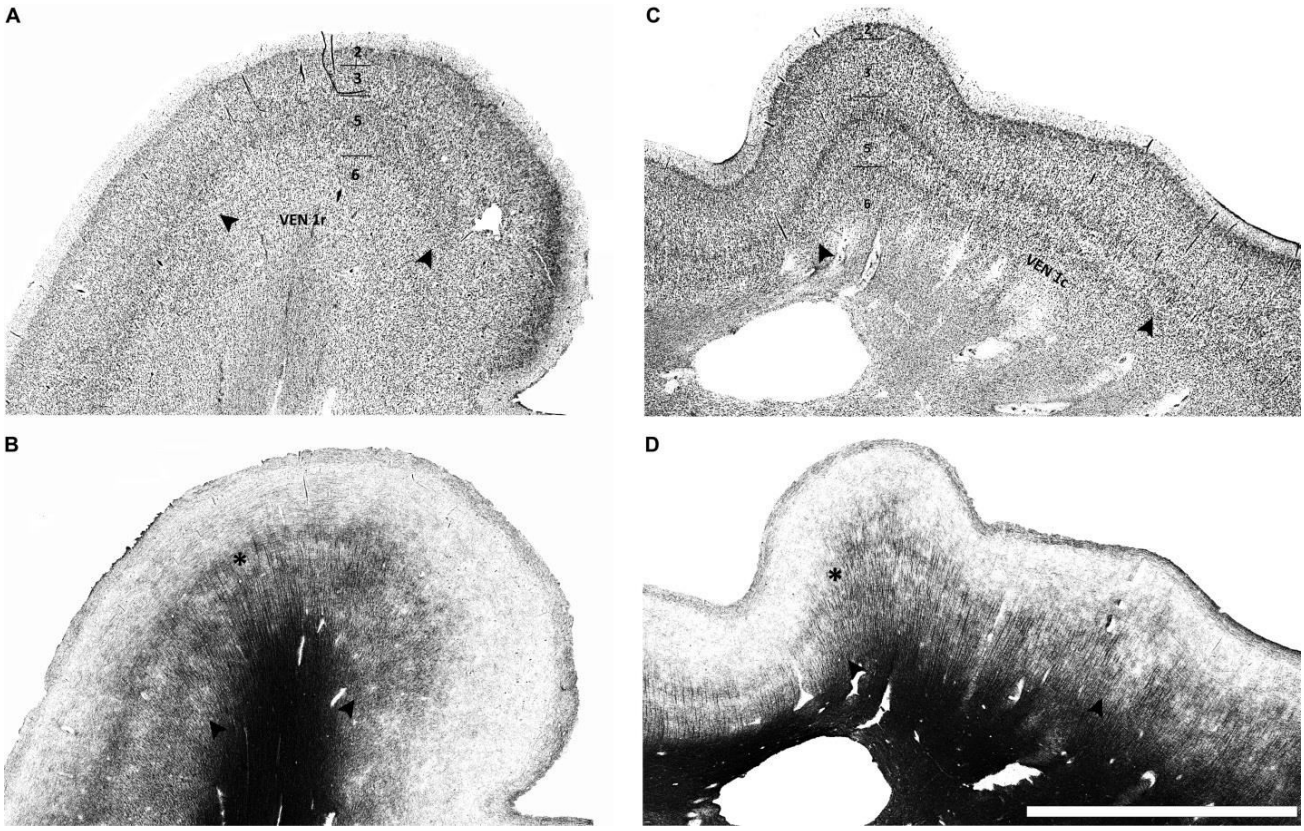

Figure 1: Medium-resolution photomicrographs of two adjacent coronal sections
A, C Nissl and **B, D** Gallyas (myelin) staining techniques. **A, B** This pairs of photomicrographs illustrates the cyto- and myeloarchitectonic characteristic of the rostral portion of VEN area 1 (VEN 1r). **C, D** This pairs of photomicrographs illustrates the cyto- and myeloarchitectonic characteristic of the caudal portion of VEN area 1 (VEN 1c). Arrowheads mark the borders of the VEN area with the neighboring regions of the anterior insular cortex. The delimitation of the cortical layers 2-6 is indicated left in the mound of the insula in panel **A** and **C;** left is dorsal, top is lateral; the asterisk marks the outer band of Baillarger; scale bar = 500 µm.

In the Nissl stain (Fig 1C) layer 2 is broader and more darkly stained; layer 3 is sublaminated with smaller and less densely packed neurons in layer 3a; layer 5 is also sublaminated with a thin horizontal gap containing less cells, which gives the appearance of two rails: layer 5a has darkly stained and densely packed cells at the border to layer 3b, and layer 5b has less but rather large

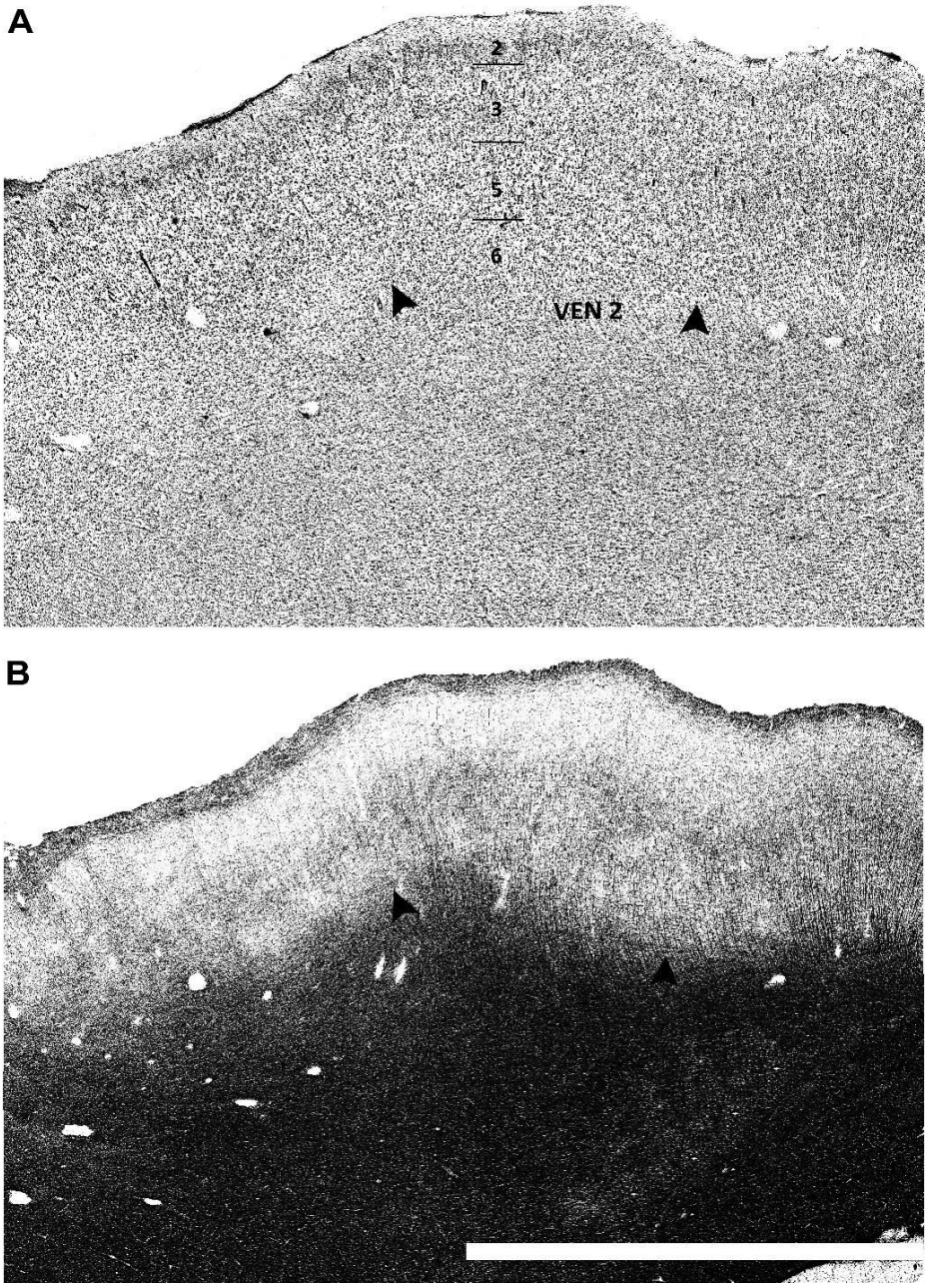

Figure 2: Medium-resolution photomicrographs of two adjacent coronal sections.
A Nissl and **B** Gallyas (myelin) staining techniques. This pair of photomicrographs illustrates the cyto- and myeloarchitectonic characteristic of the VEN area 2 (VEN2). Arrowheads mark the borders of VEN2 with the neighboring regions of the anterior insular cortex. The delimitation of the cortical layers 2-6 is indicated left in the mound of the insula in panel **A**; left is dorsal, top is lateral; scale bar = 500 µm.

and darkly stained neurons, including VEN and FN; layer 6 is also sublaminated with a compact and darkly stained layer 6a. In the Gallyas stain (Fig. 1D) *VEN 1c* is also characterized by a vertical, 'fan-like' array of thick fibers ranging from layer 6 to layer 5; it has a thick and dense horizontal plexus near the pial surface, but the outer band of Baillarger is less prominent.

In the Nissl stain (Fig. 2A) *VEN 2* has a dense but rather thin layer 2; layer 3 is sublaminated with a less dense layer 3a. The sublamination of layer 5 is rather subtle, and layer 6 is darkly stained and homogeneous. In the Gallyas stain (Fig. 2B) *VEN 2* has an array of vertical fibers that are thin

and less dense, but longer as in *VEN 1*. It has a thick and very darkly stained horizontal plexus near the pial surface, and short horizontal fibers in layer 3, but no band of Baillarger.

VEN 3 is characterized in the Nissl stain (Fig. 3A) by a thinner but densely packed layer 2; a broad layer 3, containing smaller neurons; a distinctly sublaminated layer 5 constituting of two rails, similar to *VEN 1c*; whilst layer 6 is not sublaminated and rather thin. In the Gallyas stain (Fig. 3B) *VEN 3* consists of rather short and thin vertical fibers crossed by shorter horizontal fibers in layer 3, however there is no obvious outer band of Baillarger. The horizontal plexus near the pial surface is rather light.

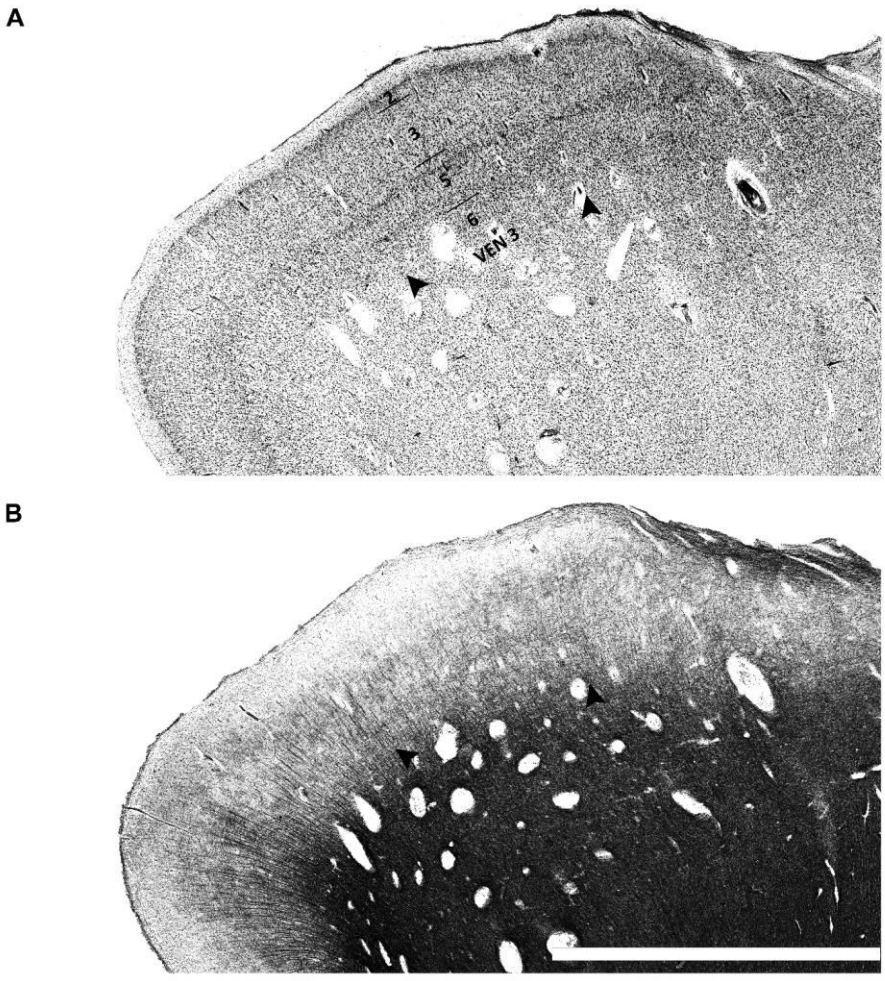

Figure 3: Medium-resolution photomicrographs of two adjacent coronal sections.
A Nissl and **B** Gallyas (myelin) staining techniques. This pair of photomicrographs illustrates the cyto- and myeloarchitectonic characteristic of the VEN area 3 (VEN3). Arrowheads mark the borders of VEN3 with the neighboring regions of the anterior insular cortex. The delimitation of the cortical layers 2-6 is indicated left in the mound of the insula in panel **A**; left is dorsal, top is lateral; scale bar = 500 µm.

In the Nissl stain, *VEN 4* has a compact layer 2 and a sublaminated layer 5, with a striped appearance similar to *VEN 3* (Fig. 4A). Myeloarchitectonic features of *VEN 4* are a very thick and darkly stained horizontal plexus near the pial surface as well as a sparse array of thin vertical fibers ranging to layer 5, with isolated long fibers ranging to layer 2 that are crossed by a broad but discontinuous horizontal band in layer 3 (Fig. 4B).

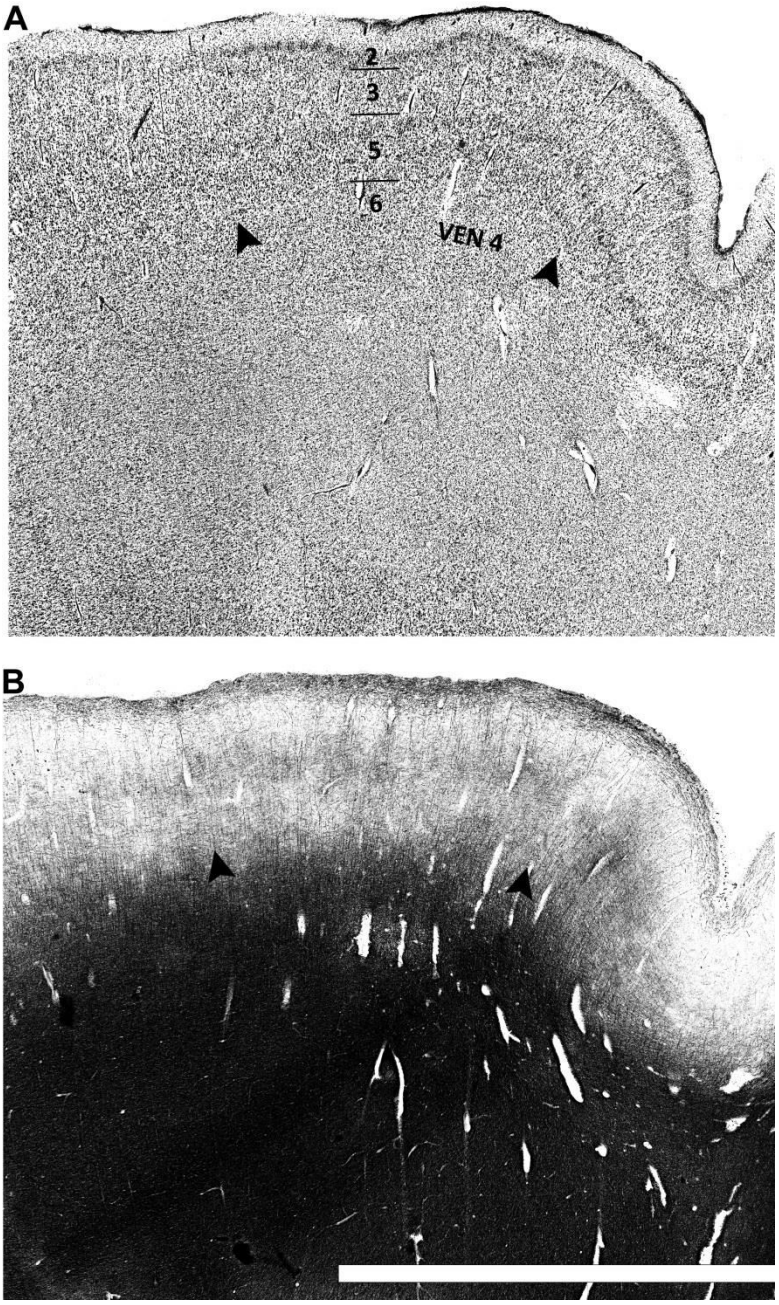

Figure 4 Medium-resolution photomicrographs of two adjacent coronal sections
A Nissl and **B** Gallyas (myelin) staining techniques. This pair of photomicrographs illustrates the cyto- and myeloarchitectonic characteristic of the VEN area 4 (VEN4). Arrowheads mark the borders of VEN4 with the neighboring regions of the anterior insular cortex. The delimitation of the cortical layers 2-6 is indicated left in the mound of the insula in panel **A**; left is dorsal, top is lateral; scale bar = 500 µm.

VEN 5 is characterized in the Nissl stain (Fig. 5A) by a rather diffuse lamination: layer 3 is undivided and not clearly distinguishable from layer 5. In the Gallyas stain (Fig. 5B) *VEN 5* consists of an array of long vertical fibers ranging until the superficial part of layer 3, and are crossed by short horizontal fibers in layer 3. It has no band of Baillarger, but a dense horizontal plexus near the pial surface.

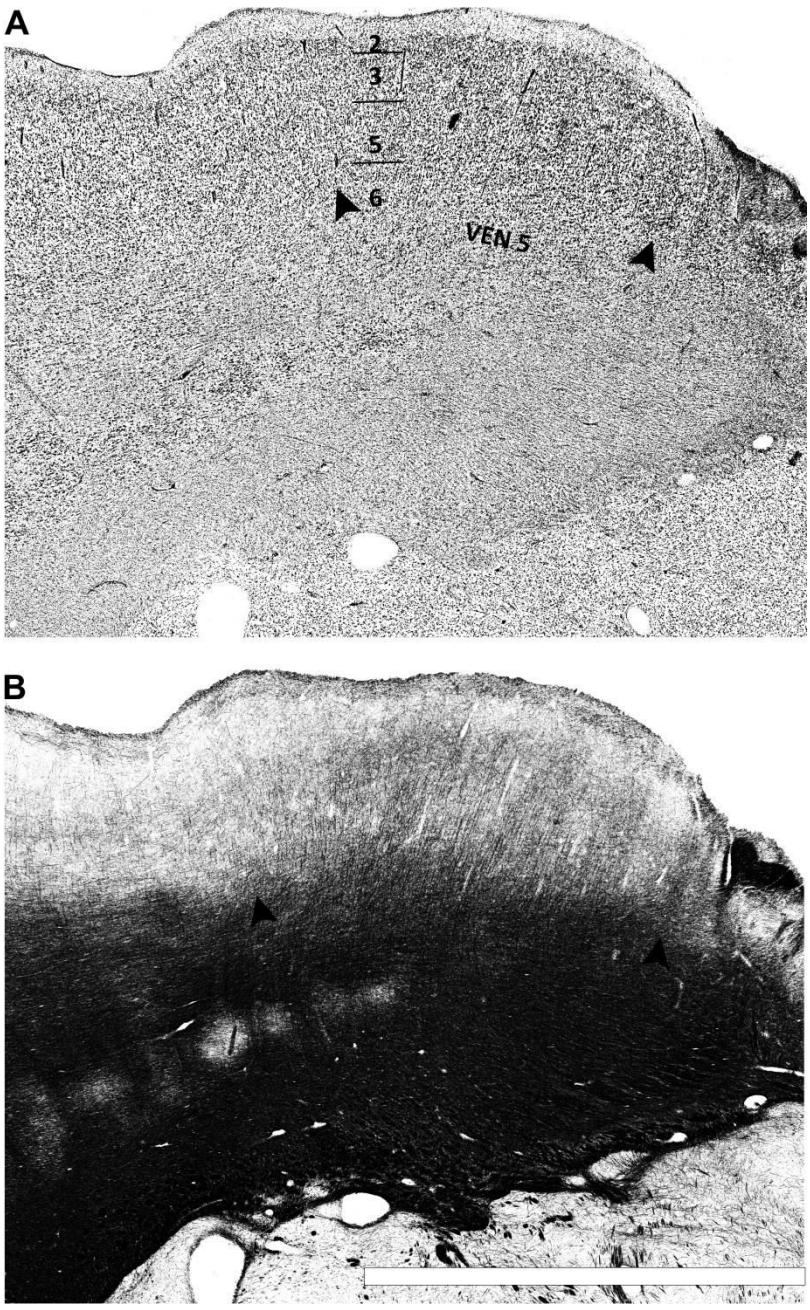

Figure 5 Medium-resolution photomicrographs of two adjacent coronal sections.
A Nissl and **B** Gallyas (myelin) staining techniques. This pair of photomicrographs illustrates the cyto- and myeloarchitectonic characteristic of the VEN area 5 (VEN5). Arrowheads mark the borders of VEN5 with the neighboring regions of the anterior insular cortex. The delimitation of the cortical layers 2-6 is indicated left in the mound of the insula in panel **A**; left is dorsal, top is lateral; scale bar = 500 µm.

Comparison of the human and monkey VEN area

The comparison of the cyto- and myeloarchitecture of all human VEN areas in the anterior insula with the VEN area of macaque monkeys shows that the architectonic characteristics of the rostral portion of the human *VEN1* corresponds to the characteristics in the rostral portion of the macaque VEN area (*VENr*). The cyto-and myeloarchitectonic features of these areas are shown in Fig. 6. In the Nissl stain (Fig. 6A and C), the VEN areas of both species show the presence of layer 2, a broad and subdivided layer 3, a darkly stained and sublaminated layer 5, with a thinner but compact layer 5a containing small neurons, and a broader layer 5b with large and darkly stained pyramidal neurons, VEN and FN; and a broad layer 6. The Gallyas stains (Fig. 6B and D) show arrays of long and rather thick vertical fibers that are crossed by short horizontal fibers in layer 3. The outer band of Baillarger is present, which is slightly more prominent in the human *VEN1r*.

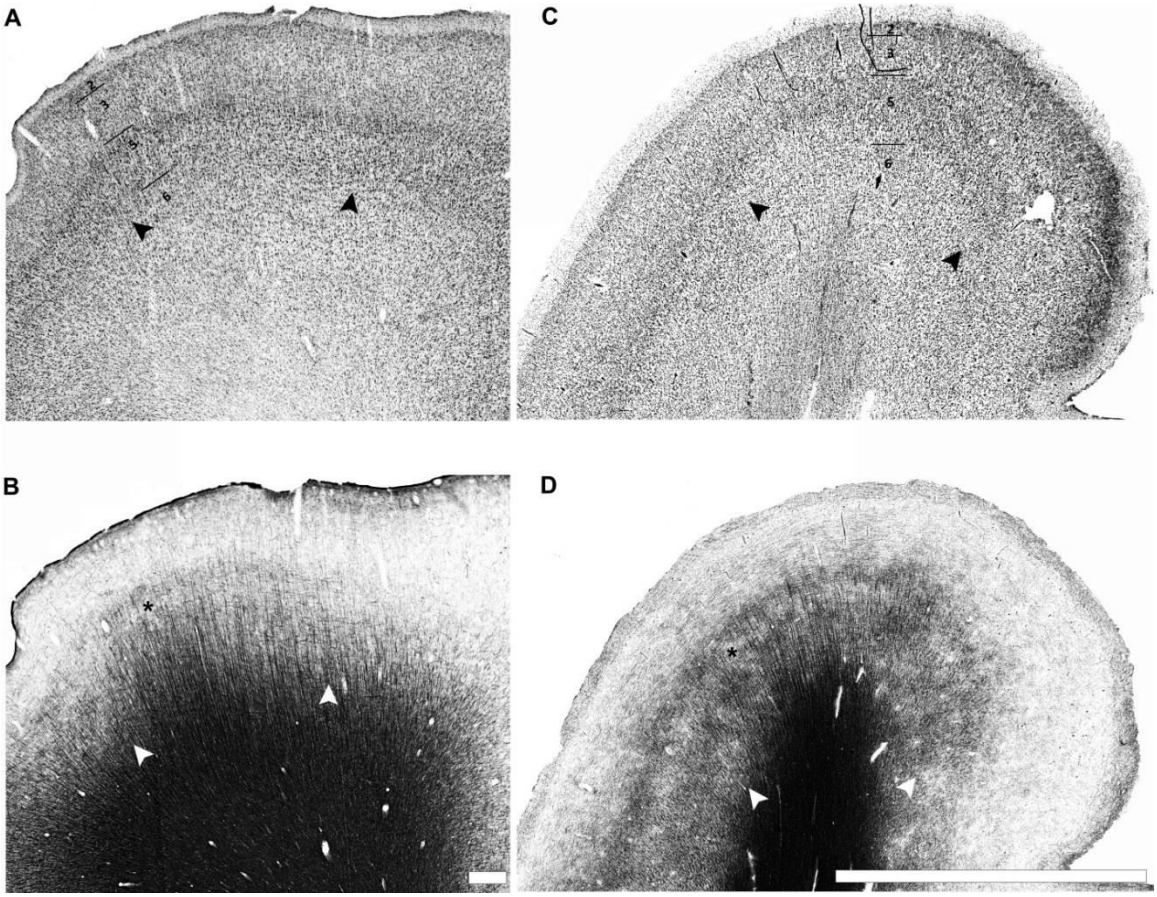

Figure 6: M**edium-resolution photomicrographs of two adjacent coronal sections of a macaque monkey (A and B) and a human (C and D)**

A, C Nissl and **B, D** Gallyas (myelin) staining techniques. These pairs of photomicrographs illustrate the cyto- and myeloarchitectonic characteristic of the rostral portion of the unique VEN area in the macaque anterior insula (**A** and **B**) and of the rostral portion of the VEN1 in the human anterior insula (**C** and **D**). Arrowheads mark the borders of VEN5 with the neighboring regions of the anterior insular cortex. The delimitation of the cortical layers 2-6 is indicated left in the mound of the insula in panel **A** and **C**; the asterisks mark the band of Baillarger; left is dorsal, top is lateral; scale bars = 500 µm.

Discussion

To analyze the areal distribution of the VEN and FN in the anterior insula in humans we used high- and low-magnification microscopy on freshly fixed tissue of the left and right hemisphere of three human brains that were histologically processed for cyto and myeloarchitectonic analyses. Our examination of the VEN and FN distribution in the human and macaque anterior insula cortex revealed a complete overlap of the delimitation of the VEN and FN clusters with architectonic boundaries. In macaque monkeys this cluster formed one unique architectonic area, or VEN area (Horn, F.M. and Evrard, HC, *in preparation*). In humans, on both the left and right FI, the VEN and FN were co-mingled in rather a vast domain consistent of five different architectonic areas. Preliminary examinations of other primates, e.g. Old World (Baboon) and New World (Spider monkey) monkeys, as well as Gibbons, Chimpanzees, and Orangutans suggest the limitation of these neurons to one architectonic area (Evrard et al., *in preparation*), similar to macaque monkeys. The highly consistent overlap of the VEN distribution and architectonic boundaries (or "elemental localization") in great apes and non-human primates indicates a robust, yet unknown, selective pressure on the development of the AIC throughout evolution. It further needs to be determined whether the single VEN area in all anthropoid primates investigated is homologue or varies in its architectonic features. Furthermore, this study only investigated the insular cortex but not the ACC. It has already been mentioned that within the human ACC, VEN and FN are also clustering (Seeley et al., 2006), however, so far, there is no study showing such an elemental localization of VEN and FN within the ACC.

In the human FI, one area containing VEN and FN can be divided into a rostral (*VEN1r*) and a caudal (*VEN1c*) portion, based on a slight rostrocaudal variation in the cyto- and myeloarchitectonic characteristics. Similarly, it has previously been found that the VEN area in macaque monkeys can also be subdivided into a rostral (*VENr*) and a caudal (*VENc*) portion (Horn, F.M. & Evrard, H.C., *in preparation*). By comparing the cyto-and myeloarchitecture of the rostral and caudal portions of these areas in macaque monkeys and humans it seemed that the *rVEN* and the rostral portion of *VEN1* (*VEN1r*) have a similar cyto-and myeloarchitecture, however, the caudal portions of this area in monkeys and humans, *VENc* and *VEN1c,* respectively, do not correspond each other. Therefore, the macaque *VENr* and the human *VEN1r* could be homologues,

whilst *VENc* and *VEN1c*, as well as the additional human VEN areas may have evolved individually. Examining the cyto- and myeloarchitectonic feature of the VEN area in the other primate species could help to answer the question whether the VEN area in these primate species is also subdivided and whether there is a homologous VEN area in all primates containing VEN and FN.

The multiplication of the VEN area to areas in humans as compared to only one area in macaque monkeys, and presumably other primates (Evrard et al., *in preparation*) likely correlates with the disproportionately faster growth of the insular cortex and in particular FI, as compared to the rest of the brain and especially as compared to other primate species (Bauernfeind et al., 2013). It has been suggested that the cognitive evolution in humans went along with neuroanatomical modifications in capacities of the anterior insula for the subjective perception of bodily feelings, self-awareness (knowing that one exists), and social and emotional intelligence (Bauernfeind et al., 2013, Craig, 2009). It is proposed that the volume of a brain area is related to the capacity of information processing and behavior necessary for the performance of a task. Additionally, with the growth of the areal volume, the amount of neurons increases, modifications in the local cortical circuitries and interconnectivity between brain areas occur, hence the fine-tuned processing is improved (Bauernfeind et al., 2013, Hofman, 2014, Kaas, 2000). The insular cortex in primates is suggested to integrate bodily, or interoceptive, feelings with homeostatic sensory and motor sensations, as well as with social, emotional, cognitive, and motivational activity, and it has been suggested that within the AIC emotions and cognitive feelings are colored by these integrated interoceptive feeling states from the body (Craig, 2002). The enlargement of the AIC and the multiplication of regions containing VEN and FN could be correlated with an increased behavioral and cognitive capacity, and may support more sophisticated cognitive processes in humans, leading to an enhanced awareness of the subjective feelings as compared to other primate species (Smaers et al., 2011). Therefore, the multiplication of VEN areas in humans might underlie the possible evolutionary emergence of human subjective awareness of feelings (Craig, 2009). Supporting this hypothesis, Stimpson and her team (2011) showed that only the VEN reveal phylogenetical differences in the gene expression profile, but not the local PN. Furthermore, among several hominid species, in humans, the highest percentage of VEN expressed the proteins ATF3, IL4Rα, and NMB. These proteins are proposed to be involved in controlling the intake of food, modulating autonomic responses, and monitoring the homeostatic state of one's body. It was

therefore suggested that human VEN might have undergone a functional specialization of biochemical features during evolution for enhanced social and emotional intelligence due to a higher sensitivity to one's own interoceptive state (Sanchez et al., 1999, Stimpson et al., 2011).

So far no model of the modular organization of the human insular cortex exists. Such a model could help understanding the topology of the areas, and answer the following questions: are the neighborhood relations consistent across both hemispheres in all cases? Are there asymmetries in the shape of the insula, and the extent and the topology of the VEN areas between the left and right hemisphere? Are the VEN areas constituting one large connected domain or are they individual areas? A model would also benefit the comparison between the human insula, in particular the anterior insular cortex, and the distribution of the VEN and FN with the established model of the macaque insula (Evrard et al., 2014), and other primate species. This could uncover which areas are homologous across primates and which are evolutionary novel and human specific. The exact organization of the human insular cortex, as well as the identification of human specific areas, including VEN areas, may provide a basis for understanding the underlying neuronal basis in human neuropsychiatric disorders which have been linked with insular and VEN functioning.

References

ALLMAN, J. M., TETREAULT, N. A., HAKEEM, A. Y., MANAYE, K. F., SEMENDEFERI, K., ERWIN, J. M., PARK, S., GOUBERT, V.

HOF, P. R. 2010. The von Economo neurons in frontoinsular and anterior cingulate cortex in great apes and humans. *Brain Struct Funct,* 214**,** 495-517.

BAUERNFEIND, A. L., DE SOUSA, A. A., AVASTHI, T., DOBSON, S. D., RAGHANTI, M. A., LEWANDOWSKI, A. H., ZILLES, K., SEMENDEFERI, K., ALLMAN, J. M., CRAIG, A. D., HOF, P. R. & SHERWOOD, C. C. 2013. A volumetric comparison of the insular cortex and its subregions in primates. *Journal of Human Evolution,* 64**,** 263-279.

BRODMANN, K. 1909. *Vergleichende Lokalisationslehre der Grosshirnrinde in ihren Prinzipien dargestellt und Grund des Zellenbaues,* Leipzig, Verlag von Johann Ambrosius Barth.

BUTTI, C. & HOF, P. R. 2010. The insular cortex: a comparative perspective. *Brain Structure & Function,* 214**,** 477-493.

CRAIG, A. D. 2002. How do you feel? Interoception: the sense of the physiological condition of the body. *Nature Reviews Neuroscience,* 3**,** 655-666.

CRAIG, A. D. 2009. How do you feel - now? The anterior insula and human awareness. *Nature Reviews Neuroscience,* 10**,** 59-70.

EBBESSON, S. O. 1980. The parcellation theory and its relation to interspecific variability in brain organization, evolutionary and ontogenetic development, and neuronal plasticity. *Cell Tissue Res,* 213**,** 179-212.

EVRARD, H. C., FORRO, T. & LOGOTHETIS, N. K. 2012. Von Economo neurons in the anterior insula of the macaque monkey. *Neuron,* 74**,** 482-9.

EVRARD, H. C., LOGOTHETIS, N. K. & CRAIG, A. D. 2014. Modular architectonic organization of the insula in the macaque monkey. *J Comp Neurol,* 522**,** 64-97.

GLASSER, M. F., COALSON, T. S., ROBINSON, E. C., HACKER, C. D., HARWELL, J., YACOUB, E., UGURBIL, K., ANDERSSON, J., BECKMANN, C. F., JENKINSON, M., SMITH, S. M. & VAN ESSEN, D. C. 2016. A multi-modal parcellation of human cerebral cortex. *Nature,* 536**,** 171.

GOODKIND, M., EICKHOFF, S. B., OATHES, D. J., JIANG, Y., CHANG, A., JONES-HAGATA, L. B., ORTEGA, B. N., ZAIKO, Y. V., ROACH, E. L., KORGAONKAR, M. S., GRIEVE, S. M., GALATZER-LEVY, I., FOX, P. T. & ETKIN, A. 2015. Identification of a common neurobiological substrate for mental illness. *JAMA Psychiatry,* 72**,** 305-15.

HOF, P. R. & VAN DER GUCHT, E. 2007. Structure of the cerebral cortex of the humpback whale, Megaptera novaeangliae (Cetacea, Mysticeti, Balaenopteridae). *Anat Rec (Hoboken),* 290**,** 1-31.

HOFMAN, M. A. 2014. Evolution of the human brain: when bigger is better. *Front Neuroanat,* 8**,** 15.

KAAS, J. H. 2000. Why is Brain Size so Important: Design Problems and Solutions as Neocortex Gets Bigger or Smaller. *Brain and Mind,* 1**,** 7-23.

KAUFMAN, J. A., PAUL, L. K., MANAYE, K. F., GRANSTEDT, A. E., HOF, P. R., HAKEEM, A. Y. & ALLMAN, J. M. 2008. Selective reduction of Von Economo neuron number in agenesis of the corpus callosum. *Acta Neuropathol,* 116**,** 479-89.

KIM, E. J., SIDHU, M., GAUS, S. E., HUANG, E. J., HOF, P. R., MILLER, B. L., DEARMOND, S. J. & SEELEY, W. W. 2012. Selective frontoinsular von Economo neuron and fork cell loss in early behavioral variant frontotemporal dementia. *Cereb Cortex,* 22**,** 251-9.

KURTH, F., EICKHOFF, S. B., SCHLEICHER, A., HOEMKE, L., ZILLES, K. & AMUNTS, K. 2010. Cytoarchitecture and probabilistic maps of the human posterior insular cortex. *Cereb Cortex,* 20**,** 1448-61.

MENON, V. & UDDIN, L. Q. 2010. Saliency, switching, attention and control: a network model of insula function. *Brain Struct Funct,* 214**,** 655-67.

MESULAM, M. M. & MUFSON, E. J. 1985. The Insula of Reil in Man and Monkey. *Peters A., Jones E.G. (eds) Association and Auditory Cortices. Cerebral Cortex.* Boston, MA: Springer, Boston, MA.

MONTGOMERY, S. H., MUNDY, N. I. & BARTON, R. A. 2016. Brain evolution and development: adaptation, allometry and constraint. *Proc Biol Sci,* 283.

NAGAI, M., KISHI, K. & KATO, S. 2007. Insular cortex and neuropsychiatric disorders: a review of recent literature. *Eur Psychiatry,* 22**,** 387-94.

NGOWYANG, G. 1932. Beschreibung einer Art von Spezialzellen in der Inselrinde-zugleich Bemerkungen über die v. Economoschen Spezialzellen. *J Psychol Neurol,* 44**,** 671-674.

NIMCHINSKY, E. A., GILISSEN, E., ALLMAN, J. M., PERL, D. P., ERWIN, J. M. & HOF, P. R. 1999. A neuronal morphologic type unique to humans and great apes. *Proc Natl Acad Sci U S A,* 96**,** 5268-73.

NORTHCUTT, R. G. & KAAS, J. H. 1995. The emergence and evolution of mammalian neocortex. *Trends Neurosci,* 18**,** 373-9.

ROSE, M. 1928. Die Inselrinde des Menschen und der Tiere. *Journal of Physchology and Neurology,* 37**,** 467-624.

SALAZAR, I., RUIZ PESINI, P., FERNANDEZ TROCONIZ, P., GONZALEZ SORIANO, J. & FERNANDEZ ALVAREZ, P. 1988. The neocortex of the dog. 1. A classical cytoarchitectonic map. *Anat Histol Embryol,* 17**,** 169-87.

SANCHEZ, M. M., YOUNG, L. J., PLOTSKY, P. M. & INSEL, T. R. 1999. Autoradiographic and in situ hybridization localization of corticotropin-releasing factor 1 and 2 receptors in nonhuman primate brain. *J Comp Neurol,* 408**,** 365-77.

SEELEY, W. W., CARLIN, D. A., ALLMAN, J. M., MACEDO, M. N., BUSH, C., MILLER, B. L. & DEARMOND, S. J. 2006. Early frontotemporal dementia targets neurons unique to apes and humans. *Ann Neurol,* 60**,** 660-7.

SMAERS, J. B., STEELE, J., CASE, C. R., COWPER, A., AMUNTS, K. & ZILLES, K. 2011. Primate prefrontal cortex evolution: human brains are the extreme of a lateralized ape trend. *Brain Behav Evol,* 77**,** 67-78.

STIMPSON, C. D., TETREAULT, N. A., ALLMAN, J. M., JACOBS, B., BUTTI, C., HOF, P. R. & SHERWOOD, C. C. 2011. Biochemical Specificity of von Economo Neurons in Hominoids. *American Journal of Human Biology,* 23**,** 22-28.

Summary and Conclusion

The primate AIC and ACC harbor a high concentration of two specialized neuronal morphotypes, the spindle-shaped von Economo neuron (VEN) and the triangularly shaped Fork neuron (FN). Within these regions, the VEN and FN were described to form clusters instead of being homogeneously dispersed over the cortex. The exact function of these neurons is still unknown. However, the discovery of their precise localization may contribute to the understanding of their role within the brain. Therefore, the three experiments discussed in the present work researched the exact localization of the VEN and the FN within the agranular, anterior insular cortex (AIC) and dysgranular, mid-insular cortex (DIC) in two species of macaque monkeys and in the agranular frontoinsula (FI) in humans. Consecutive coronal sections of six macaque monkey brains and three human brains were histologically processed and analyzed using pre-established multi-architectonic comparison criteria. High magnification microscopy was used to accurately localize these neurons, whilst cyto- and myelo-architectonic areas were determined with low-magnification microscopy.

Upon independent analyses of the architecture of the AIC and the distribution of the VEN and FN in macaque monkeys, the first experiment demonstrated an exact overlap of the distribution of the VEN and the FN with the borders of a previously defined architectonic area, Ial, which is always located in an around a characteristic cortical curvature of the agranular anterior insula. This containment of neuronal elements within one architectonic area was defined as “elemental localization” (EL) by Brodmann in 1909. Area Ial, now referred to as VEN area, was divided into a rostral and a caudal subarea, which varied slightly in their architecture. However, both subareas were still more similar to each other compared to adjacent areas of the AIC.

The subsequent second study showed a further EL of the VEN and FN within the dysgranular insula in macaque monkeys. Similar to the VEN area of the AIC, the VEN area was allocated within a cortical convexity, also defined as the mound area of the dysgranular insula (Idm). The dysgranular VEN area revealed the same separation into a rostral and caudal portion as described for the agranular VEN area.

The third experiment showed that the concept of the EL of the VEN and FN is also valid within the human FI. In contrast to the AIC in macaque monkeys, the FI

contained five different architectonic VEN areas. Nonetheless, one human VEN area, VEN1, which was also permanently located within a specific cortical curvature, revealed the segmentation into a rostral and a caudal portion similar to the macaque VEN areas.

Taken together, the research described here shows that in both species, the localization of the VEN and FN at high magnification enabled the prediction of the architectonic boundaries of the macaque and human VEN areas at low magnification and vice versa. Furthermore, the rostral portion of the agranular macaque VEN area and of the human VEN1 area showed a similar architecture and therefore could be neuroanatomical homologues, while there are clear indications that the caudal portion of the macaque VEN area and of the human VEN1 area, as well as the additional human VEN areas, have evolved separately. The results further support the theory that the primate orbital prefrontal cortex and adjacent ventral agranular and dysgranular insula are heterogeneously organized into smaller, sharply delimited areas, instead of being lumped together into larger, gradually changing periallocortical (agranular) and proisocortical (dysgranular) regions.

Additionally, the concept of an EL suggests that the neuron and its host area have a common functional, hodological pattern as well as identical evolutionary and developmental features. The findings of this EL within both species cortices offers an advantage in future examinations of the function of these neurons, which are associated with the representation of the homeostatic state of one’s body and are selectively affected in several neuropsychiatric disorders. This may also further the understanding of the structural organization of the insular cortex in primates.

Outlook

The comparison of the architecture of the rostral and caudal portions of the agranular VEN area in macaque monkeys and the VEN1 area in humans revealed the rostral portion of the macaque VEN area and the human VEN1 to have a similar cyto- and myeloarchitecture. However, the caudal portions of this area in monkeys and humans do not exhibit the same features. Therefore, the rostral portions of the agranular macaque VEN area and the human VEN1 could be homologues, while the caudal portions of both areas, as well as the additional VEN areas in the human agranular insula, may have evolved individually. To answer the question whether the VEN area in all primate species, which harbor VEN and FN within the agranular insula, is also subdivided into a rostral and caudal portion and whether there is a homologous area in all these primates, an examination of the cyto- and myeloarchitectonic feature of the VEN area in other primate species is needed. Furthermore, so far only the dysgranular insular cortex in macaque monkeys has been examined for the presence of VEN and FN. To uncover whether there are additional VEN areas in the dysgranular insula of humans and other primate species, more studies need to be conducted. Similar studies on the ACC are also needed.

In general, the comparison of the architectonic organization of the entire human insular cortex with the existing model of the macaque monkey (Evrard et al., 2014), and eventually other primate species, might reveal which areas are homologous across all primate species and which are newly evolved and human specific. For this comparison, a model of the human insular cortex would be necessary in order to understand the topology of the insular areas and to understand the following questions: Are there robust interhemispheric and interindividual neighborhood relations? Is there an asymmetry in the shape, size, and number of VEN and FN between the left and right hemisphere? Are all the VEN areas connected, forming one large domain, or are they separate areas? The exact organization of the human insular cortex and the identification of areas that are human specific could provide the framework to further understanding the underlying neuronal basis in human neuropsychiatric disorders which have been linked to insular and VEN functions.

Additionally, the VEN and FN have been shown to be selectively depleted in several neuropsychiatric disorders such as bvFTD. The study in this thesis was the first one that examined the exact localization of these neurons within the human

frontoinsula. To discover whether in different neuropsychiatric diseases different VEN areas are affected or if all of them are affected equally, examinations of the exact distribution of VEN and FN in post-mortem brain of patients suffering from several neuropsychiatric disorders are required. This may also extend the understanding of the VEN and FN role in the healthy and diseased brain.

Acknowledgements

I would like to thank my supervisor Dr. Henry C. Evrard for his support during my PhD and for providing the resources.

I am especially grateful for my sister Caterina Z. Horn, who I lived with, and my boyfriend Julian F. Stauss, for all their warm love, patience, encouragement and faith in me. I appreciate their faithful support during all the phases of this PhD. Thank you.

A special acknowledgement goes to my colleague Jennifer Smuda, who has been a source of friendship and as well as good advice and collaboration and I am grateful for the time we spent together.

I am also grateful to Johannes Boldt for our lovely lunch meetings once a week, and especially for becoming a good friend.

I am thankful to Katharina Happ, who worked as a HIWI in our laboratory, for her professional support with the lab work and especially for our friendship.

I would like to thank Ana Vedoveli for her collaboration and Joachim Werner for the technical support and his patience.

I would also like to thank all of my friends for their emotional support and last but not least I am truly grateful to my family, especially my parents Claudia G. und Pius M. Horn for their love, emotional encouragement, financial support and their faith in me.